Dark Matter, Baryogenesis, and Inflation in the Higgs era

Hogan, Robert Joseph

Awarding institution:
King's College London

King's College London

Doctoral Thesis

Dark Matter, Inflation, and Baryogenesis in the Higgs Era

Author:

Robert Hogan

Supervisor:

Dr. Malcolm Fairbairn

A thesis submitted in fulfilment of the requirements

for the degree of Doctor of Philosophy

in the

Theoretical Particle Physics and Cosmology Group

Department of Physics

December 2015

Declaration of Authorship

I, Robert Hogan, declare that this thesis titled, ' Dark Matter, Inflation, and Baryogenesis in the Higgs Era' and the work presented in it are my own. I confirm that:

- This work was done wholly or mainly while in candidature for a research degree at this University.
- Where any part of this thesis has previously been submitted for a degree or any other qualification at this University or any other institution, this has been clearly stated.
- Where I have consulted the published work of others, this is always clearly attributed.
- Where I have quoted from the work of others, the source is always given. With the exception of such quotations, this thesis is entirely my own work.
- I have acknowledged all main sources of help.
- Where the thesis is based on work done by myself jointly with others, I have made clear exactly what was done by others and what I have contributed myself.

Signed:

Date:

Abstract

Despite the successes of particle physics and cosmology there are still some big unanswered questions. We still do not have a complete understanding of the nature of dark matter, the origin of the baryon asymmetry of the Universe, and the mechanism behind cosmic inflation. In this thesis we will address these problems by proposing minimal extensions of the Standard Model of particle physics in which the recently discovered Higgs boson often plays a central role. The aim is to provide an economical explanation for these phenomena by introducing as few new ingredients as possible. As a results these models are easily interpretable and testable with complementary particle physics and cosmological observations.

Acknowledgements

There are many people I want to thank for their help in the production of this thesis. First of all I want to thank my supervisor Malcolm for his guidance and trust and especially for his willingness to let me satisfy my curiosity with diverse topics. I want to thank him, and my other collaborators Philipp and Doddy, for their contributions to the research that makes up this thesis. I have also had many invaluable discussions with other members of the TPPC group that helped me learn so much more than I could have alone. For that I want, in particular, to thank Philipp, John, Tom, Thomas, Tevong, Chakrit, Katy, Peter, and James.

I received a lot of help proof reading this thesis for which I am extremely grateful. I would like to sincerely thank Philipp, John, Tevong, Krzysiek, and Chakrit for their generous help with such a dull task.

I would like to thank everyone in the Physics department for making it great to come to work (especially to Jean for introducing me to craft beer and Philipp for withstanding countless thrashings on the squash court). Finally, I want to thank my girlfriend Ally for making coming home even better and my family and friends for their constant support.

Contents

List of Figures

Chapter 1

Introduction

Research in the field of particle physics and cosmology has for some time been propped up by two standard models. The standard cosmological model (ΛCDM) is based on a homogeneous and isotropic Universe described by a Friedmann-Lemaître-Robertson-Walker (FLRW) model containing baryonic matter, radiation, cold dark matter, and a cosmological constant and impressively fits all observational evidence to date. While the phenomenological success of ΛCDM has been fantastic there are some theoretical problems related to the initial conditions of the model. The consensus solution to these problems, which we will discuss later in this chapter, is a period of exponential expansion in the very early Universe, known as inflation. While the generic predictions of inflation[1] are well tested and cosmologists are as confident as ever in its existence, we are still far from understanding the microscopic particle physics that underpins inflation. But this may change in the coming years. Many possible theories have been ruled out by measurements of the cosmic microwave background (CMB) (by e.g. *Planck* [1]) and several experiments are searching for primordial gravitational waves that would provide both a smoking gun signal for inflation and a strong constraint on the possible underlying particle physics theories.

[1] A vanilla inflation model predicts an almost scale invariant, Gaussian, and adiabatic spectrum of primordial fluctuations which has been observed in measurements of the cosmic microwave background.

The Standard Model (SM) of particle physics, based on an $SU(3)_c \times SU(2)_L \times U(1)_Y$ gauge theory, is also a remarkably successful theory having undergone numerous precise experimental tests. The recent discovery of a 125 GeV Higgs boson by the ATLAS [2] and CMS [3] collaborations at the LHC has confirmed the existence of the last piece of the puzzle. It is well understood however that the SM has many shortcomings. Some of these, such as the hierarchy problem and a desire for grand unification, are theoretical problems which, while very suggestive that some ingredients are missing, do not conflict with any experimental measurements directly. Perhaps more importantly, the SM is incapable of explaining some well established observational results. In addition to accounting for non-zero neutrino masses, two of the most notable of these are the presence of non-baryonic dark matter in the Universe and the asymmetry between matter and anti-matter. It seems unavoidable that the resolution of these two problems will need additional, as yet undiscovered degrees of freedom to be incorporated into the SM.

Predicting the nature of the new degrees of freedom needed to solve these three (and other) problems has been the charge of particle physicists for the last 50 or more years. In this thesis we will continue that endeavour and we will see that the recent discovery of the Higgs boson may provide the most promising avenue for exploration.

In the rest of this chapter we will introduce the problems of dark matter, the baryon asymmetry of the Universe, and inflation in more detail and discuss some candidate solutions. We will then finish the chapter by motivating the approach taken in this thesis of using minimality as a guiding principle and providing an outline of the thesis.

1.1 Dark matter

In this section we will introduce the problem of dark matter. We will first discuss the evidence for dark matter from astronomical and cosmological observations. We will

then describe the best candidates mechanisms for the production of a dark matter relic compatible with that observed today.

1.1.1 Observational evidence

The observational evidence for the existence of dark matter is now overwhelming [4]. The gravitational signature of dark matter can be seen on various length scales from galaxies up to cosmological scales. The first indication of dark matter was found more that 80 years ago by Zwicky [5] who, by measuring the velocities of galaxies in the Coma cluster and inferring its mass, noticed an apparent lack of visible matter. The mass-to-light ratio was $\sim$ 400 times what would be expected if all the mass was made up of stars like the Sun. Modern studies also use gravitational lensing by these clusters (see Fig. 1.1) to get an independent measurement of the mass and the 'missing mass' problem persists. This can be explained if there is a large contribution of weakly interacting, non-luminous (or dark) matter to the mass of the cluster.

FIGURE 1.1: *The gravitational potential of the galaxy cluster lenses light from background galaxies to create streak-like images. The inferred mass of the galaxy cluster is much larger than that expected from the visible matter alone suggesting presence of a large dark matter contribution. Credit: NASA*

Similarly on galactic scales, the rotational velocities of stars can be used to infer the gravitational potential, and hence the mass, of galaxies. Again there is a discrepancy from what would be expected if the visible matter was the only mass in the galaxy. In the absence of dark matter we would expect the outer stars of galaxies to be

orbiting much slower than observed. The inferred gravitational potential can then be used to reconstruct the expected dark matter density profile (e.g. [6]).

The most constraining and convincing evidence for dark matter however comes from cosmological scale observations. In an FLRW spacetime the Einstein equations yield the Friedman equation (in units with the speed of light, $c = 1$),

$$H^2 = \left(\frac{\dot{a}}{a}\right)^2 = \frac{8\pi G}{3}\rho + \frac{\Lambda}{3} - \frac{k}{a^2} = \frac{8\pi G}{3}\rho_{\text{tot}} - \frac{k}{a^2} \tag{1.1}$$

where H is called the Hubble parameter, a is the scale factor, G is the Newton constant, ρ is density of matter and radiation, Λ is a cosmological constant and $k \in \{-1, 0, 1\}$ describes the spatial curvature as open, flat, and closed respectively. In the last equality we define ρ_{tot} as the total energy density of the Universe which includes the contribution of matter, radiation, and the cosmological constant. This equation can then be used to define a critical density,

$$\rho_{\text{crit}} = \frac{3H^2}{8\pi G}, \tag{1.2}$$

such that for $\rho_{\text{tot}} = \rho_{\text{crit}}$ we have $k = 0$ and the Universe is flat. It is convenient to then describe the energy density contribution of the various components as $\Omega_i = \rho_i/\rho_{\text{crit}}$, and constrain the various Ω_i with cosmological observations. Among the most important of these observations was that of high redshift Type Ia supernovae [7]. The observation of the redshifts of these standard candles indicates that the Universe today is undergoing *accelerated* expansion. This is then evidence for $\Lambda \neq 0$ because the acceleration of the scale factor is governed by

$$\dot{H} + H^2 = \frac{\ddot{a}}{a} = -\frac{4\pi G}{3}(\rho + 3p) + \frac{\Lambda}{3}, \tag{1.3}$$

where p is the pressure of the cosmological fluid so for ordinary matter (with $\rho + 3p > 0$) the right hand side can only be positive for $\Lambda > 0$. The supernovae data can then be best explained in a cosmology with $\Omega_m \simeq 0.3$ and $\Omega_\Lambda \simeq 0.7$, where the subscript m includes both baryonic matter and any non-baryonic dark matter.

The density of matter can also be constrained by measuring the CMB. The CMB was produced at the time of last scattering $\sim 380,000$ years after the big bang when the first atoms were formed and photons decoupled from matter. The photons then propagated freely throughout the Universe and were redshifted by the cosmic expansion. The observation of the CMB is an extremely important tool for cosmology. It is in fact the earliest time that we can hope to observe because the Universe is opaque prior to its formation. Our best hope of understanding the physics of the Universe at earlier times is therefore to study its imprint on the CMB.

The CMB contains inhomogeneities that were imprinted at the time of last scattering as a result of under/over-densities of the cosmic fluid (see Fig. 1.2). The presence of different kinds of matter affects the cosmological evolution of density perturbations so observations of the CMB can give us information about the overall density of the Universe. Overdensities collapse under gravity and then re-expand from radiation pressure. The overdensities therefore oscillate about a critical scale called the sound horizon in a process known as baryon acoustic oscillation. The scale of the sound horizon in then imprinted as peaks in the CMB and matter power spectra. The first acoustic peak of the CMB is visible at $\ell \simeq 200$ in Fig. 1.3 and the amplitude and position of this peak in particular is very sensitive to the value of Ω_m, largely due to the baryonic contribution, Ω_b.

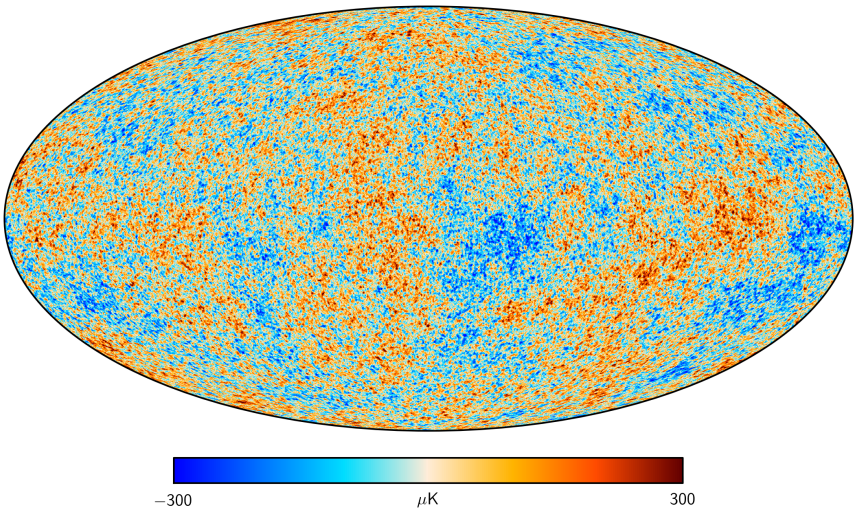

FIGURE 1.2: *This figure shows the inhomogeneities in the cosmic microwave background as seen by Planck. The statistics of these inhomogeneities are an invaluable tool for cosmology. Credit: ESA*

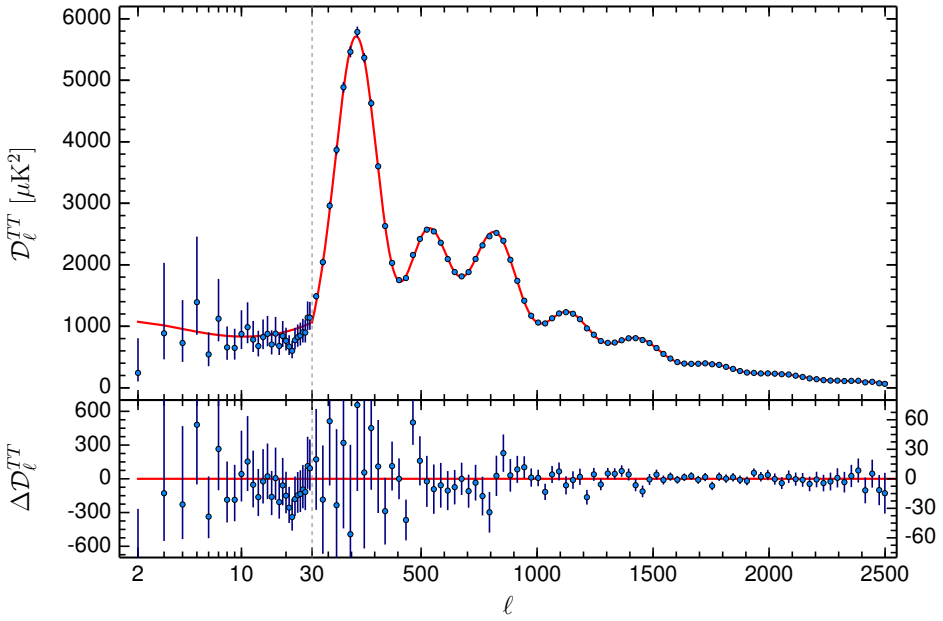

FIGURE 1.3: *This figure (taken from [8]) shows the temperature power spectrum data from the CMB observations of the Planck satellite. The best fit ΛCDM model is overlaid on the data and show a remarkable agreement between theory and experiment.*

All of these complementary observations conspire to constrain $\Omega_m \simeq 0.3$. We also have a very tight complementary constraint on the contribution of baryons, Ω_b, coming from big bang nucleosynthesis (BBN) that predicts very well the abundances of light elements in the Universe today [9]. The success of BBN requires $\Omega_b \simeq 0.05$ thus requiring a non-baryonic cold dark matter component of $\Omega_{\rm cdm} \simeq 0.25$.

Finally, there has been much work on understanding structure formation using N-body simulations of cold dark matter (e.g. [10, 11]). These studies have been very successful in reproducing the large scale structure we observe in the Universe and so further emphasise the need for a large dark matter component in the Universe.

1.1.2 Production

The combination of all this evidence demands a microscopic explanation of the origin of dark matter. There is an abundance of candidate explanations of the particle

physics models for dark matter but they all fall into two broad categories: thermal and non-thermal. The most common way to create a cosmological abundance of thermal dark matter is through what is known as the 'freeze-out' mechanism. In this mechanism all species including dark matter are in thermal equilibrium with approximately equal number densities in the early Universe. As the Universe expands, particles must interact with the cosmic fluid quickly enough to maintain this thermal equilibrium. The number density of massive particles in equilibrium will be Boltzmann suppressed, $n \propto \exp(-m/T)$, and will quickly decay at temperatures, T, below the particle mass m. If the particles are stable then they can only be destroyed by annihilation. If, however, the annihilation rate is less than the expansion rate of the Universe then the particles will be unable to find an annihilation partner and will fall out of equilibrium with the thermal bath. This process can produce a thermal relic that can play the role of dark matter. Dark matter particles produced in this way are known as Weakly Interacting Massive Particles (WIMPs).

The freeze-out dynamics is governed by the Boltzmann equation for the dark matter number density, n,

$$\frac{dn}{dt} + 3Hn = -\langle \sigma v_{rel} \rangle (n^2 - n_{\rm eq}^2), \tag{1.4}$$

where $n_{\rm eq}$ is the equilibrium number density, σ is the annihilation cross-section, v_{rel} is the relative velocity of the dark matter, and the angle brackets denote thermal averaging. In the non-relativistic limit, assuming a Maxwell-Boltzmann distribution for the dark matter at equilibrium we can solve this (e.g. [4]) to relate the relic density to the thermally averaged annihilation cross section via

$$\Omega_{\rm cdm} h^2 \simeq \frac{(1.07 \times 10^9 \text{ GeV}^{-1}) x_F}{\sqrt{g_\star} M_{\rm pl} \langle \sigma v_{rel} \rangle}, \tag{1.5}$$

where $h \simeq 0.7$ is the Hubble constant in units of 100 km s^{-1} Mpc^{-1}, T_F is the freeze-out temperature, $x_F = m/T_F$, $M_{\rm pl} = (8\pi G)^{-1/2}$ is the reduced Planck mass, and $g_\star$ is the effective number of relativistic degrees of freedom in thermal equilibrium at

T_F. The freeze-out temperature is solved for iteratively using

$$x_F = \log\left(\frac{m}{2\pi^3}\sqrt{\frac{45M_p^2}{2g_\star x_F}}\langle\sigma v_{rel}\rangle\right). \tag{1.6}$$

To understand what type of particles could give rise to a successful dark matter candidate we can approximate the solution as

$$\Omega_{\rm cdm}h^2 \simeq \frac{3\times 10^{-27}{\rm cm}^3{\rm s}^{-1}}{\langle\sigma v_{rel}\rangle}. \tag{1.7}$$

Therefore if there is a particle with $\langle\sigma v_{rel}\rangle \simeq 3\times 10^{-26}$ cm^{3}s^{-1} we can achieve the correct relic density for dark matter. For a particle that interacts via the weak interactions we have $\sigma \sim G_F^2 m^2$ and $v \sim c/3$ for particles that freeze-out with $x_F \sim 20$. If we plug in the numbers with $m \sim 100$ GeV we find $\sigma v_{rel} \simeq 3\times 10^{-26}$ cm^{3}s^{-1} which is remarkably exactly what we need. This coincidence, known as the 'WIMP miracle', has inspired a lot of research in the area of weak scale dark matter candidates. The estimate was of course very loose and there is plenty of room for manoeuvre with the dark matter mass and annihilation rate. The dependence of the comoving number density of dark matter on the thermally averaged cross section can be see in Fig. 1.4 where we see that increasing $\langle\sigma v_{rel}\rangle$ decreases the dark matter yield for freeze-out processes.

Perhaps the most popular example of a WIMP candidate uses the supersymmetric framework where the lightest supersymmetric particle plays the role of the dark matter [12]. In this case the R-parity symmetry which is required to prevent $B+L$ violation can also be used stabilise the dark matter. The simplest example of thermal freeze-out dark matter however is provided by SM singlets [13] that are stabilised by some new global symmetry. These models have recently grown in popularity under the name Higgs portal dark matter and we will present an example in Chapter 3 of this thesis.

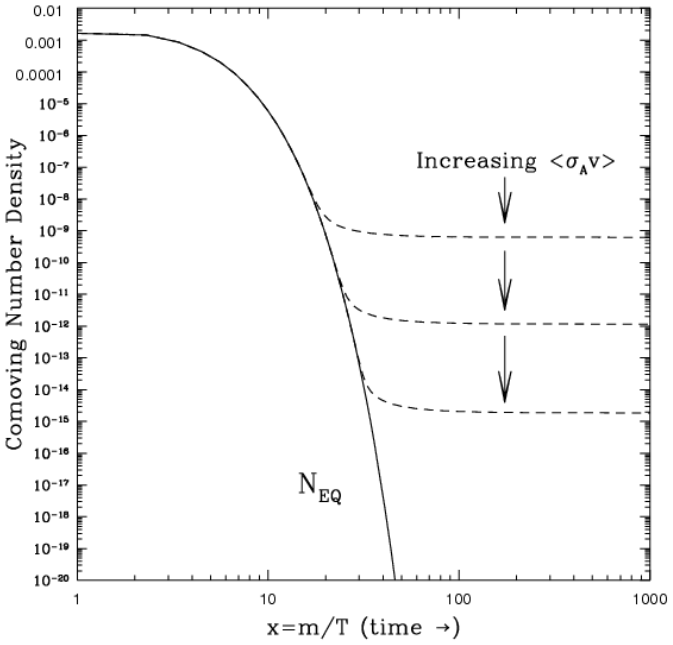

FIGURE 1.4: *This figure (taken from [14]) shows the dependence of the comoving number density of dark matter on the thermally averaged cross section for freeze-out. Large cross sections result in lower yields of dark matter.*

Another possible way to produce a dark matter relic is through 'freeze-*in*' [15]. In this case, the initial dark matter abundance is negligible and dark matter is produced by collisions and decays of the thermal bath. As T drops below the dark matter mass m this production becomes exponentially suppressed by a Boltzmann factor and the dark matter abundance freezes-in. Contrary to the freeze-out case we will therefore get larger dark matter abundances for larger interaction strengths with the thermal bath. The required interactions strengths are extremely weak so the particles are known as Feebly Interacting Massive Particles (FIMPs).

Dark matter can also be produced non-thermally. Non-thermal production occurs when dark matter is produced during phase transitions or by the decay of heavy unstable particles. One very popular realisation of non-thermal dark matter is the axion. Axions are the pseudo-Nambu-Goldstone bosons of a broken $U(1)$ symmetry and are theoretically motivated by their solution of the strong-CP problem. We will postpone further discussion of axions until Chapter 4 where we will present a new model that explains both the dark matter abundance and inflation.

1.2 Baryon asymmetry of the Universe

The most plausible initial condition for the Universe is a totally symmetric one. We would therefore expect that the Universe began with equal parts matter and anti-matter. There is no obvious mechanism by which the SM would prevent this symmetry from maintaining until today. In fact, we would expect matter and anti-matter to annihilate leaving only a tiny amount left when the annihilations freeze-out in the same way as dark matter giving rise to a Universe almost devoid of matter. The abundance of baryonic matter in the Universe today, of course, refutes this conclusion. Moreover, even if it were possible to retain large numbers of baryons and anti-baryons we would expect to see evidence of their annihilation today in a diffuse γ-ray background or at the very least at the boundaries of possible 'islands' of separated matter and anti-matter. Again this is counter to observations [16] suggesting that matter and anti-matter do not coexist in equal quantities today.

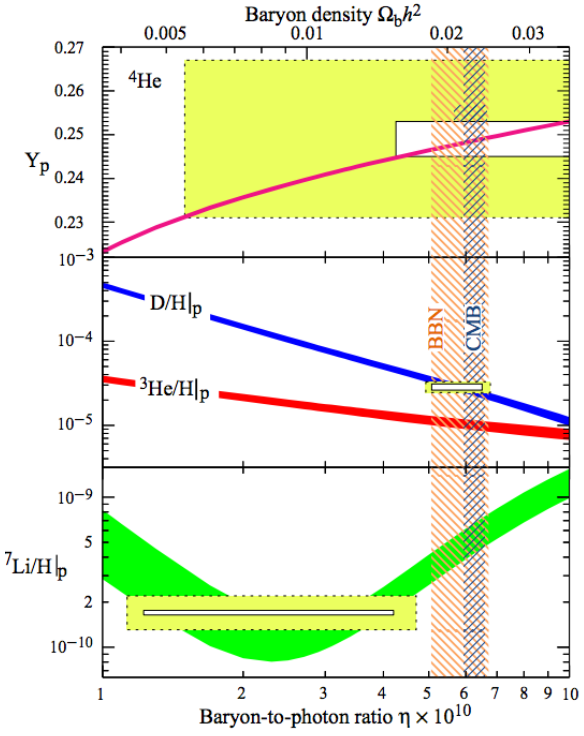

FIGURE 1.5: *This figure (from [17]) shows the abundance of light elements as function of the asymmetry parameter, η, that is predicted by BBN. There is good agreement between theory (solid curves) and the 95% confidence regions (boxes) over several orders of magnitude constraining η and hence Ω_b tightly.*

The strongest evidence for a baryon asymmetry however comes from cosmology. It is common to normalise the asymmetry with respect to the photon density to yield the asymmetry parameter,

$$\eta = \frac{n_b - n_{\bar{b}}}{n_\gamma}, \tag{1.8}$$

where n_i is the number density of species i. The quantity can be constrained directly using the power spectrum of the CMB and it is found that $\eta \simeq 6 \times 10^{-10}$ [8].

There is also a strong consistency check coming from BBN. The predicted abundances of light elements are very sensitive to the values of η and they agree with that expected from the CMB observations (with the exception of a slight discrepancy for Li^7 [18] as seen in Fig. 1.5) providing very strong evidence for a baryon asymmetry of the Universe (BAU).

This conflict between the observed BAU and the desire for symmetric initial conditions is a problem with the standard cosmology that must be resolved. Even if an initial asymmetry is conceded then it would be diluted away in an inflationary Universe. There must therefore be some dynamical mechanism for the creation of a small asymmetry. Such a mechanism is referred to as baryogenesis. The necessary conditions for a successful theory of baryogenesis were first written down almost 50 years ago by Sakharov [19]. The Sakharov conditions are

(i) baryon number (B) violation,

(ii) C and CP violation,

(iii) non-equilibrium dynamics.

Condition (i) is self-evident; without B violation we can never create a baryon excess. Condition (ii) is required because the rate of baryon production must exceed the rate of the conjugate process of baryon destruction in order to increase the net B. Finally, condition (iii) is required to ensure the process is not time reversible. This is necessary because the CPT theorem would otherwise guarantee that CP violating baryon creating processes would be exactly balanced by anti-baryon creating processes in thermal equilibrium because they are energetically equivalent.

There have been several different approaches to creating a theory to satisfy these conditions. The most popular theories are electroweak baryogenesis (EWBG) [20], leptogenesis [21], GUT (grand unified theory) baryogenesis [22], and Affleck-Dine baryogenesis [23]. In the first two cases the B violation comes from non-perturbative electroweak processes known as sphalerons. EWBG then uses the electroweak phase transition to facilitate the non-equilibrium dynamics. Leptogenesis on the other hand first creates a lepton asymmetry through the out-of-equilibrium decay of right handed neutrinos. This is later converted into a baryon asymmetry by the sphalerons. GUT baryogenesis relies on the fact that because quarks and leptons are combined into a single representation of the simple GUT group there will be B violating interactions mediated by the new gauge bosons of the GUT. The decay of these boson in the early Universe can then account for the baryon asymmetry. Affleck-Dine baryogenesis uses supersymmetric flat directions corresponding to a combination of fields with non-zero net B charge. During inflation these combination fields will get large expectation values. The supersymmetry breaking terms then give a small mass to these fields and when this mass is less than Hubble scale the field begins to oscillate and decay producing a baryon asymmetry.

Of all these options, EWBG is arguably the easiest to test because all the relevant physics is at the weak scale. We will see later that in order to make it successful it is necessary to modify the electroweak symmetry breaking of the SM. After the discovery of the Higgs we now have a promising avenue to probe this sector and possibly shed light on whether EWBG is a viable solution to generating the baryon asymmetry. In contrast, the key physics of other theories of baryogenesis lie well above the weak scale and so are difficult to test.

1.3 Inflation

In this section we will discuss another as yet unexplained aspect of cosmology: cosmic inflation. We will first introduce the problems that motivated the idea of an

inflationary Universe and then discuss the inflationary solution in both its original incarnation and the modern view.

1.3.1 Problems with hot big bang model

The standard picture of cosmology discussed in Sec. 1.1 presents some theoretical problems. Let us first consider the so called flatness problem. We saw earlier that cosmological observations find that $\Omega = \sum \Omega_i = 1$ to very good accuracy (i.e the spatial curvature is very well constrained with $|\Omega_K| < 0.005$ today [24] where $\Omega_K \equiv \Omega - 1$). This level of flatness does not necessarily seem to pose any problem until we consider how this number evolves in time. We can rearrange Eq. (1.3) to write

$$\frac{\rho_{\rm tot} - \rho_{\rm crit}}{\rho_{\rm tot}} = \Omega_K = \frac{k}{a^2 H^2} = \frac{k}{\dot{a}^2} \ . \tag{1.9}$$

In a radiation dominated Universe we have $a \sim t^{1/2}$ whereas in a matter dominated Universe we have $a \sim t^{2/3}$, which gives

$$|\Omega_K| \ \sim t \ \text{ or } \ \sim t^{2/3} \ . \tag{1.10}$$

We can see therefore that $\Omega_K = 0$ is an unstable solution. In order to ensure $\Omega_K < 0.005$ today ($t_0 \sim 10^{17}$ s) we need to tune $\Omega_K \lesssim 10^{-63}$ or 10^{-43} at the Planck time ($t_p \sim 10^{-43}$ s) for matter and radiation dominated Universes respectively (since in reality the Universe undergoes a period of radiation dominance followed by a matter dominance the true number is somewhere in between these two estimates). This clearly represents an extreme tuning of initial conditions.

Another problem, known as the horizon problem, has to do with the observation of a remarkably homogeneous Universe. The temperature of the CMB is homogeneous up to fluctuations $\delta T/T \sim 10^{-5}$. This suggests that the entire observable Universe must have been in causal contact in the past in order for it to reach thermal equilibrium.

The comoving particle horizon (the conformal time since the big bang),

$$h_p = \Delta\eta = \int_{t_i}^{t} \frac{dt'}{a(t')}, \tag{1.11}$$

is the maximum distance a photon could have travelled from a time t_i to t (where we take $t_i = t_p$ as the initial condition). For particles at the time of last scattering we have $h_p \sim 200$ Mpc. If we compare this to the scale of the Universe today ~ 14 Gpc we find that the CMB is composed of many different patches that were causally disconnected when it was formed. The horizon problem is then why do we observe such global uniformity on the CMB?

Finally, we have the monopole problem [25]. If we assume that SM gauge groups unify into a GUT at some high scale (as is suggested by the *almost*[2] unification of the SM gauge couplings) then when this GUT breaks in the early Universe we generically expect monopoles to be produced in abundance. These monopoles are extremely heavy and would overclose the Universe in contradiction to observation of an approximately flat Universe. There must therefore be some mechanism that prevents the production of magnetic monopoles or sufficiently reduces their energy density.

1.3.2 Solutions old and new

The horizon and flatness problems both depend critically on the history of the comoving Hubble radius $r_H = (aH)^{-1}$. From Eq. (1.9) we see that

$$\Omega_K = k\ r_H^2. \tag{1.12}$$

The comoving particle horizon can also be rewritten as,

$$h_p = \int_{t_i}^{t} \frac{dt'}{a(t')} = \int_{a_i}^{a} \frac{da'}{a'\dot{a}'} = \int_{\ln\ a_i}^{\ln\ a} r_H\ d\ \ln a. \tag{1.13}$$

[2]If the unification was precise we might in fact be a bit suspicious because we would naively expect there to be some important threshold effects near the GUT scale.

We can therefore see that if we have $\dot{r}_H < 0$ at sometime in the past then $|\Omega_K|$ would decrease, flattening the Universe and the integrand of h_p would also decrease such that patches of the Universe that were originally in causal contact would exit each others Hubble sphere. Therefore today h_p could be very large compared with r_H. From our perspective today, our expectation that $h_p \sim r_H$ (as is the case for a radiation/matter dominated Universe) would cause us to conclude that these patches were never in causal contact. This can be seen diagrammatically in Fig. 1.6, where we can see that a period of shrinking Hubble radius can result in causally connected patches appearing to be out of casual contact.

The condition needed then to solve these problems is therefore that

$$\dot{r}_H = \frac{d}{dt}\,\frac{1}{\dot{a}} = -\frac{\ddot{a}}{\dot{a}^2} < 0, \tag{1.14}$$

which is satisfied for $\ddot{a} > 0$ i.e. accelerated expansion of the Universe. This accelerated expansion would also solve the monopole problem by diluting away the monopoles produced in phase transitions.

The amount of inflation required to sufficiently solve the horizon problem is somewhat dependent on the realisation of inflation but we can estimate it by considering the ratio of comoving Hubble radius at the end of inflation to that today,

$$\frac{r_H^0}{r_H^e} = \frac{a_e H_e}{a_0 H_0} = \frac{a_0}{a_e}, \tag{1.15}$$

where in the last equality we have assumed $H \sim a^{-2}$ for a radiation dominated Universe. We also have that $a \sim T^{-1}$, and using $T_0 \simeq 3$ K $\simeq 10^{-2}$ eV, and assuming $T_E \sim 10^{15}$ GeV for the energy scale during inflation. Then,

$$\frac{a_0}{a_e} \simeq 10^{28} \simeq e^{64}. \tag{1.16}$$

We therefore need approximately 60 'e-folds' of inflation (at least) such that the largest scales we observe today were within the same horizon at the beginning of inflation.

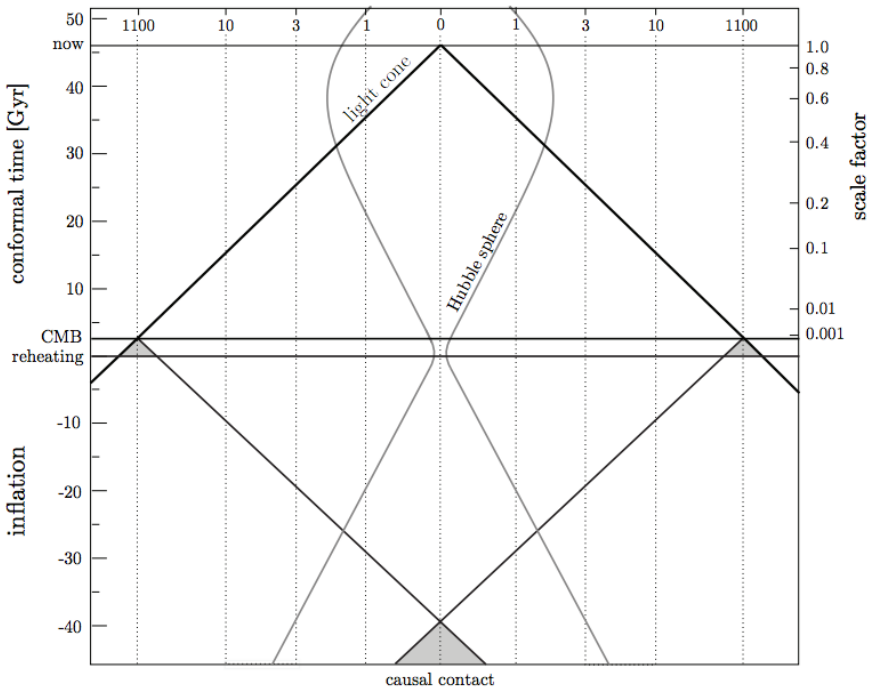

FIGURE 1.6: *This figure (taken from [26]) that two separated patches of the CMB appear to be causally disconnected but if there was a period of accelerated expansion such that the Hubble radius was shrinking then these patches could have been in causal contact at an earlier time.*

If we examine Eq. (1.3) we see that this accelerated expansion could be achieved with a large positive cosmological constant Λ. This must however be a transient effect so we cannot simply rely on a cosmological constant. Setting $\Lambda = 0$ in Eq. (1.3) we see that we need

$$w = \frac{p}{\rho} < -\frac{1}{3}. \tag{1.17}$$

This inflationary solution was first presented by Guth in 1980 [27]. He showed that if the Universe was supercooled many orders of magnitude below the temperature of some phase transition this effect could be achieved. The Universe becomes stuck in a false vacuum whose energy will play the role of a large cosmological constant. As the Universe tunnels from this false vacuum inflation will end. However, as was pointed out by Guth himself in the original paper, this theory (now known as old inflation) has a problem achieving a 'graceful exit'. As the Universe rapidly expands the nucleated bubbles of true vacuum do not expand quickly enough to coalesce and form a homogeneous and isotropic Universe.

Modern incarnations of inflation are mostly based on Linde's chaotic inflation model of a slowly rolling scalar field [28]. In such a scalar field theory we have

$$w = \frac{p}{\rho} = \frac{\frac{1}{2}\dot{\phi}^2 - V(\phi)}{\frac{1}{2}\dot{\phi}^2 + V(\phi)}. \tag{1.18}$$

If we can arrange that $V(\phi) \gg \frac{1}{2}\dot{\phi}^2$ then we will have $w \simeq -1$ and the Universe will inflate. That is, we need the potential energy to dominate over the kinetic energy, which can be arranged at large field values for a suitably flat potential. As ϕ rolls down the potential we will eventually reach a situation with $w > -1/3$ and inflation will end gracefully.

The conditions for successful slow roll can be summarised as

$$\epsilon = -\frac{\dot{H}}{H^2} = \frac{1}{2}M_{\rm pl}^2\left(\frac{V'}{V}\right)^2 < 1, \tag{1.19}$$

which guarantees $\ddot{a} > 0$, where we have neglected the $\ddot{\phi}$ terms. In order to ensure this approximation is valid we can introduce the second slow roll parameter

$$\eta = \frac{1}{H}\frac{\ddot{\phi}}{\dot{\phi}} = M_{\rm pl}^2\frac{V''}{V}, \tag{1.20}$$

and require $|\eta| \ll 1$.

Although inflation was invented to solve the various problems with the hot big bang model, perhaps its most attractive feature came as a side product. Quantum fluctuations of the inflaton field ϕ are stretched out by inflation and act as the seeds for structure formation in the Universe. The scalar and tensor perturbations will then be imprinted in the CMB. The spectrum of scalar perturbations has been measured many times, most recently to an impressive accuracy by the *Planck* satellite [1] and agree with the generic expectations of inflation. The observation of the tensor modes however would be a fantastic victory for inflation. A recent claimed measurement of tensor modes from inflation by the BICEP2 experiment [29] was therefore met with great excitement. Alas, the claim has since been withdrawn so we must wait a little longer.

While these measurements are important to test the theory of inflation they are also essential to discriminate between various microscopic models i.e. we can start to answer questions like

- can inflation be described by slow roll?
- what are the allowable forms for $V(\phi)$?
- is there only a single inflaton or multiple inflatons?

Although the *Planck* data has made some steps in selecting from the various models that can produce inflation, we are still a long way from pinning down what features the precise microscopic mechanism responsible for inflation needs.

1.4 The effective potential

In this section we will briefly introduce the quantum corrected effective potential. In particular we will discuss its renormalisation group improvement and generalisation to finite temperature, both of which will be relevant in the context of the Higgs field in the remainder of the thesis.

1.4.1 Renormalisation group improvement

The potential of classical field theory will receive quantum corrections that can play a large role at high energies. Thess corrections can have profound consequences, such as inducing spontaneous symmetry breaking [35]. In order to account for quantum effects we must replace the classical action with the quantum effective action, which, for a massless scalar field theory, can be expanded as

$$\Gamma = \sum_n \int d^4x_1 ... d^4x_n \Gamma^{(n)}(x_1, ..., x_n)\phi(x_1)...\phi(x_n), \tag{1.21}$$

where ϕ is a scalar field and $\Gamma^{(n)}$ is the sum of all one-particle-irreducible (1PI) Feynman diagrams with n external legs. If we expand in terms of the classical field ϕ we can write

$$\Gamma = \sum_n \int d^4x \left[-V(\phi) + \frac{1}{2} \left(\partial_\mu \phi\right)^2 Z(\phi) + ... \right]. \tag{1.22}$$

Here, $V(\phi)$, called the effective potential, is the sum of all 1PI Feynman diagrams with only scalar external legs. This potential therefore contains all quantum corrections and its minimum describes the vacuum state of the quantum theory. In practice we can only compute Feynman diagrams with a small number of quantum loops and higher order effects must be neglected. We therefore expand the effective potential as the sum of a contribution at each loop order [35],

$$V(\phi) = V_0 + V_1 + V_2 + ..., \tag{1.23}$$

where V_0 is the tree-level (no loops) contribution and is equivalent to the classical potential, V_1 is the 1-loop contribution etc. When computing these loop diagrams however we find that the result diverges at high energy. This of course cannot be physical because physical observables like the scattering cross-sections depend on this result and must be finite.

The solution to this problem is renormalisation. Renormalisation is a procedure to cancel these divergent parts of the integrals by introducing counter terms. To compute the counter terms we must first regularise the loop integrals e.g. by introducing a UV cut-off, and then chose the counter terms in order to cancel any would be divergent parts. This procedure redefines the *bare* couplings in terms of *renormalised* couplings. In [35] this procedure was applied to the theory of a massless scalar field and they found the renormalised 1-loop approximation to the effective potential

$$V = \frac{\lambda}{4!}\phi^4 + \frac{\lambda^2 \phi^4}{256\pi^2} \left(\ln \frac{\phi^2}{\mu^2} - \frac{25}{6} \right). \tag{1.24}$$

Here μ is an arbitrary mass scale that must be introduced to avoid a logarithmic

singularity in the effective potential. Since we have only computed the effective potential up to 1-loop we require both λ and $\ln\frac{\phi^2}{\mu^2}$ to remain small for our approximation to remain valid. Changing the renormalisation scale μ amounts to a redefinition of λ and rescaling of ϕ but the physics is unchanged. It was noted in [35] however that this inter-dependence of λ and μ can have profound implications. The requirement that the effective potential remain unchanged under these redefinitions can be written as

$$\left(\mu\frac{\partial}{\partial\mu}+\beta\frac{\partial}{\partial\lambda}+\gamma\phi\frac{\partial}{\partial\gamma}\right)V=0. \tag{1.25}$$

This can be solved to yield the so called renormalisation group equations (RGEs),

$$\frac{d\lambda}{d\ln\mu}=\beta(\lambda) \tag{1.26}$$

$$\frac{d\phi}{d\ln\mu}=-\gamma(\lambda)\phi \tag{1.27}$$

where the functions β and γ require computation of all Feynman diagrams at every loop order. If we however approximate these functions using a loop expansion as before then we can solve the RGEs to find a μ dependent solution for λ and ϕ. The key thing to note is that if we insert these μ dependent solutions into the effective potential then it will be valid as long as λ is small and the restriction on $\ln(\phi^2/\mu^2)$ is dropped. This is called RGE improvement of the effective potential and it is allows us to study the physics of the potential at high energies without perturbation theory breaking down. This will be important to us when we examine the Higgs potential in the next chapter.

If we have the effective potential up to L-loop order and we use the $(L+1)$-loop RGEs to resum the leading logs then we will have a potential that is accurate to the L^{th}-to-leading log terms. We have still performed a truncation however because we did not compute the effective potential to all loops. As well as missing some corrections to the potential we will not have removed all μ dependence from the potential that we have computed [36]).

1.4.2 Effective potential at finite temperature

So far we have been considering field theory in empty space. This is an appropriate approximation for many applications e.g. collider physics. In the early Universe however know that space contains matter and radiation. We must therefore consider a theory in which the quantum fields interact with a thermal bath of particles, i.e. finite temperature field theory. This will be of interest to us later in this thesis when we discuss the Electroweak phase transition and reheating after inflation.

In thermal field theory the key point is that computing quantum correlation functions should be replaced with taking thermal averages. An analogy between these procedures can be made apparent by comparing the correlation function of and operator $\mathcal{O}$ in quantum field theory at zero temperature,

$$\langle \mathcal{O} \rangle = \frac{\int \mathcal{D}\phi \; e^{i \int \mathcal{L}(t)} \mathcal{O}}{\int \mathcal{D}\phi \; e^{i \int \mathcal{L}(t)}}, \tag{1.28}$$

with the thermal average of an observable A in quantum statistical mechanics,

$$\langle A \rangle = \frac{\mathrm{Tr}\left[\rho(\beta) A\right]}{\mathrm{Tr}\left[\rho(\beta)\right]}, \tag{1.29}$$

where $\rho(\beta) = \exp(-\beta H)$ is density matrix for a system with Hamiltonian H and inverse temperature β. We see that for thermal theory the density matrix plays a directly analogous role to the time evolution operator.

An important implication of computing thermal averages by taking the trace over all the states is that states must have periodic boundary conditions in time due to the cyclicity of the trace. We can use this fact to recast thermal averages to as ordinary correlations function by taking a Wick rotation $t \to -i\tau$ to Euclidean space time with a finite and periodic time dimension $\tau \in [0, \beta]$,

$$\langle \mathcal{O} \rangle_\beta = \frac{\int \mathcal{D}\phi \; e^{-\int_0^\beta \mathcal{L}_E(\tau)} \mathcal{O}}{\int \mathcal{D}\phi \; e^{-\int_0^\beta \mathcal{L}_E(\tau)}}. \tag{1.30}$$

In Fourier space, integrals over the Euclidean time coordinate then reduce to a Fourier series of discrete modes known as Matsubara modes.

In analogy to zero temperature field theory we may use this formalism to construct a thermal effective action which is formally given by the Gibbs free energy functional $G[\phi, \beta] = -(1/\beta) \log Z[\beta, J] + \int J\phi$ where J is a external current source for an interacting theory and Z is the partition function. From this we can derive a finite temperature effective potential as before. We will see an example of this in Chapter 3 when we look at phase transition in the finite temperature effective potential of the Higgs.

1.5 Top-down or bottom-up? Minimality as a guiding principle

The shortcomings of our current best theories for particle physics and cosmology have been the inspiration for much theoretical investigation. The approach to tackling these problems can be generally split into two classes: top-down and bottom-up. Top-down models take the ambitious approach of trying to find a fundamental theory of the Universe. This approach can be guided by symmetry principles, elegance, and naturalness. Equipped with such a theory, we can then ask questions about what its phenomenology looks like.

The greatest of triumphs of this approach is undoubtedly Einstein's general relativity (GR). The apparent fine-tuning of the gravitational 'charge' (or mass) to equal the inertial mass in Newtonian gravity lead Einstein to the principle of equivalence and a radical reformulation of gravity in terms of the curvature of spacetime. The elegance of GR was soon bolstered by the successful prediction of the precession of Mercury's perihelion and bending of starlight by the Sun.

This success has inspired many after Einstein to seek a similarly elegant theory to provide a unified picture of everything. This has lead to great interest in the very

beautiful string/M-theory picture which provides both the most promising theory of quantum gravity and also reformulates all other forces and degrees of freedom in terms of the geometry and topology of a 10/11 dimensional spacetime. The main criticism of this approach however is that there exists an enormous number of possible vacua when the theory is reduced to 4 dimensions. This makes phenomenology very difficult.

One key feature of these theories is supersymmetry which was discovered separately and has more promising discovery potential. Supersymmetry can be formulated as a generalisation of the Poincaré algebra of spacetime to a super-algebra (or $\mathbb{Z}_2$ graded algebra). Not only does this seem like a natural extension but it is also able to avoid a 'no-go' theorem that seemed to prevent extensions to the symmetries of spacetime [30]. The real interest in supersymmetry from the perspective of particle physics however came from its provision of a solution to the aforementioned hierarchy problem. Simply put the hierarchy problem is that the mass of any fundamental scalar (e.g. the Higgs boson) is radiatively unstable. Quantum loop corrections result in $M_h \sim \Lambda_{\text{cut-off}}$ where $\Lambda_{\text{cut-off}}$ is the cut-off scale of the effective theory. We expect $\Lambda_{\text{cut-off}} \sim M_{\text{pl}}$ or $M_{\text{GUT}} \sim 10^{16}$ GeV but instead we know that M_h must be weak scale (~ 100 GeV). This hierarchy of scales seems to require a large degree of fine-tuning between the bare Higgs mass and the quantum corrections. Supersymmetry solves this in a very neat way because it predicts each boson will have a fermionic superpartner (and vica-versa). This means that the loop corrections will cancel at leading order leaving only a logarithmic dependence of the Higgs mass on the cut-off scale, rendering the theory natural. Supersymmetry is now perhaps the most popular extension of the SM and has been used to explain dark matter, baryogenesis, inflation, and many other phenomenon. Its original purpose of providing a solution to the hierarchy problem, however, requires supersymmetry to be found at or below the TeV scale. Some pressure has been applied in this regard by the non-observation of a signal of supersymmetry during Run 1 of the LHC (e.g a global fit in [31] suggests squark masses $\gtrsim 1.5$ TeV and gluino masses $\gtrsim 1$ TeV). The jury, however, is far from out on whether natural supersymmetry is still viable

and we can look forward to results of Run 2 of the LHC to shed some more light on this.

The other approach to explaining the shortcomings of our theories is then to build theories from the bottom-up where phenomenology is at the forefront and theoretical motivation comes second. This method for model building is much more tightly linked with experiment and is often easier to falsify because simpler models make more clear predictions. If such models are successful then it may be that they merely represent a subset of a more complete picture. A good example of this is the recent trend of producing simplified models to constrain at the LHC and later mapping these constraints onto your favourite top-down model (see e.g. [32, 33]).

In light of the lack of signals for supersymmetry and other top-down models we argue here that this shift towards a more bottom-up approach is a good one. While both approaches are of course worthwhile, in this thesis we prefer to leverage simple models to explain as many unexplained phenomena as possible. This provides a much more economical solution compared to models with many new degrees of freedom and can offer an informative starting point from which a fuller picture can be built. As an example, if supersymmetry fails in its motivating purpose of solving the hierarchy then a model for supersymmetric dark matter is perhaps less appealing than a simple one based on, say, gauge singlet dark matter. This minimal approach has also recently inspired a new idea for the hierarchy problem (which is a rare thing) by coupling the Higgs to an axion (see Chapter 4) which ensures a natural mass for the Higgs emerges from their interaction during inflation [34]. We take this as an encouraging sign for the use of minimality as a guiding principle for building particle physics models.

1.6 Thesis outline

This thesis is organised as follows:

- In chapter 2 we will discuss what role the recently discovered Higgs can play in an inflationary Universe. We will consider the consequences of the two possibilities: the Higgs is the inflaton, and the Higgs is not the inflaton. In the first case we will review the attempts at Higgs inflation and provide a new analysis of the Higgs inflating from a false vacuum that can appear in the effective potential. In the second case we will investigate the implications of the having the Higgs as a spectator during inflation. We will see that instability of the potential can have dramatic consequences for the fate of the Universe. This chapter is based on the published work [37, 38].

- In chapter 3 we will address the problems of baryogenesis and dark matter. We will describe a model based on electroweak baryogenesis and gauge singlet dark matter and see that both can be explained simultaneously in a minimal model. We will also discuss the phenomenological implications of this model in terms of modifications to Higgs physics and the search for dark matter. This chapter is based on the published work [39].

- In chapter 4 we will present a new model of axion physics that can successfully explain inflation, dark matter, and the strong-CP problem by adding a single complex field to the SM. This model contains a mechanism to suppress isocurvature perturbations of the axion field and so opens up a new region of the parameter space that was previously ruled out. This new window for axion phenomenology can be probed by several complimentary measurements and so offers exciting discovery potential in the near future. This chapter is based on the published work [40].

- Finally, in Chapter 5 we will present our conclusions.

Chapter 2

The Higgs and Inflation

2.1 Introduction

The discovery of the Higgs boson of the Standard Model (SM) has rightly been heralded as one of the most significant scientific discoveries of recent years [2, 3]. At present there is no evidence to suggest that the particle is anything other than a fundamental scalar field [41, 42] and there is not yet any evidence for the existence of particles beyond the SM of particle physics (see e.g. [43]). This monumental discovery therefore presents perhaps our most promising new avenue for phenomenology. The Higgs is an invaluable tool for exploring theories beyond the SM of particle physics and cosmology.

As discussed in chapter 1 inflationary cosmology is one such theory that, while accepted as a general consensus, has yet to be fully understood at the microscopic level. Theories of inflation almost always rely on scalar fields and, having just found the first example of a fundamental scalar field, it is a perfect time to test the implications of the Higgs discovery on inflation. This will be the topic of this chapter. We will first introduce the Higgs potential and its quantum corrections which will be of central importance to the rest of the chapter. In the remainder of the chapter we will consider in turn the implications of the two possible scenarios:

(i) the Higgs is the inflaton, (ii) the Higgs is not the inflaton. We will see that both cases have important implications for particle physics.

2.1.1 The Higgs potential and its quantum corrections

The role of the Higgs field is to spontaneously breaking the $SU(2)_L \times U(1)_Y$ electroweak symmetry of the SM down the $U(1)_{\rm em}$ of electromagnetism. This is achieved using the potential,

$$V = -\mu^2 H^\dagger H + \lambda (H^\dagger H)^2, \tag{2.1}$$

with $\mu^2,\ \lambda > 0$, which can be rewritten in the unitary gauge, with $H = \frac{1}{\sqrt{2}}(0, h)^T$ and $v = \sqrt{\mu^2/2\lambda}$, as

$$V = \frac{1}{4}\lambda \left(h^2 - v^2\right)^2, \tag{2.2}$$

where the extra constant can be absorbed into the cosmological constant. This potential is of course minimised for $h = v$ and the symmetry is broken. But this potential is only part of the story. The preceding description is entirely classical and will be modified by quantum effects. As we discussed in Sec. 1.4.1 the quantum corrected effective potential is the important object in quantum field theories. In the case of the Higgs, the effective potential can have important physical consequences.

To illustrate there importance let's consider a theory with just the Higgs and the top quark (the top contributes most to the quantum corrections of the Higgs in the SM) and apply the reproduce the machinery introduced in Sec. 1.4.1. At 1-loop order after renormalising to remove the infinities we find that λ gets an additional contribution $\sim (4\pi)^{-2} y_t^4 \log(h/\mu)$ where y_t is the Higgs-top Yukawa coupling.

We can also account for the running of the couplings with energy using renormalisation group equations (RGEs) of the theory. In the case of our toy theory the 1-loop beta functions are given by,

$$\beta_\lambda = \frac{d\lambda}{d\log\mu} = \frac{1}{(4\pi)^2}\left(-6y_t^4 + 12 y_t^2 \lambda + 24\lambda^2\right), \tag{2.3}$$

$$\beta_{y_t} = \frac{dy_t}{d\log\mu} = \frac{1}{(4\pi)^2}\left(\frac{9}{2}y_t^3\right). \tag{2.4}$$

We can solve the RGEs to find the couplings as a function of renormalisation scale e.g. $\lambda = \lambda(\mu)$, and plug these back into the effective potential. We can see from these equations that the large negative contribution y_t to the running of λ could potentially cause λ to become negative at high energies which, as we will see, could have interesting physical implications.

In this chapter we are concerned with inflationary cosmology which occurs at very high energies in the very early Universe. We therefore will need to describe the behaviour of the Higgs potential up to very large scales (e.g. the Planck mass $M_{\rm pl} = 2.435 \times 10^{18}$ GeV). In this case the quantum effects described above are expected to play an important role. In what follows we will use the state of the art calculation of the effective potential to NNLO (2 loop effective potential improved with 3 loop RGEs) from [44, 45]. We will also follow these works and package all the additional contributions to the effective potential into a redefinition of λ to $\lambda_{\rm eff}$. So we have,

$$V_{\rm eff}(h) = \frac{1}{4}\lambda_{\rm eff}(h)h^4, \tag{2.5}$$

where we have made the convenient choice $\mu = h$ so the running is contained in the h dependence of $\lambda_{\rm eff}$ and because we are concerned with large field behaviour ($h \gg v$) we have dropped the v contribution.

2.2 The Higgs as the inflaton

As we have already mentioned, the Higgs may be the first fundamental scalar we have detected. Inflationary cosmology requires a hypothetical fundamental scalar called the inflaton. It is therefore natural to ask whether the Higgs can be the field responsible for two key epochs in particle cosmology: electroweak symmetry breaking and inflation. Such a theory would be attractive both for its minimality and for the possibility to learn about Planck scale physics by studying the Higgs at the electroweak scale.

A naive first response would be that it is impossible because we know that for $V(\phi) \simeq \frac{1}{4}\lambda\phi^4$ the measured spectrum of perturbations requires[1] the quartic coupling $\lambda \simeq 10^{-13}$ whereas the measured Higgs mass requires $\lambda \sim 0.13$. This is of course too simplistic because as we have just seen the bare tree-level potential can receive large quantum corrections. The hope is therefore that when we study the quantum corrections in detail we might find a potential that has the correct low energy behaviour to break electroweak symmetry and give rise to a Higgs boson of mass $M_h \simeq 125$ GeV while at the same time have the correct shape at high field values to allow for slow roll inflation and generate the perturbations observed in the CMB.

In this section we will first review previous attempts to build a theory of Higgs inflation that uses a non-minimal coupling to gravity. We will then examine the effect of the quantum corrections and see that when properly considered they give some hint that the quantum corrected potential might yield successful inflation.

2.2.1 Higgs inflation with a non-minimal coupling

The idea that the SM Higgs could play the role of the inflaton is not new. It has been a popular idea since a working model was first introduced in [46, 47]. In this model the problem with the size of λ is overcome by introducing a non-minimal coupling, ξ, between the Higgs and gravity,

$$\mathcal{L} = \mathcal{L}_{SM} - \frac{M^2}{2}R - \xi R H^\dagger H, \tag{2.6}$$

where M is a mass parameter, and R is the scalar curvature. If we consider only the Higgs we therefore have the action in the Jordan frame as

$$S_J = \int d^4x\sqrt{-g}\left[-\left(\frac{M^2+\xi h^2}{2}\right)R + \frac{1}{2}\partial_\mu h \partial^\mu h - V(h)\right]. \tag{2.7}$$

[1]This requirement is to fit the perturbations for $N = 60$ e-folds before the end of inflation. This model is also excluded by *Planck*'s $n_S - r$ plane constraints [1], where n_S is the spectral index and r is the tensor-to-scalar ratio

We therefore see that as long as $\sqrt{\xi} \ll 10^{17}$ then M is just equal to $M_{\rm pl}$ to good approximation (we will take this approximation in what follows). We can now make a conformal transformation to the Einstein frame defined by

$$\hat{g}_{\mu\nu} = \Omega^2 g_{\mu\nu}, \qquad \Omega^2 = 1 + \frac{\xi h^2}{M_{\rm pl}^2}. \tag{2.8}$$

In order to have canonical kinetic terms we then make a redefinition of the Higgs field using

$$\frac{d\sigma}{dh} = \frac{\sqrt{\Omega^2 + 6\xi^2 h^2/M_{\rm pl}^2}}{\Omega^2}. \tag{2.9}$$

This results in an Einstein frame action given by

$$S_E = \int d^4x \sqrt{-\hat{g}} \left[-\frac{1}{2} M_{pl}^2 \hat{R} + \frac{1}{2} \partial_\mu \sigma \partial^\mu \sigma - U(\sigma) \right], \tag{2.10}$$

where

$$U(\sigma) = \frac{V(h(\sigma))}{\Omega^4} = \frac{\frac{1}{4}\lambda \left(h(\sigma)^2 - v^2\right)^2}{\left(1 + \xi h(\sigma)^2/M_{\rm pl}^2\right)^2}. \tag{2.11}$$

Examining this potential we see that it will be a negligible modification to the usual Higgs potential for $h \ll M_{\rm pl}/\sqrt{\xi}$. On the other hand, for $h \gtrsim M_{\rm pl}/\sqrt{\xi}$ the potential will start to significantly flatten out (see Fig. 2.1). This allows for viable slow-roll inflation with the Higgs boson. In order to reproduce the correct amplitude for the scalar perturbations on the CMB however ξ must be quite large ($\sim 10^4$). It is important to note that we are using inflationary observables computed in the Einstein frame directly and not transforming them back to the Jordan frame. This is justified because we are interested in physics at late times when h^2 is small compared to $\xi/M_{\rm pl^2}$ so $\Omega \to 1$ and the Jordan and Einstein frames are identical.

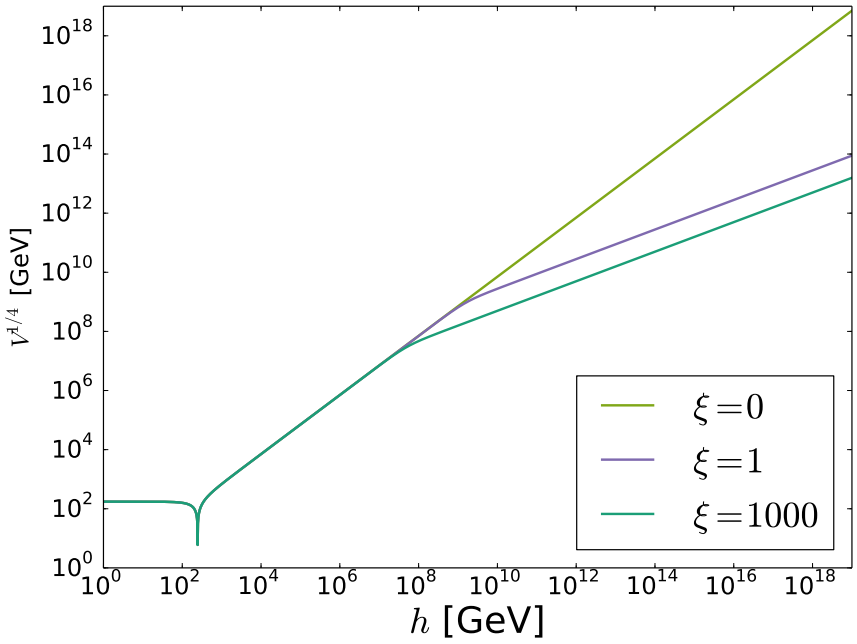

FIGURE 2.1: *This figure shows the effect of introducing an non-minimal coupling on the tree-level Higgs potential. Large values of ξ cause the potential to flatten out at high field values opening up the possibility of the Higgs playing the role of the inflaton.*

Although this model has been quite popular in recent years [48–59] it does have a problem. It has been much discussed in the literature [60–65] that the theory must have a cut-off imposed by perturbative unitarity of,

$$\Lambda \simeq \frac{M_{\rm pl}}{\xi}. \tag{2.12}$$

For large values of ξ graviton mediated Higgs-Higgs scatterings can saturate the unitarity bound for the partial wave amplitudes much below the Planck scale[2]. This is problematic because during inflation we are working at energies very close to this cut-off and we might worry that our calculations are no longer valid. The relevant scale to compare with the bound (2.12) is the Hubble scale during inflation. This is approximately given by,

$$H \simeq \sqrt{\lambda}\frac{M_{\rm pl}}{\xi}, \tag{2.13}$$

[2]Note that this problem only arises when, in the unitary gauge, the longitudinal gauge boson fields are included (or, equivalently, the Goldstone modes in the covariant gauge) [62–64].

so we see that it is comparable with (2.12) for $\lambda \sim 0.13$ of SM Higgs. It has however been pointed out in [55, 66] that the cut-off is background dependent. If we include the effect of the background Higgs field the cut-off derived for graviton-Higgs interactions will be modified to,

$$\Lambda \simeq \frac{M_{\rm pl}^2 + (1+6\xi)\,\xi\langle h\rangle^2}{\xi\sqrt{M_{\rm pl}^2 + \xi\langle h\rangle^2}}. \tag{2.14}$$

Note that $\langle h\rangle$ will be very large ($\sim M_{\rm pl}$) during inflation so the bound will be significantly higher and we may therefore trust the result of the inflationary calculation. We can also see that in the limit $\langle h\rangle \to 0$ the previous cut-off is recovered.

There is, however, still a need to cure this unitarity violation in the Universe today and therefore either new physics must appear or perhaps perturbation theory breaks down as we enter the strong coupling regime. There has been some work to build a unitary Higgs inflation model (see e.g. [67, 68]). It was argued in [65] however that since the mechanism that cures the apparent unitarity violation must enter at the same scale that inflation is taking place then it will likely take part in the inflationary dynamics and modify the predictions (see for example [67] where new terms are included to make the theory unitary and the predicted value of n_s is modified). From the model building perspective the need to introduce these extra ingredients makes this solution to inflation less minimal and somewhat reduces its appeal.

The problem of having a large ξ therefore still lingers in Higgs inflation with a non-minimal coupling. In the remainder of this section we will try to circumvent these issues by investigating Higgs inflation scenarios with $\xi = 0$[3].

For completeness we also note that the above picture has generalisations [55] and alternatives [69, 70]. For example it has also been shown [69] that non-minimal derivative couplings to gravity can give successful Higgs inflation and makes different

[3]We will see in the next section that it may not be possible to simply neglect the effects of ξ by setting it to zero at tree-level because it is expected to be generated by radiative corrections.

predictions for inflationary observables (notably r can be as large as 0.3 compared to $r \simeq 0.003$ for regular Higgs inflation) [71].

2.2.2 Higgs plateau inflation

We have seen that the tree-level Higgs potential needs to be modified in order for the Higgs to play the role of the inflaton. We have just discussed one such modification that introduced a direct coupling between the Higgs and gravity but which was not without problems. We now instead investigate whether replacing the classical Higgs potential with the effective potential of the quantum theory can give successful inflation.

The effect of quantum corrections was discussed in Sec. 2.1.1. Properly considered, these effects can lead to substantial modifications to the tree-level potential and a significant scale dependence of λ. In [44, 45] a state of the art 3-loop RGE improved 2-loop effective potential for the SM Higgs was presented and discussed. This calculation showed that, within the current experimental errors on the Higgs and top masses and ignoring possible contributions of new physics, we appear to be living in a very special Universe. The first result of interest is that the running of the Higgs quartic coupling λ is such that it appears to become negative at $\mu \sim 10^{10}$ GeV. If this is so then the electroweak vacuum is no longer the true vacuum. Instead we have the possibility of tunnelling to a vacuum with large negative energy density at $h \gg 10^{10}$ GeV. If such a vacuum exists and the tunnelling time is less than or of the order of the age of the Universe then our vacuum is unstable and should have decayed by now. Instead if the decay time is much longer that the current age of the Universe then we may have survived until now in this meta-stable Universe (whether or not this is true in an inflationary Universe is the subject of the next section).

The story gets even more interesting however when we use experimental constraints to investigate whether the Universe is unstable or meta-stable. The two most important parameters in determining the shape of the effective potential are the values of λ and the top Yukawa, y_t, at the electroweak scale. These can be constrained

experimentally by measuring the Higgs and top masses respectively. The resulting "phase diagram" for the SM is shown in Fig. 2.2 (from [44]) where we can see that the current experimental data places the electroweak vacuum at the boundary between stable and meta-stable.

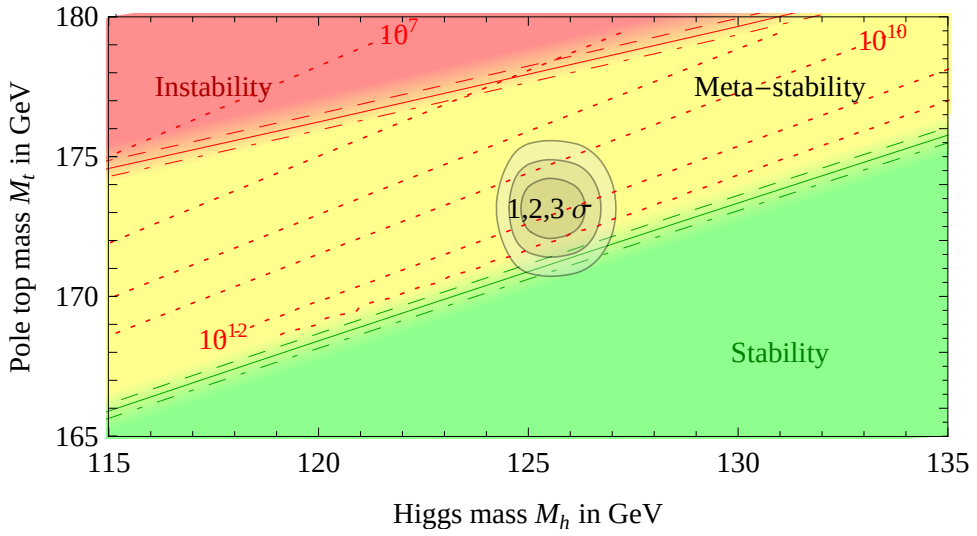

FIGURE 2.2: *This figure (from [44]) shows the phase diagram of the SM in the M_h-M_t plane. The experimental measurements at 1, 2, and 3 sigma are included and reveal that our Universe appears to be quite close (within experimental errors) to the boundary between stable and meta-stable. The dotted lines indicate the scale at which $\lambda_{eff} = 0$.*

The appearance of instability/meta-stability boundary offers an opportunity for further investigation and has been much discussed in the literature [44, 45, 72–76]. It is remarkable that we find ourselves so close to this boundary. This is a result of the peculiar fact that both λ_h and β_{λ_h} can vanish at the same scale, which is a highly non-trivial result. It should of course be noted that any new physics above the electroweak scale (even Planck suppressed operators [77]) could significantly change this story. What is interesting however is that if we ignore these extra contributions we get such an interesting criticality. If, with more precise experimental measurement, we move closer to the critical boundary we might begin to suspect that all additional contributions really are zero and that there is some symmetry principle or perhaps anthropic reasoning that could be applied to understand the origin of the criticality.

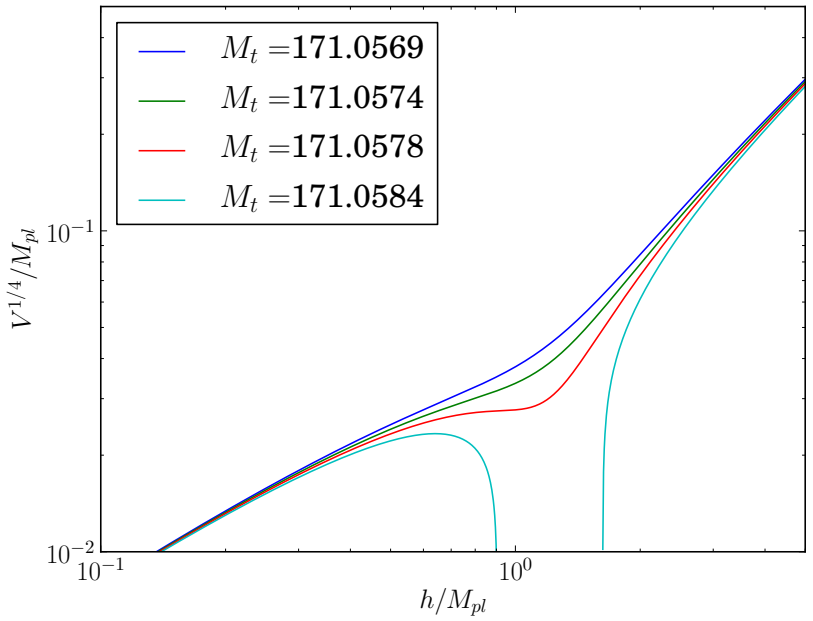

FIGURE 2.3: *The figure shows the effective potential for $M_h = 125$ GeV. The top mass is tuned in order to show the appearance of a plateau or an instability. The four curves plotted differ by 0.5 MeV in M_t.*

Here we will, for a moment, take this near-criticality seriously and attempt to use it to explain inflation. The appearance of criticality could then be explained by its necessity to inflate the Universe and make it habitable [78]. If we examine the effective potential very near the critical boundary we find the development of a plateau. Such a plateau could lead to slow roll inflation [73] and, remarkably, it appears at approximately the correct scale to generate the observed perturbations. In Fig. 2.3 we can see the effect of tuning the top mass on the effective potential. The figure shows that tuning on the order of $0.1 - 1$ MeV can interpolate between a stable and meta-stable vacuum. At the boundary of this transition we see the appearance of a plateau.

In order to test the suitability of this scenario for inflation we can initialise the field above the plateau and let it roll down the potential and calculate the number of e-folds of inflation that take place. The field, h, will evolve according to the field equations,

$$\ddot{h} + 3H\dot{h} = \frac{dV_{\text{eff}}}{dh}, \tag{2.15}$$

with

$$H = \frac{1}{M_{pl}}\sqrt{\frac{\rho}{3}} \qquad \text{and} \qquad \rho = \frac{1}{2}\dot{h}^2 + V_{\text{eff}}, \tag{2.16}$$

where V_{eff} is given by Eq. (2.5). The total number of e-folds is then given by,

$$N_{tot} = \int H dt, \tag{2.17}$$

where the integral is taken over the duration of inflation.

The result is shown in Fig. 2.4. We see that in order to get the required number of e-folds (50-60) to solve the horizon and flatness problems we need $M_h \gtrsim 129$ GeV which is inconsistent with the value observed at the LHC. It is possible to try to relieve this constraint by, say, introducing another scalar that mixes with the Higgs such that our input λ is smaller for the same M_h. This will delay the appearance of a plateau and push it to higher scales, allowing more e-folds for lower M_h values. This does not resolve the matter, however, because in both cases the inflationary scale is too high to fit the amplitude of the scalar perturbations.

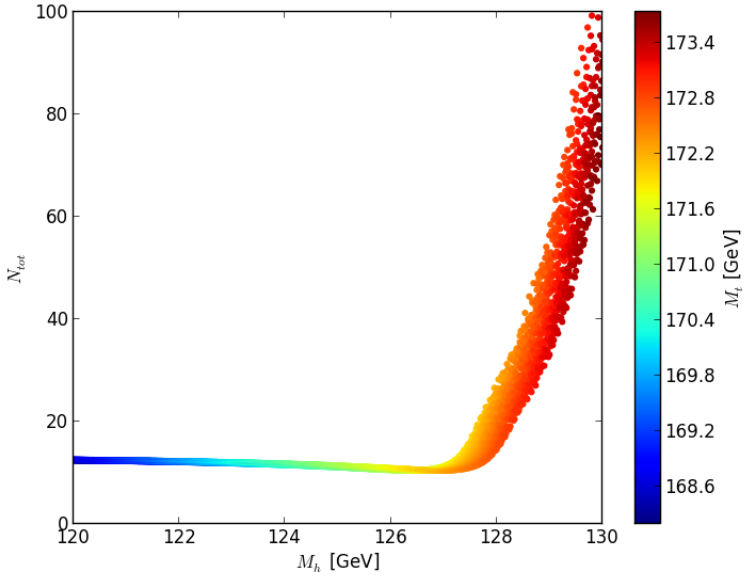

FIGURE 2.4: *This figure shows the total number of e-folds of inflation caused by a Higgs rolling from rest at 10 M_{pl}. The thickness in the band is set by the $\pm 1\sigma$ error on $\alpha_s(M_Z)$ and the color bar indicates the value of M_t required for a plateau. For smaller M_h the plateau is shorter and occurs at a lower scale and so has only a very small effect on the rolling of the field. For larger M_h the plateau is significant enough to cause an extended period of slow roll.*

The power spectrum of scalar perturbations can be written as,

$$\mathcal{P}(k) = A_s \left(\frac{k}{k_*}\right)^{n_s - 1}, \tag{2.18}$$

where n_s is called the scalar spectral index, k_* is a reference scale known and the pivot scale, and we have ignored possible k dependence of n_s. In the slow-roll regime the amplitude, A_s, is given by

$$A_s = \frac{V_*}{24\pi^2 \epsilon M_{pl}^4} \simeq 2 \times 10^{-9}, \tag{2.19}$$

where V_* is the value of the potential $N_* = 50 - 60$ e-folds before the end of inflation. For slow-roll $\epsilon_{\max} = 1$ so we can put an upper bound on the inflationary scale of

$$\max\left(\frac{V_*^{1/4}}{M_{pl}}\right) \sim 2.5 \times 10^{-2}. \tag{2.20}$$

We find that whenever enough e-folds are generated by a plateau this upper bound is exceeded. In Fig. 2.4 we see that 60 e-folds requires $M_h \sim 129$ GeV which results in a plateau forming at $\left(\frac{V_*^{1/4}}{M_{pl}}\right) \sim 3 \times 10^{-2}$ so we see that even $\epsilon = 1$ we will not be able to fit Eq. 2.19. We could try a similar game by adding in extra fermionic degrees of freedom, *e.g.* right-handed neutrinos. Again this does not work because, to a good approximation, this is equivalent to increasing the value of the top quark Yukawa (ignoring QCD running of course), or, equivalently, increasing the effective top mass of the SM. Note however that the occurrence of the plateau in the Higgs potential fixes a linear relationship between the Higgs mass and the top mass (see Fig. 2.2). Introducing new fermions therefore only gives us some freedom on the Higgs or top mass inputs but cannot change the shape of the potential significantly enough to allow for successful inflation.

It is also possible to consider very careful choices of initial conditions such that a large number of e-folds could be generated by the field rolling very slowly passed the inflection point. This was addressed in the slow roll regime in [79] and it was found that simultaneously achieving enough e-folds of inflation and generating scalar

perturbations with the observed amplitude is impossible. Finally, you could imagine repeating the above calculation and allowing for a shallow potential well instead of a plateau to slow the Higgs as it rolls past, producing more e-folds. We found however that in order to avoid being trapped in the minimum by Hubble friction, the Higgs can only be slowed by a tiny amount. We found that this impacted the e-folds less than varying $\alpha_s(M_Z)$ by 1σ. We must therefore abandon the plateau in the Higgs potential as a candidate for inflation.

2.2.3 False vacuum inflation

Although successful inflation cannot be achieved in the simple case of the Higgs plateau it may still be possible that the Higgs may be connected to inflation in a slightly less minimal way. To see this we can imagine starting with the plateau situation and increasing the top mass by a few$\times 0.1$ MeV. In this way we can create a false vacuum with large positive energy density that can be used to inflate the universe [80–82].

This is then the scenario of old inflation [83] and we are therefore burdened with the graceful exit problem. The necessity for this exit strategy is what makes false vacuum inflation slightly less minimal than the Higgs plateau approach. One possible solution [80] is to extend general relativity to a scalar-tensor theory. This allows the expansion rate of the universe with a constant inflaton energy density to decrease with time, eventually becoming slow enough to allow successful exit through tunnelling. Here we revisit an alternative solution, proposed in [81], that introduces an extra scalar whose dynamics during inflation slowly lifts the Universe out of the false vacuum such that it can roll classically down to the true vacuum. At this point the reader may worry that if we are introducing an extra scalar why we are not just letting that extra scalar to be the inflaton with, say, a quadratic potential. While this is a reasonable position to take, it ignores the peculiar possibility of the false vacuum in the Higgs potential that results from being so close to the critical boundary discussed in the previous section. We also expect that the Higgs will be

coupled to any additional scalars (e.g. the scalar responsible for Peccei-Quinn symmetry breaking) that appear above the electroweak scale through the Higgs portal coupling regardless of whether these scalars can achieve inflation on their own. We therefore consider the approach that the Higgs is responsible for inflation and the additional scalar merely facilitates the graceful exit.

Our calculation improved upon a previous treatment in [81] by using the state-of-the-art expression for V_{eff} [44, 45], including the 1-loop RGE's for the new scalar field and its threshold effect at the matching scale. Also, we account for the movement of the Higgs during inflation and further address a degeneracy in the initial depth of the false vacuum. We will see that these improvements can dramatically affect the conclusions.

The mechanism will require the additional scalar to obtain a vev so that, through its interaction with the Higgs, it can modify the effective mass of the Higgs. The tree-level potential in the unitary gauge is then given by,

$$V(h,s) = \frac{1}{4}\lambda_s\left(s^2 - w^2\right)^2 + \frac{1}{4}\lambda_h\left(h^2 - v^2\right)^2 + \frac{1}{4}\lambda_{hs}\left(s^2 - w^2\right)\left(h^2 - v^2\right), \quad (2.21)$$

where s is the real part of a possibly complex SM singlet scalar field and respects a global $\mathbb{Z}_2$ (real field) or $U(1)$ (complex field) symmetry and (v, w) is the global minimum of the potential. The tree-level Higgs quartic coupling is now denoted by λ_h. Such a complex field, S, arises in the context of invisible axion models, where the symmetry is identified with the $U(1)$ of Peccei and Quinn that solves the strong CP problem (we will discuss this further in chapter 4).

During inflation the s field will roll towards its minimum $\langle s \rangle$ and the mixing term between h and s will grow and lift the false vacuum as shown in Fig 2.5. The end of inflation is taken as the value of s, denoted s_{end}, for which the false minimum disappears. In reality, tunnelling will become highly probable when the well depth is sufficiently small (when $\Gamma_{\text{tunnel}} \gg H$) causing inflation to end slightly earlier. Additionally the subsequent free rolling of the field down to the global minimum can still produce some inflation. Both of these effects however are small and change the

calculation by a negligible number of e-folds [81] which will not alter our conclusions and so we neglect these contributions.

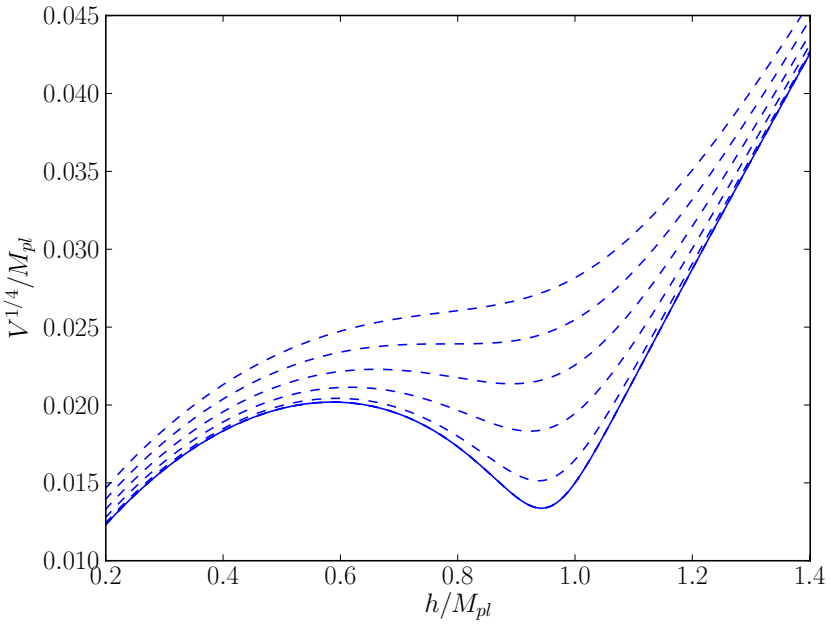

FIGURE 2.5: *This plot shows the effect of the mixing between the singlet, s, and the Higgs, h, on the Higgs contribution to V as s rolls towards its minimum. The solid line is for $s = 0$ and the dashed lines are the result of increasing s. The singlet field manages to successfully remove the false vacuum allowing the Higgs to roll down to the true vacuum.*

We therefore have a setup similar to hybrid potential [84] in which the rolling of s triggers the waterfall field h but in this case the false vacuum is created purely by quantum effects.

It is possible to treat this as a quasi-single field model for s because h is trapped in the false minimum throughout inflation. The renormalized potential can then be written as a function of s

$$V_s = \frac{1}{4}\lambda_s \left(s^2 - \langle s\rangle^2\right)^2 + \frac{1}{4}\left(\lambda_{\text{eff}} - \frac{\lambda_{hs}^2}{4\lambda_s}\right)\left(h_0^2 - v^2\right)^2 , \tag{2.22}$$

with

$$\langle s\rangle = \frac{1}{\sqrt{2\lambda_s}}\sqrt{M_s^2 + \lambda_{hs}(v^2 - h_0^2)} \ , \tag{2.23}$$

where M_s is the mass of the new scalar. Note that h_0 is the vev in the false vacuum and is not equal to v, the vev in the electroweak vacuum. After inflation ends and h rolls to the global minimum $\langle s \rangle$ relaxes to its ground state value given by

$$w = \langle s \rangle|_{h_0=v} = \frac{M_s}{\sqrt{2\lambda_s}}. \tag{2.24}$$

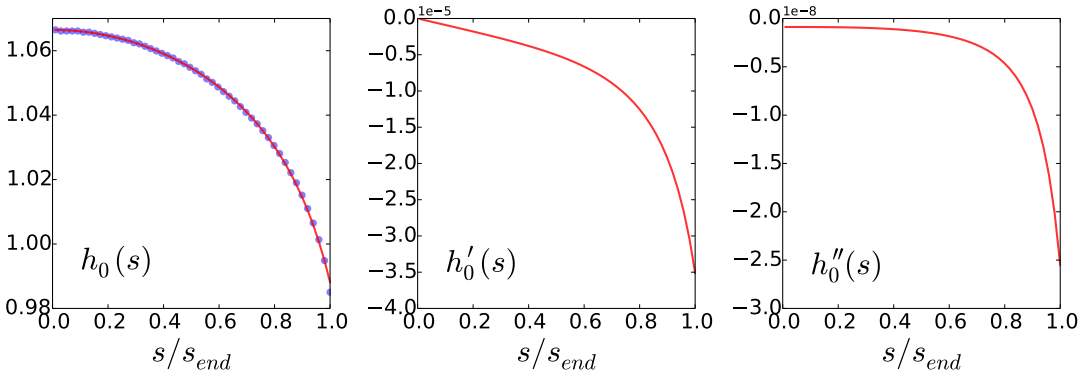

FIGURE 2.6: *This plot shows an example of the fit performed for movement of h as a function of s during inflation. The first and second derivative of this function that are needed for slow roll calculations are also included. The y-axes are in Planck units.*

The position, h_0, of the false vacuum will in fact change slightly during inflation as can be seen in Fig. 2.5. In order to take this into account while still working in the single field regime we treat the motion of h_0 as a function of s. To compute this function we record the position of both h_0 and s during inflation and preform a polynomial fit to this data. A typical example of this procedure is shown in Fig. 2.6. This allows smooth derivatives to be computed and used in the slow roll calculations.

The total number of e-folds is then calculated using

$$N = \frac{1}{M_{pl}} \int_{s=0}^{s_{\rm end}} \frac{ds}{\sqrt{2\epsilon}} \,, \tag{2.25}$$

with

$$\epsilon = \frac{M_{pl}^2}{2} \left(\frac{V_s'}{V_s} \right)^2 , \tag{2.26}$$

and

$$V_s' = \lambda_s s(s^2 - \langle s \rangle^2) + h_0'(s) \left(\lambda_{hs} h \left(s^2 - \frac{1}{2} \langle s \rangle^2 \right) + \lambda_{\rm eff} h^3 \right). \tag{2.27}$$

The amplitude of the scalar perturbations are then calculated $N_* = 50 - 60$ e-folds before the end of inflation using equation (2.19).

Before we can proceed however we must consider the effect that the presence of a new scalar will have on the effective potential of the Higgs. Since there is a mixing between the scalar and the Higgs, the low energy Higgs parameters will be modified. Quantum corrections involving new scalar loops will also modify the RGEs relative to the SM. Firstly, when the mass of the extra scalar is much larger than the electroweak scale (as will always be the case here) it can be integrated out to yield an effective theory below M_s. In this effective theory the Higgs quartic coupling will be modified compared to that of the SM as a result of the λ_{hs} mixing term. It was shown in [85] that below M_s we must replace

$$\lambda_h \to \lambda = \lambda_h - \frac{\lambda_{hs}^2}{4\lambda_s}, \tag{2.28}$$

where $\lambda \simeq 0.129$ is what is inferred from the Higgs mass measurement and is what enters the SM running below M_s. At M_s we must therefore apply a threshold effect to match to the full theory by replacing λ with $\lambda_h = \lambda + \frac{\lambda_{hs}^2}{4\lambda_s}$. Above M_s we must then also include the s field in the RGEs. Here we include them up to one loop and they are given by,

$$(4\pi)^2\beta_{\lambda_h} = (4\pi)^2\beta_{\lambda_h}^{SM} + \frac{1}{2}\lambda_{hs}^2, \tag{2.29}$$

$$(4\pi)^2\beta_{\lambda_{hs}} = \frac{1}{4}\lambda_{hs}\left(12y_t^2 - \frac{9}{5}g_1^2 - 9g_2^2\right) + \lambda_{hs}(6\lambda_h + 4\lambda_s) + 2\lambda_{hs}^2, \tag{2.30}$$

$$(4\pi)^2\beta_{\lambda_s} = \lambda_{hs}^2 + 10\lambda_s^2. \tag{2.31}$$

In order for this mechanism to work both λ_s and λ_{hs} will need to be very small so the RGE contribution will be relatively minor. The threshold effect however can still be significant because even small changes in λ_h can substantially change the position of the false vacuum. This effect also helps to push the experimental fit in Fig. 2.2 closer to the boundary because the input λ_h will be larger which is equivalent to having a larger Higgs mass for the SM. This is helpful because we need to be extremely close

to the boundary in order for a false vacuum to appear.

The setup for testing this model is to:

- select our 5 inputs $\{M_h, \alpha_s(M_Z), \lambda_s, \lambda_{hs}, M_s\}$,
- carefully tune M_t to generate a false vacuum in the potential (see below for more details),
- determine s_{end}, the value of s for which the false vacuum disappears and inflation ends,
- calculate the amplitude of the scalar perturbations N_* e-folds before the end of inflation using equation (2.19),
- calculate the χ^2 of this model point using the experimental values: The χ^2 was derived from fitting the experimental value of $M_h = 125.66 \pm 0.34$ GeV (see [44] and references therein) and $M_t = 173.35 \pm 0.76$ GeV [86], the world average of $\alpha_s(M_Z) = 0.1184 \pm 0.0007$ [87], and observed value of $A_s = (2.196 \pm 0.060) \times 10^{-9}$ [1].

Note, however, that there is a degeneracy in such an approach resulting from the freedom of tuning the initial depth of the well using M_t. Different well depths will result in different s_{end}, and hence A_s, values for the same set of input parameters. To resolve this we tune M_t for each set of inputs such that the resulting well depth generates the best possible fit to A_s. We therefore choose only the best possible point in the degenerate set of outputs given our 5 inputs.

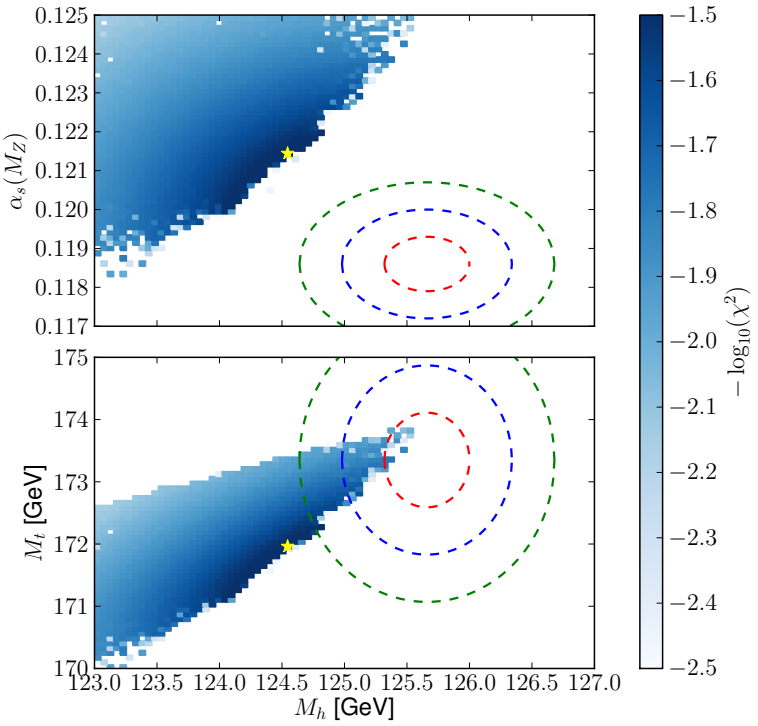

FIGURE 2.7: *This plot shows the binned best fit point in the M_h-$\alpha_s(M_Z)$ plane (top) and the M_h-M_t plane (bottom) for $N_* = 50$. The colourbar shows $-\log(\chi^2)$ for each point when fitting to all 4 observables $\{M_h, \alpha_s(M_z), M_t, A_s\}$. For comparison the $1-$, $2-$, and $3-\sigma$ experimental contours for the plotted parameters are also depicted. The global best fit point, marked with a yellow star, is inconsistent with experiment at more than 5σ.*

The result of an extensive nested sampling scan using MultiNest [88] is shown in Fig 2.7. The best fit point has a $\chi^2 = 29.4$ largely due to poor fits of M_h and $\alpha_s(M_z)$. There is a clearly visible sharp boundary in Fig. 2.7. This marks the point when the scale of inflation exceeds the maximum value allowed by equation (2.20) preventing any chance of achieving a good fit to A_s by tweaking ϵ. We also see that allowing a variation of $\alpha_s(M_Z)$ gives considerably more freedom in M_t for a particular M_h while still achieving a false vacuum.

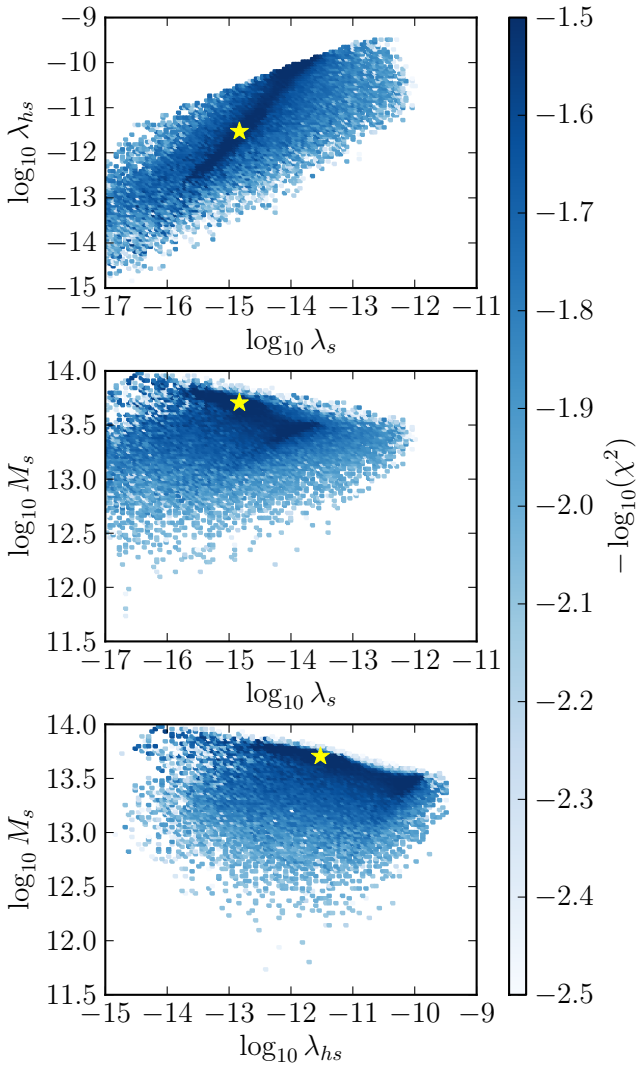

FIGURE 2.8: *This figure shows the binned best fit point for λ_s, λ_{hs}, and M_s with $N_* = 50$. The global best fit point is marked with a yellow star.*

The corresponding distributions for λ_s, λ_{hs}, and M_s and their best fit value are shown in Fig. 2.8. It is clear that in order to fit the scalar perturbations and the e-folds simultaneously, quite small values for the couplings are needed, which would result in a very large (Planckian) expectation value $\langle s \rangle|_{h_0=v}$ for the extra scalar field. The sharp line in the λ_s-λ_{hs} plane marks the region above which the threshold effect becomes too large and results in a push of the false vacuum to too large scales.

Although we do not consider the spectral index, n_s, or the tensor-to-scalar ratio, r, as constraints for our fit, this model is capable of reproducing a large range of r and $n_s < 1$ in the region preferred by Planck. This is, however, secondary to the difficulties encountered when fitting M_h and $\alpha_s(M_Z)$.

2.2.4 Is the Higgs the inflaton?

In this section we have discussed the idea that Higgs might be the inflaton. We first discussed Higgs inflation with a non-minimal coupling and found that there is some complicating details involving the UV completion of such as theory that make it somewhat less appealing. Next we examined two possible implementations of minimal Higgs inflation: Higgs plateau inflation and false vacuum Higgs inflation. For the case of Higgs plateau inflation we found that a simultaneous fit of the number of e-foldings and the scalar perturbations turned out to be impossible. We argued that inclusion of extra fermionic or scalar singlets to the SM cannot change this conclusion. As such we conclude that a different approach is required for the Higgs to be the inflaton.

Next we considered a slightly less minimal approach where we introduced an additional singlet scalar field s and looked at a hybrid scenario. In this case, the Higgs sits in a local minimum of the potential and s slowly rolls towards the minimum of its potential. The mutual coupling between s and the Higgs field removes the barrier during the rolling of s such that the Higgs can then roll towards its global minimum and successful exit is guaranteed. To ensure a correct treatment, we included the 1-loop RGEs for the new scalar, the threshold effect in the Higgs potential occurring at the mass of the singlet scalar, the movement of the Higgs field during inflation and the degeneracy in the well depth. The results are summarised in Fig. 2.7 where one can see that, although it is now possible to fit A_s for $N_* = 50 - 60$, these points are clearly excluded by measurements of the Higgs mass and the strong coupling constant. This result challenges claims in the literature that false vacuum Higgs inflation is viable (e.g. [81]).

We therefore find that Higgs inflation without a non-minimal coupling appears to be impossible. If we are determined to have the Higgs be the inflaton we must therefore address the problems with non-minimal Higgs inflation. As mentioned already there has been some works to create a UV complete Higgs inflation model [67, 68]. There has also been some recent work that attempts to combine both approaches discussed here i.e. they leverage both a non-minimal coupling and fine-tuning of quantum effects to inflate with the Higgs [58, 59]. Here they use a non-zero ξ to flatten out the potential above the Higgs plateau to give successful inflation. This approach also evades the unitarity problem because the use of the plateau means that values of $\xi \sim \mathcal{O}(10)$ are viable. At this point however the original argument for Higgs inflation in terms of minimality begins to work against us. It would seem that a far more economical choice would be to have a separate field that plays the role of the inflaton. This of course ignores the possible hint of near-criticality, but perhaps some new ideas are needed to make this theory attractive again.

In the next section we consider the case where the Higgs is not the source of inflation. We must still however properly consider the behaviour of the Higgs during inflation.

2.3 The Higgs as a spectator

In light of the somewhat discouraging findings in the last section, this section deals with the case where there is an additional field, separate from the Higgs, that plays the role of the inflaton. We do not however consider this field in isolation. The Higgs has been discovered and therefore it is important to consider any effect it might have on the dynamics of inflation. This section therefore deals with the implications of having the Higgs as a spectator field during inflation. The behaviour of the Higgs field during inflation has started to get a lot of attention in recent years and following its discovery at the LHC is perhaps the most promising avenue for particle physics to elucidate early Universe physics. Several studies have considered the contributions of the Higgs to cosmological perturbations [89–92] and several others have raised the

issue of stability of the electroweak vacuum during inflation [93–95]. Here we will be concerned with the latter.

2.3.1 Meta-stable Higgs and high scale inflation

As we have seen already in this chapter, quantum corrections have a large effect on the structure of the Higgs potential. In the previous section we considered the case when the Higgs was on the cusp of stability. This was made easier by introducing a new scalar field that could have a positive contribution to the running of the quartic self-coupling, λ_h. Without this field the observed central values of the SM parameters, in particular the top mass and the Higgs mass, imply that λ_{eff} becomes negative at large values of the Higgs field h [44, 45]. For example, we can see in Fig. 2.9 that for the central value of $M_t = 173.34$ GeV and $M_h = 125.66$ GeV the Higgs potential becomes negative at a scale Λ just above $h = 10^{10}$ GeV. As we discussed this had lead to lots of interest in the tunnelling rate from our vacuum to the unstable vacuum in order to put bounds on the lifetime of our metastable minimum at $h = 246$ GeV [44, 45, 72–76].

These calculations however are for the Universe today and might not apply to the very early Universe. If we accept that there was a period of inflation in the very early Universe then it is possible that the very large energy density of the inflationary Universe might alter the tunnelling rate. During inflation all fields lighter than the Hubble scale H will receive stochastic quantum fluctuations of order $H/2\pi$ per Hubble time from the Gibbons-Hawking temperature [96]. The $H/2\pi$ factor corresponds to the amplitude of the power spectrum of scalar perturbations on super-horizon scales and so will be present in any spacetime with a causal horizon which is the case during inflation. Since successful inflation with generation of scalar perturbations which fit the data well can be achieved for a wide variety of inflationary energy scales, the magnitude of these quantum fluctuations can be relatively small. If, however, we find evidence for high scale inflation then these quantum fluctuations might become extremely important.

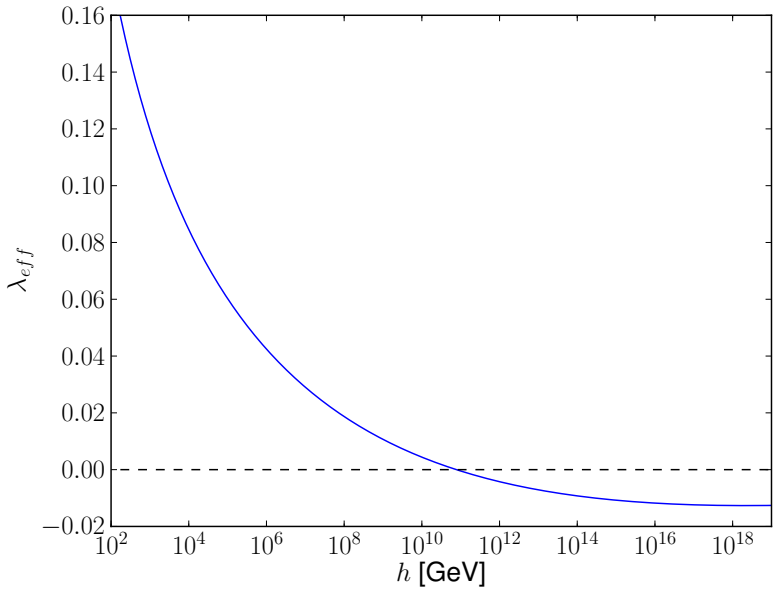

FIGURE 2.9: *The running of the RGE improved effective coupling for* $M_h = 125.66$ *GeV and* $M_t = 173.34$ *GeV. An instability develops when* λ_{eff} *crosses zero.*

There were recently some hints that the scale of inflation was very high indeed[4]. The BICEP2 experiment reported a measurement of B-modes in the CMB radiation at degree angular scales [97]. A detection of B-modes at this scale is intriguing because it is too large to be caused by gravitational lensing of CMB E-modes by large scale structure and so might have primordial origin. If this were the case then the measurement would be a direct probe of the scale of inflation. Another possible source of the signal however is from E-mode to B-mode conversion by dust in the Galaxy. Using a simple dust model BICEP2 reported an excess in B-modes and attributed their origin to primordial gravitational waves. This lead them to an estimate of the tensor-to-scalar ratio, $r = 0.16^{+0.06}_{-0.05}$. This would set the scale of the energy density during inflation to be very large $\sim 10^{13-14}$ GeV. This caused quite a stir in the community as many worked frantically to understand the implications of such a measurement. There were several works that revisited the issue of vacuum stability [98–100] including [38] which is presented here. Unfortunately, it has since come to light that dust model used in the BICEP2 analysis underestimated the contribution of dust [101–103]. With a more accurate dust model the observed B-mode signal is now consistent with $r = 0$ ($r < 0.12$ at 95% confidence) [104].

[4]Henceforth we will use high scale inflation to mean inflation with $H \gg \Lambda$.

Although the signal has disappeared the possibility of high scale inflation is still something to be considered. More data from *Planck* and future ground, balloon, and space based experiments (e.g. SPIDER [105], and the KeckArray [106]) could detect primordial gravitational waves and therefore probe the scale of inflation. It is immediately clear that if there is indeed high scale inflation then the quantum fluctuations of the Higgs during inflation might be large enough for the Universe to fluctuate over the barrier and into the true minimum. This therefore presents a very interesting avenue for investigation into particle physics models of inflation.

If we restrict our interest to the case of high scale inflation, i.e. $H \gg \Lambda$ then fluctuations of the Higgs field will be very large during inflation. In this case we may treat them stochastically using the Fokker-Planck equation as long as the classical motion is always treatable by slow roll [107, 108]. In this picture we treat the quantum motion of the field like a random walk with step size $H/2\pi$. The Fokker-Planck equation then describes the probability distribution for the Higgs field at a time, t, via

$$\frac{\partial P}{\partial t} = \frac{\partial}{\partial h}\left[\frac{V'_{\rm eff}(h)}{3H}P + \frac{H^3}{8\pi^2}\frac{\partial P}{\partial h}\right]. \tag{2.32}$$

This is is a diffusion equation for $P(h,t)$ with diffusion coefficient equal to $H^3/8\pi^2$. We therefore see the critical role that Hubble scale plays in the evolution of the Higgs field during inflation. If $H \gg \Lambda$ then we expect there to be a high probability for $h > \Lambda$ after a few e-folds of inflation. If we multiply Eq. 2.32 by h^2 and integrate over all h we find an equation for the second moment of the Higgs field,

$$\frac{d\langle h^2\rangle}{dt} + \frac{2}{3H(t)}\langle hV'_{\rm eff}\rangle = \frac{H^3(t)}{4\pi^2}, \tag{2.33}$$

where we have required the boundary conditions $P,\ \partial P/\partial h \to 0$ as $h \to \pm\infty$. Given SM inputs at the weak scale we can then determine the effective potential for the Higgs and solve (2.33) to track the behaviour of the Higgs during inflation. Note that (2.32) and (2.33) are space-independent so refer to behaviour of entire Hubble volume. During inflation many such Hubble volumes are produced so we will have a sample of this probability distribution for each Hubble volume.

2.3.2 Test case: $m_\phi^2\phi^2$ potential

In this section we consider the simplest inflationary model: the quadratic potential $V = \frac{1}{2}m_\phi^2\phi^2$. Using this model as a test case we can investigate the effect of high scale inflation on the dynamics of the Higgs during inflation. Of course, no matter what the shape of the potential, if the energy density during inflation is as high as the GUT scale, then the Higgs field will receive stochastic fluctuations which will push it to expectation values typically of order 10^{13} GeV or higher during the 50-60 e-folds of inflation, even if one assumes that its value at the beginning of those final e-folds was zero. If the Higgs field has instabilities above 10^{10} GeV the tunnelling calculation would therefore be rendered irrelevant - at or before the end of inflation the Higgs field will roll classically into the unstable minimum leading to a Universe incompatible with the one we live in (in which at the *very* least the particle physics would be very different from what we observe).

To make this more quantitative let's turn to the example of quadratic inflation. First, we use the slow roll approximation to get an estimate of the Hubble scale during inflation. We find that

$$\epsilon = \frac{M_{\rm pl}^2}{2}\left(\frac{V'}{V}\right)^2 = \frac{2M_{\rm pl}^2}{\phi^2}, \tag{2.34}$$

therefore inflation ends at $\phi_{\rm end} = \sqrt{2}M_{\rm pl}$. We then have

$$N_* = \frac{1}{M_{\rm pl}}\int_{\phi_{\rm end}}^{\phi_*}\frac{1}{\sqrt{2\epsilon}} = \frac{\phi_*^2 - \phi_{\rm end}^2}{4M_{\rm pl}^2} \tag{2.35}$$

For $N_* = 50$, we get $\phi_* \simeq \sqrt{200}\ M_{\rm pl}$. There is also then a simple relationship $N = (2\epsilon)^{-1}$ for general N. We can use the amplitude of the scalar perturbations (Eq. (2.19)) to set $m_\phi \simeq 10^{13}$ GeV. Finally, we find that the Hubble scale is given by,

$$H = \sqrt{\frac{V}{3M_{\rm pl}^2}} \simeq 6 \times 10^{13}\ \text{GeV}. \tag{2.36}$$

We therefore see that indeed this model of inflation has $H \gg \Lambda$ so the instability is likely to be problematic. Here we will consider the best case scenario where the Higgs is sitting at the origin 50 e-folds before the end of inflation. It is perhaps natural to expect Planckian initial conditions for the Higgs field in which case, without additional contributions to the Higgs potential, the Higgs would roll straight into the unstable vacuum in the early Universe before the inflaton dominates the energy density of the Universe (see e.g. [94]). There is no explicit reason however that the Higgs does not begin at the origin however and it does allow *some* possibility of survival so it is a conservative choice in that respect.

The solution to (2.33) at $t = t_{\rm end}$ gives the variance of the probability distribution of h at the end of inflation. The probability of fluctuating into the unstable region is then given by the fraction of this distribution with $h > \Lambda$. This calculation of the probability is slightly complicated by the fact that there is a different value of the Higgs field h in each Hubble volume during inflation. Whether or not the tunnelling of any one Hubble volume to the true minimum is detrimental to our survival or not depends on its post-inflationary evolution. If the bubble expands quickly enough it may consume all the surrounding spacetime before collapsing. On the other hand it could quickly collapse and leave the other Hubble volumes safe. This is a subject of ongoing research and we will discuss it further in the next section. Here we will take the simplifying assumption that the collapse of any Hubble volume in our horizon is unacceptable. This would be the case if all Hubble volumes survive until the end of inflation and any with $h > \Lambda$ will quickly expand to fill spacetime before collapsing. The approach that we use therefore is to evaluate at each e-fold of inflation the probability in a single Hubble volume and weight that with the number of independent Hubble volumes at each e-fold which end up within our horizon. This can be written as

$$P_{\rm surv} = \prod_{N=1}^{N_*} \left[1 - \int_{\Lambda}^{\infty} \sqrt{\frac{2}{\pi \langle h^2 \rangle_N}} \exp\left(-\frac{1}{2} \frac{h^2}{\langle h^2 \rangle_N} \right) \right]^{j_N} \tag{2.37}$$

where N is the number of e-folds, $\langle h^2 \rangle_N$ is the variance of h after N e-folds evaluated

using equation (2.33) and $j_N = e^{3N}$ is the number of separate Hubble volumes at e-fold N which end up within our past light cone today. The field equations of the inflation can be solved numerically to determine $H(t)$ which is then fed into (2.33) and (2.37) to determine $P_{\rm surv}$. In order to solve (2.33) numerically for $\langle h^2 \rangle$ we neglect the h dependence of $\lambda_{\rm eff}$ and use a Hartree-Fock (HF) approximation to write $\langle h^4 \rangle \simeq 3\langle h^2 \rangle^2$ which yields $\langle h V'_{\rm eff} \rangle \simeq 3\lambda_{\rm eff}\langle h^2 \rangle^2$ [93]. The HF approximation is very good for small fluctuations but neglects non-Gaussianity which can contribute for large h. In order to properly take this into account we must instead solve the full Fokker-Planck equation. The two approaches were compared in [109] and it was found that the resulting probability distribution showed some quantitative difference in the tails where the HF approximation slightly underestimates the probability of very large fluctuations. The HF approximation can therefore be seen as a conservative one but in practice it will have no bearing on our conclusions.

Note that because here we have a slowly rolling scalar field H will not be constant with time/e-fold. Given,

$$\epsilon = -\frac{\dot{H}}{H^2} \qquad \text{and} \qquad \dot{H} = \frac{dH}{dt} = \frac{dH}{dN_r}\frac{dN_r}{dt}, \tag{2.38}$$

where we have defined N_r as the number of e-folds of inflation remaining, and using

$$\frac{dN_r}{dt} = -H \implies \dot{H} = -H\frac{dH}{dN_r}, \tag{2.39}$$

we can write

$$\epsilon = \frac{1}{H}\frac{dH}{dN_r} \implies \frac{dH}{dN_r} = \frac{H}{2N_r}, \tag{2.40}$$

which can be integrated to yield $H = H_*\sqrt{N_r/N_*}$, where H_* is the Hubble scale N_* e-folds before the end of inflation. We therefore see that H decreases by an order of magnitude over the course of the inflation. This means that the largest quantum fluctuations will occur in the early stages of inflation when $\langle h^2 \rangle$ is close to zero.

As expected, if the Higgs ends up on the other side of the instability it will most likely rapidly roll away to very high field values. This will happen as soon as the

classical evolution dominates the quantum fluctuations, where we have

$$\Delta h_{\text{classical}} = -\frac{V'_{\text{eff}}(h)}{3H^2}, \tag{2.41}$$

and

$$\Delta h_{\text{quantum}} = \frac{H}{2\pi}. \tag{2.42}$$

In [99] a critical scale, Λ_c, was defined as the point at which classical motion begins to dominate. This scale can be estimated by approximating λ_{eff} as constant above the instability scale such that $V'_{\text{eff}}(h > \Lambda) \simeq \lambda_{\text{eff}} h^3$. Then by equating (2.41) and (2.42) at $h = \Lambda_c$ we find

$$\Lambda_c \simeq \left(\frac{-3}{2\pi\lambda_{\text{eff}}(\Lambda_c)}\right)^{1/3} H \sim \mathcal{O}(H). \tag{2.43}$$

So we see that even when $h > \Lambda$ there is a possibility that it will fluctuate back over the barrier. However, within a few e-folds it will quickly reach Λ_c from which point on there is no chance of recovery.

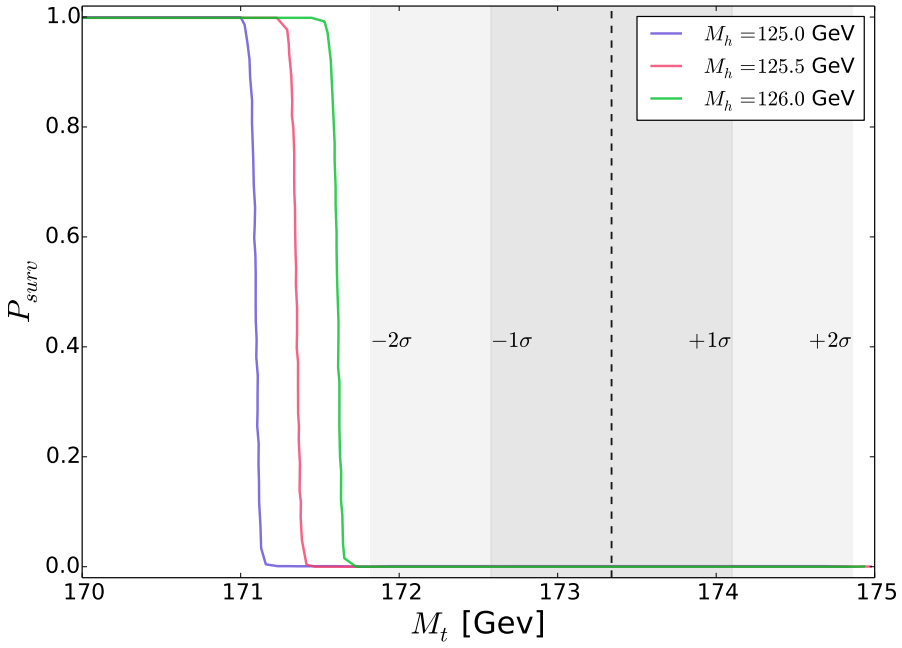

FIGURE 2.10: *The probability of the Higgs field not ending up above the instability scale Λ in any of the Hubble volumes in our past horizon during inflation as a function of top mass M_t. We plot the results for three values of the Higgs mass M_h. We also plot the 1σ and 2σ limits on M_t.*

In Fig. 2.10 the probability of finding the Higgs field below Λ in each Hubble volume after 50 e-folds of inflation is shown. The figure shows that naively, without further physics, inflationary fluctuations would push the Higgs field over the top of the potential to above the instability scale Λ for the best favoured values of the Higgs mass and top-quark mass into a (presumably anti de-Sitter) vacuum. Since we are working under the assumption that any such transition will spread to the entire Universe this is clearly incompatible with observation. In order to have an acceptable theory of the inflationary Universe with high scale inflation we must introduce some new effects that will modify V_{eff} in some way such that the probability of transitioning to the true vacuum is reduced to an acceptable level.

The most obvious solution would be to introduce some new physics, e.g. supersymmetry, that modifies the running of the Higgs above the energy scale of the new physics. Bosonic fields are needed to give positive contributions to λ_{eff} so, if we find evidence for high scale inflation, lights stops for example would be a good candidate to cure the problem. Another solution would be to have a non-minimal coupling of the Higgs to gravity [93, 110]. This will generate an effective contribution to the Higgs mass squared of $12\xi H^2$ during inflation which can stabilise the potential. In [110] the quantum corrections to this theory were considered and it was shown that even if ξ is set to zero at some scale (e.g. the electroweak scale) then the radiative corrections will create a non-zero ξ at higher scales which could play an important role. The situation is complicated however by the rapidly changing spacetime at the end of inflation that could cause the Universe to transition into the true vacuum [111]. It therefore seems that non-zero ξ hinders rather than helps.

Another point of view is that the solution to this problem could lie with the inflaton itself and may be the first clue concerning its couplings to SM particles. In [38] we presented two ways that the inflaton could affect the vacuum stability. The first is the situation where the Higgs has a sufficiently large direct coupling to the inflaton itself such that the instability is prevented from appearing during inflation when the inflaton has a large expectation value [94, 95]. Such a coupling is to be expected by symmetry considerations for a SM singlet inflaton. The second way is through

dissipative effects during inflation which could create temperature corrections to the Higgs mass which would result in it rolling into the electroweak minimum at $h = 246$ GeV.

If we first allow a direct coupling between the Higgs and the inflaton there are two ways this result could be affected. Firstly, the inflaton coupling would add a positive contribution to the beta function for λ and so could prevent the instability from appearing and thus solve the problem in a non-dynamical way. For values of the coupling between the Higgs and the inflaton of order 10^{-1} the entire Higgs potential becomes stable up to the Planck scale. Such a large coupling will also affect the inflaton dynamics however. Furthermore, if we assume the inflaton does not get a vev (which would cause it to mix with the Higgs) the quartic coupling would only be altered above the mass scale of the inflaton. Many simple models of high scale inflation require an inflaton mass close to 10^{13} GeV, above the energy scale required to stabilise a quartic coupling which becomes negative at 10^{10} GeV. We therefore instead look for a dynamical solution.

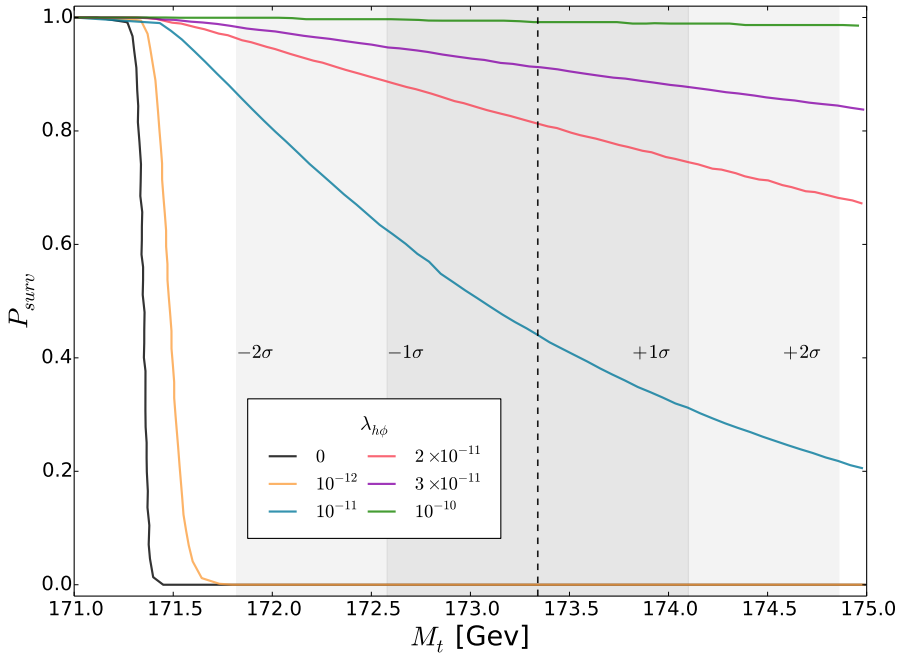

FIGURE 2.11: *The probability of the Higgs field remaining in the electroweak vacuum in any of the Hubble volumes in our past horizon during inflation as a function of top mass M_t. We plot the results for different values of the Higgs-inflaton coupling $\lambda_{\phi h}$.*

Including this additional coupling modifies the effective potential to,

$$V_{\text{eff}} \to V_{\text{eff}} + \frac{1}{4}\lambda_{\phi h}\phi^2 h^2. \tag{2.44}$$

During inflation, ϕ has a large value so this contribution behaves like a large effective mass for the Higgs field. If $\lambda_{\phi h}$ is large enough this could stabilise the vacuum completely, or at least push Λ to larger scales and reduce the probability of collapse if the Higgs starts with a low expectation value. The effect of such a direct coupling is shown in Fig. 2.11 where we find that for $\lambda_{\phi h}$ a few $\times 10^{-11}$ the modified effective mass of the Higgs is such that the probability of surviving until the end of inflation increases dramatically.

In the absence of a sufficiently large direct coupling between the Higgs and the inflaton the problem must be cured in a different way. A second possibility is that dissipative effects could generate a non-zero temperature during inflation which would result in corrections to the Higgs mass. That is,

$$V_{\text{eff}} \to V_{\text{eff}} + \frac{1}{2}c_h T^2 h^2, \tag{2.45}$$

where $c_h \simeq 0.308$ in the SM. Such a temperature might be generated in the context of warm inflation, where the inflaton equation of motion is modified to

$$\ddot{\phi} + (3H + \Upsilon)\dot{\phi} + \frac{dV_\phi}{d\phi} = 0, \tag{2.46}$$

where Υ is a model dependent dissipation term that sources a thermal bath. Warm inflation is a well studied subject that tries to use this thermal viscosity to slow the roll of the inflaton and drive inflation [112]. However here we are not interested in the effect of the thermal bath upon the inflaton, but rather its effects on the Higgs potential. We therefore do not require Υ to be anywhere near as large as $3H$. Since the functional dependence of Υ on ϕ and T is highly model dependent (see e.g. [113–123]) we do not deal with it directly here. Instead we adopt a phenomenological approach and concern ourselves only with the temperature required to stabilise the

Higgs field.

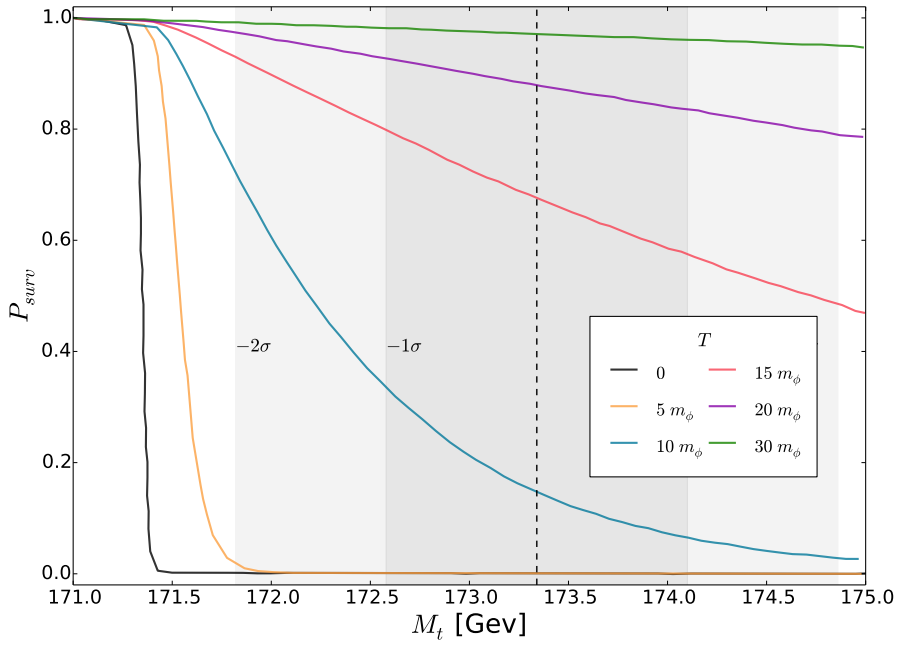

FIGURE 2.12: *The probability of the Higgs field not ending up above the instability scale Λ in any of the Hubble volumes in our past horizon during inflation as a function of top mass M_t. We plot the results for different values of the temperature, T, during inflation.*

Figure 2.12 shows the result of inflation occurring in the presence of a thermal bath of temperature T which prevents the Higgs field from destabilising if it starts with zero expectation value. Note that we do not require the potential to be completely stable, merely that thermal effects both increase the value of Λ via equation (2.45) and decrease the variance of the Higgs field $\langle h^2 \rangle$ by changing the effective mass in equation (2.33). A temperature of a few tens times the inflaton mass, m_ϕ, would therefore prevent the Higgs field from destabilising.

2.3.3 Post inflationary evolution: is the SM incompatible with high scale inflation?

The previous discussion shows that if we assume that the transitioning of any Hubble volume to the true minimum causes the rest of the observable Universe to follow

suit the consequences are drastic. Under this assumption some new physics must be introduced to stabilise the Higgs field during high scale inflation. Now, however, we will question the legitimacy of the assumption that the transition of a single Hubble volume is catastrophic. Following the appearance of [38] there were two papers [99, 109] that considered this question in more detail.

The fundamental uncertainty that must be addressed is the evolution of the Hubble patches with $h > \Lambda_c$. In the preceding discussion we assumed that these patches will not crunch to a singularity before inflation ends. In this situation, when inflation ends and the horizons of the separate Hubble volumes begin to grow they will come back into causal contact with each other. We would then have a Universe with patches of true vacuum and patches of false vacuum separated by domain walls. Depending on wall tension and the energy difference between the separate vacua, the true vacuum (with negative energy density) could expand to fill the Universe or collapse. The collapse could be a result of the wall tension or gravitational collapse due to the negative energy density inside the bubble. If they expand rapidly and fill space the Universe will collapse to a singularity shortly afterwards.

An alternative to this is to assume the patches with $h > \Lambda_c$ very quickly crunch. In this regime we would hope that the patches that transition to the true vacuum early on in inflation would not pose any threat to the existence of the rest of the Universe. Several questions must then addressed. Firstly, we must ask whether the rate of crunching volumes is so great that it stops inflation from proceeding. This was addressed first in [99] and then in more detail in [109] where it was concluded that inflation can proceed for a maximum number of e-folds $N_{\max} \sim 50 - 70$ after which the fraction of Hubble patches crunching becomes $\mathcal{O}(1)$ and inflation ends. Another consideration is that we must also allow for few extra e-folds of inflation to compensate for the those lost to crunching volumes while still solving the horizon and flatness problems [109]. The allowable window for phenomenologically successful inflation is therefore quite tight.

The second question raised in this scenario concerns the phenomenological consequence of the collapsed regions. If they comprise a large fraction of the sky at the

end of inflation then we might expect to see large inhomogeneities in the CMB. The nature of the defects resulting from the crunch of a Hubble patch is therefore also important. If we assume that the the crunching patches result in primordial black holes (PBH) then the fraction of crunched patches is constrained to be extremely small[5]. The only remaining escape is to hope that primordial black holes are very light and quickly evaporate without leaving any relics. If they leave behind Planck-mass relics they could still overclose the Universe. Avoiding this requires the fraction of patches that transition to the true vacuum to be tiny ($\mathcal{O}(10^{-9})$ [109]) which runs counter to the results presented here.

The final consideration we must make is the fate of Hubble patches which transition to $h > \Lambda_c$ very close to the end of inflation such that they could not have had time to crunch. These unstable patches could then expand to consume the rest of the Universe before collapsing as mentioned above. It would only take one such patch out of e^{3N} to make the resulting universe inconsistent with observation. One final hope, suggested in [109], is that a sufficiently high reheating temperature will quickly re-stabilise these patches before crunching.

If all the conditions that we just discussed are met then it is in fact possible that our Universe could have arisen from high-scale inflation with an unstable Higgs potential. We do however still need to be lucky enough to find ourselves in one of the Hubble volumes that did not transition to the true vacuum. It therefore seems that even a more optimistic view of the post-inflationary evolution of Hubble patches with $h > \Lambda_c$ than that of the previous subsection meets opposition at every turn. It is easy then to argue that a much more economical solution would be to take the point of view that high scale inflation requires the existence of some new physics to stabilise the Higgs potential. It would be very interesting to study the evolution of the Hubble patches that transition to the true vacuum more quantitatively. This might be possible in the coming years after the development of sophisticated numerical GR

[5]Constraints on the fraction of energy density stored in PBHs are very tight (ranging from $10^{-5} - 10^{-30}$ depending on mass of the PBH [124])

codes [125] that could illuminate the precise conditions for expansion or collapse of these volumes.

Having knowledge of the energy scale of inflation has radical implications for the thermal history of the Universe, which in turn has a huge bearing upon particle physics. State of the art calculations have shown that for a Higgs mass of $M_h = 125.5$ GeV the time scale for tunnelling into the true vacuum is larger than the age of the Universe for top masses up to around $M_t \sim 178$ GeV [44]. Here we have argued that if the Hubble scale during inflation is a high ($> \Lambda \simeq 10^{10}$ GeV for central values of M_h, M_t, and α_s) then the instability of the Higgs potential likely requires new physics to step in and protect our vacuum. This new physics could be in the form of a direct coupling between the Higgs and the inflaton, a non-zero temperature during inflation, a non-minimal coupling of the Higgs to gravity, Planck suppressed operators, or any new particles that will effect the running of the quartic coupling. A direct measure of the energy scale of inflation by observing primordial gravitational waves can therefore give us key insight not only to the nature of inflation but also potentially as yet undiscovered aspects of particle physics.

2.4 Conclusion

In this chapter we have seen some of the consequences of a theory of inflationary cosmology that contains the Higgs. We first discussed the possibility that the Higgs itself was the inflaton but find that, while initially appealing, these theories are quickly confronted with either theoretical problems with unitarity or contrary experimental evidence. In particular we revisited the idea of false vacuum Higgs inflation. Using an additional scalar singlet the false vacuum can be lifted to end inflation. We found that although it is possible to reproduce the inflationary observables in this setup this comes at the expense of significant modifications of the Higgs mass that are excluded by experiment.

It is still possible to successfully invent Higgs inflation models that use both non-minimal coupling to gravity and fine-tuning of the Higgs potential. These models are able to avoid the above issues but in the process some of the gloss is taken of the idea as the attractive minimality is lost. These theories still offer a promising avenue of research however because a successful theory would offer a concrete link between electroweak scale particle physics and early Universe cosmology.

We then discussed the implications of having an unstable Higgs field as a spectator during high scale inflation. A large Hubble scale during inflation induces large fluctuations in the Higgs field resulting in a high probability of transitions to the unstable vacuum. Although there are several subtleties in considering the consequences of these transitions we have argued that a conservative interpretation is that such a situation is incompatible with observation. A measurement of primordial B-modes indicative of high scale inflation would therefore require new physics and so offers a great opportunity for inflationary observables to inspire particle physics models. In the event of such a measurement we have presented two possible solutions to the problem that can teach us about the couplings of the inflaton to the SM. A direct coupling between the Higgs and the inflaton could give a large effective mass contribution to the Higgs during inflation which prevents destabilisation. Alternatively, couplings of the inflaton to other particles could give rise to significant dissipation of the inflaton energy into a thermal bath of particles. Interactions with the thermal bath would then contribution to the effective mass of the Higgs and, again, prevent destabilisation.

The discovery of the Higgs has thus ushered in an exciting era for those working at the boundary of particle physics and cosmology. The complementarity between particle physics experiments at the LHC and CMB experiments like *Planck* and the Keck-Array therefore offer the potential for fruitful discoveries in the coming years.

Chapter 3

Electroweak Baryogenesis and the Higgs Portal

3.1 Introduction

In Sec. 1.2 we discussed the problem of the Baryon Asymmetry of the Universe (BAU). With symmetric initial conditions the CPT symmetry of the Standard Model (SM) seems to prevent any matter-antimatter asymmetry being generated. This is of course contrary to observation so requires a physical explanation. Additionally, any asymmetry in the initial conditions would be washed away in an inflationary Universe. As we discussed earlier we therefore need a dynamical solution that meets the Sakharov conditions. One promising solution that meets these requirements is electroweak baryogenesis (EWBG) which we will investigate in this chapter. As we will see below the utility of this solution demands new degrees of freedom at the weak scale. With Run 2 of the LHC under way this is therefore fertile ground for phenomenology that could be tested in the near future.

Another hallmark of new physics at the weak scale is dark matter. The WIMP miracle (Sec. 1.1) suggests that searching for traces of dark matter at the weak scale is a promising endeavour. With many complimentary experiments looking for dark

matter directly (with nuclear recoil experiments and the LHC) and indirectly (by searching for gamma ray emission from the Galactic centre and dwarf spheroidal galaxies, and for excesses in the cosmic ray background) the parameter space of electroweak scale dark matter is being explored more and more comprehensively.

In this chapter we will discuss the possibility of a connection between EWBG and dark matter with the Higgs at the fulcrum. We will first review EWBG and introduce Higgs portal dark matter models before presenting the results of a model that can account for both phenomena.

3.1.1 Electroweak baryogenesis

The goal of EWBG is to take advantage of the apparent ability of the electroweak theory to satisfy the first and third Sakharov conditions. If the electroweak phase transition is first order then during the transition we will have the non-equilibrium dynamics to satisfy the third Sakharov condition. The baryon number violation required by Sakharov's first condition is provided by non-perturbative processes in the SM.

The vacuum structure of $SU(2)$ is such that there are an infinite number of physically equivalent but topologically distinct vacua that can be labelled by an integer winding number. This can be understood as a result of the non-trivial homotopy of $SU(2)$ which is topologically S^3. The possible gauge field configurations when we topologically identify points at spatial infinity are then described by $\pi_3(S^3) = \mathbb{Z}$, where we call the integers $\mathbb{Z}$ the winding number. Each vacuum is equivalent to the others under these large gauge transformations. These vacua are separated by an energy barrier provided by intermediate gauge field configuration with non-zero energy. It was shown by 't Hooft [126] that non-perturbative effects called instantons allow tunnelling between these different vacua. Changing the winding number by 1 through an instanton transition will violate baryon number, B, and lepton number, L, by 3 units each as result of the triangle anomaly [127, 128] that violates the classical conservation of fermion currents under these large gauge transformations. A

vacuum transition will therefore violate $B+L$ while preserving $B-L$. The amplitude of these tunnelling events is extremely low, $\mathcal{A} \sim e^{-4\pi/\alpha_{EW}} \sim e^{-170}$, so they don't appear to be useful for baryogenesis. In [20, 129] however it was shown that there is another process called a sphaleron that can have a much larger amplitude at high temperatures. The sphaleron is a finite energy, static solution to the Electroweak field equations found at a saddle point in the Electroweak action. The sphaleron solution corresponds to the barrier separating the two topologically distinct vacua and carries half integer winding number. In this way it can be thought of as the "midpoint of an instanton". Contrary to the instanton, the sphaleron can be interpreted as a physical (albeit unstable) object. For temperatures $\gtrsim 100$ GeV (the electroweak scale) thermal fluctuations mean that transitioning between the topologically distinct vacua via sphaleron production and decay becomes unsuppressed and the baryon number violation is possible.

There are two important implications of this result. Firstly, the high rate of sphaleron transitions in the early Universe would washout any initial asymmetry even without inflation and so demands a dynamical generation of the asymmetry. Secondly, once the asymmetry is established, it is important that sphaleron transitions are sufficiently suppressed to prevent subsequent washout of the asymmetry.

During a first order phase transition, space becomes populated with bubbles of the broken phase that expand, collide, and coalesce to eventually fill all of space, marking the end of the transition. The idea is to have efficient baryon number violation through sphaleron processes outside the bubbles while suppressing washout inside the bubbles. If we fulfil Sahkarov's second condition and there are CP violating interactions of particles with the walls, then the reflection/transmission probabilities of particles will be different to their CP conjugates. This causes a CP-asymmetry to build up on either side of the bubble walls i.e there will be excess of $f_L + \bar{f_R}$ on one side of the wall and $f_R + \bar{f_L}$ on the other, where f denotes SM fermions. Since the sphalerons are from the $SU(2)_L$ gauge group they will only interact with the left-handed fermions. There will therefore be an excess in sphaleron-mediated particle creation (destruction) whenever there is an excess in left-handed anti-fermions

(fermions). In the symmetric phase the sphaleron rate can be approximated as [130, 131],

$$\Gamma \propto (\alpha_{ew} T)^4. \tag{3.1}$$

The rate is therefore unsuppressed and the sphalerons are still in thermal equilibrium so they can efficiently remove the the excess left-handed anti-fermions to accumulate a baryon asymmetry outside the bubble walls. As the walls expand throughout space the baryons will move into the broken phase. In the broken phase, the sphaleron rate is suppressed by a Boltzmann factor,

$$\Gamma \propto \exp\left(-\frac{E_{\rm sph}(T)}{T}\right), \tag{3.2}$$

where $E_{\rm sph}$ is the height of the energy barrier separating the different vacua. If this rate is sufficiently suppressed in the broken phase then the excess baryons will not be destroyed and a baryon asymmetry is achieved. The mechanism can be seen schematically in Fig. 3.1, where the CP-asymmetry is converted to a B asymmetry in the symmetric phase by sphalerons but not in the broken phase where sphalerons are suppressed.

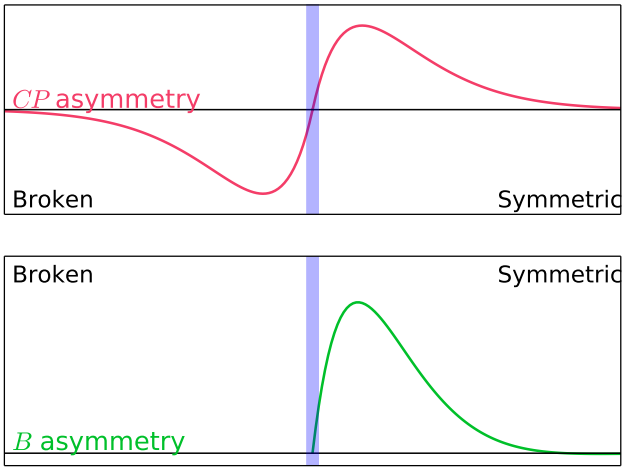

FIGURE 3.1: *A schematic representation of the baryon asymmetry generation near the bubble walls (blue). A CP asymmetry is created by the CP violating bubble wall interactions which is converted to a B asymmetry outside the bubble wall. The sphalerons are suppressed in the broken phase so no compensating asymmetry is created there resulting in a net overall B asymmetry.*

The condition to prevent washout in the broken phase is therefore that $E_{\rm sph}(T_c)/T_c$ is sufficiently large (> 45 [129]), where T_c is the critical temperature for the phase transition (the temperature at which the two phases are degenerate). In the 1-loop approximation [132] this is equivalent to requiring[1]

$$\frac{v_c}{T_c} \gtrsim 1, \tag{3.3}$$

where v_c is the Higgs vev at T_c. This measure takes into account that there is usually some supercooling and the phase transition only occurs at a bubble nucleation temperature $T_n < T_c$. This condition can be difficult to achieve and is the most constraining aspect of theories of electroweak baryogenesis. In what follows whenever we say a phase transition is strongly first order we mean that this additional condition has been met. A schematic of the electroweak phase transition is shown in Fig. 3.2. The schematic shows the appearance of a potential barrier between the broken and unbroken minima at $T = T_c$ as is required for a first order phase transition.

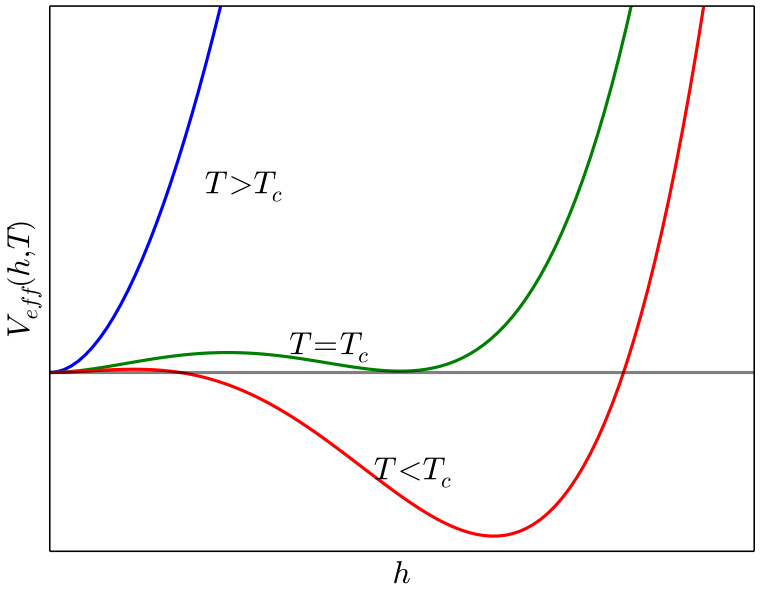

FIGURE 3.2: *Schematic of the electroweak phase transition. At $T = T_c$ the symmetric and broken and minima are degenerate. For a first order phase transition that proceeds via bubble nucleation these must be separated by a potential barrier.*

[1]There are issues with gauge dependence of this measure that we will return to later.

From this discussion we can see that the role of significant CP-violation in this mechanism is crucial. Without sufficient CP-violation the CP asymmetry that accumulates near the bubble walls will not be large enough to produce the required baryon asymmetry when converted by sphalerons (see Fig. 3.1). The SM provides some CP-violation through the CP-odd phase of the CKM matrix. Unfortunately, this is insufficient to establish the observed BAU [133–135]. An additional source of CP-violation is required for successful electroweak baryogenesis. In the remainder of this chapter we will set aside the detailed calculation of baryon asymmetry and focus on the most constraining aspect of electroweak baryogenesis theories i.e. the requirement of a strongly first order phase transition. We will therefore remain agnostic about the source of additional CP-violation but emphasise that its inclusion in a final theory is crucial.

3.1.2 Electroweak phase transition in the SM

In the SM, the properties of the electroweak phase transition are determined by the mass of the Higgs, M_h, and a first order phase transition requires $M_h < 72$ GeV [136–138]. The requirement (3.3) that the sphaleron processes are out of equilibrium introduces an even stronger bound of $M_h \lesssim 35$ GeV [139]. Unfortunately, the discovery of the Higgs with $M_h = 125$ GeV means that EWBG is not possible in the SM. This does, however, present an opportunity to postulate the existence of new physics at the electroweak scale that will modify this bound. It is therefore interesting to investigate models that give rise to a first-order phase transition and look for their signatures in collider experiments.

The usual approach to studying the behaviour of the electroweak phase transition is to take the 1-loop approximation to the effective potential,

$$V_{\text{eff}} \simeq V_0 + V_{1-\text{loop}}^{T=0} + V_{1-\text{loop}}^{T\neq 0}, \tag{3.4}$$

where V_0 is the tree-level potential and we have included both the zero-temperature corrections and the thermal corrections at 1-loop. At zero temperature we have the

Coleman-Weinberg correction,

$$V_{1-\text{loop}}^{T=0} = \frac{1}{64\pi^2}\sum_i (-1)^{n_F^i} N_i M_i(h)^4 \log\left(\frac{M_i^2}{\mu^2} + A_i\right), \tag{3.5}$$

where the sum is over all fields with field-dependent masses $M_i(h)$, N_i is the number of degrees of freedom, $n_F = 1, 2$ for fermions/bosons respectively, $A_i = 3/2$ for scalars and fermions and 5/6 for gauge bosons, and μ is the renormalisation scale. We also have the thermal contribution (e.g. [140]),

$$V_{1-\text{loop}}^{T\neq 0} = \sum_i \frac{T^4}{2\pi^2} N_i \int_0^\infty dx x^2 \log\left(1 - (-1)^{n_F^i} e^{-\sqrt{x^2 + M_i^2(h)/T^2}}\right) \tag{3.6}$$

$$+ \delta_{n_F^i}^1 \frac{T}{12\pi} N_i \left(M_i(h)^3 - M_{i,T}^3(h,T)\right), \tag{3.7}$$

where $M_{i,T}(h,T)$ is the thermally corrected field dependent mass of the particle i. This may be approximated using a high temperature expansion ($M_i \ll T$), which yields (e.g. [141])

$$V_{\text{eff}}(h,T) \simeq V_0 + \frac{1}{2} c_h T^2 h^2 - \frac{eT}{12\pi} h^3, \tag{3.8}$$

where c_h is a coupling dependent factor which we will give later, and $e \sim \sum_i N_i g_i^{3/2}$, where the sum is over light bosonic degrees of freedom and g_i are their couplings to the Higgs. In this approximation the important order parameter can be written as

$$\frac{v_c}{T_c} \simeq \frac{e}{6\pi\lambda}, \tag{3.9}$$

where λ is the Higgs quartic coupling. This therefore explains the earlier statement that prevent sphaleron washout is more difficult for larger M_h (and hence λ). With λ fixed by the Higgs measurement and EWBG impossible in the SM we can instead try to enhance e by introducing new bosonic fields that couple strongly to the Higgs and generate the barrier in Fig. 3.2. This has been the traditional approach to EWBG in beyond the SM theories like the MSSM [142] but the large value of the Higgs mass requires the superpartners to be very light ($\sim$ 100 GeV) which is in tension with experiment [31, 143].

This need for large couplings in order to overcome the loop suppression is a problem that must be addressed by any EWBG theory that relies on large thermal loop contributions. There has therefore been considerable focus in the literature [140, 141, 144–149] on the need for tree-level barriers in the electroweak potential rather than appealing to large loop corrections. With a tree-level barrier there is no longer a need for large e and so the collider constraints can be relaxed. This can be readily achieved by including extra scalar degrees of freedom in the Higgs sector (*e.g.* [140, 141, 146–154]). For example, a direct coupling between the Higgs and an extra scalar of the form $\lambda_{hs}(S^\dagger S)(H^\dagger H)$ can generate such a tree-level barrier in the scalar potential.

There is however a problem with the above discussion. The effective potential is an inherently gauge-dependent quantity. As emphasised in [155, 156] this gauge dependence is present in the the order parameter v_c/T_c which is therefore not the correct physical quantity to use when calculating $E_{\rm sph}$ to ensure the sphalerons freeze-out after the phase transition. In these works, the order parameter is instead $\bar{v}(T_c)/T_c$, where $\bar{v}$ is a gauge independent quantity related to $E_{\rm sph}$. Here, however, we will avoid this difficulty. Motivated by the need for tree-level barriers and the desire for a gauge independent measure we will work in the high-T expansion with only the gauge invariant T^2 terms retained where the scale $\bar{v}(T_c)$ coincides with v_c. In this regime the effective potential will therefore only have terms quadratic and quartic in h and we cannot generate a barrier. Without the addition of a tree-level barrier the phase transition will therefore be second order. In this chapter we will describe a model with an additional scalar coupled to the Higgs that can generate such a barrier.

3.1.3 Higgs portal dark matter

With the discovery of the Higgs boson at the LHC we now have an excellent effective field theory that can explain all non-gravitational physics. With this effective field theory in hand we can start to examine its operators and ask how well they are

constrained. Constraining the dimension 6 operators has now become a very active and promising avenue of research (e.g. [43, 157–159]). The most intriguing operator, however, is perhaps the dimension 2, super-renormalisable operator known as the "Higgs Portal" operator [160],

$$\mathcal{O}_2 = H^\dagger H. \tag{3.10}$$

This operator is gauge invariant under the SM gauge group and so can easily form other useful operators by combining it with more singlet operators. For example we could write down and dimension 4 or 5 operators using singlet scalars, fermions or vectors,

$$\mathcal{O}_S = (S^\dagger S)(H^\dagger H), \tag{3.11}$$

$$\mathcal{O}_F = (\psi\bar{\psi})(H^\dagger H), \tag{3.12}$$

$$\mathcal{O}_V = (V^\mu V_\mu)(H^\dagger H). \tag{3.13}$$

It is important to note that $\mathcal{O}_F$ has mass dimension 5 and so is non-renormalisable, and $\mathcal{O}_V$ is not gauge invariant. It is assumed that these operators are generated in a gauge invariant, renormalisable UV completion. We met $\mathcal{O}_S$ already as an example of an operator that can help generate a barrier in the scalar potential and result in a first order electroweak phase transition.

The interactions of these particles with other SM particles are then mediated by the Higgs (which explains the name "Higgs Portal") and as a result would be very weak. These operators have therefore frequently been suggested as minimal models of dark matter (see *e.g.* [13, 161–174]). In this case an additional symmetry must be introduced to render the dark matter candidate absolutely stable. For example, if using the $\mathcal{O}_S$ operator for dark matter a $\mathbb{Z}_2$ symmetry for the S would provide the simplest possible dark matter model.

It is an attractive idea because it opens up the possibility of illuminating the properties of dark matter by studying the recently discovered Higgs boson. For example, the decay width of the Higgs could be modified through scalar mixing or decays to these dark matter particles.

3.2 Dark matter and the electroweak phase transition

In the last section we discussed two outstanding physics problems that may both be solved by coupling new particles to the Higgs boson, namely, dark matter and baryogenesis. It is therefore natural to ask if these minimal models can solve both problems at the same time. Many attempts were made in this direction using scalar extensions [148, 162, 175–178] and it was found that in the case of the real scalar singlet it was impossible to solve both problems together. Recently for example, it was found [148] that the addition of $\mathbb{Z}_2$ symmetric singlet can provide a strong electroweak phase transition but only account for at most 3% of the DM (the remaining $\gtrsim 97\%$ is assumed to come from some other mechanism). This was due to a conflict between the requirement of a large barrier and direct detection constraints that both depend strongly on one parameter: the Higgs-scalar coupling.

In this section we describe a simultaneous solution of the total DM relic density and a strongly first order phase transition. The key is to relax the $\mathbb{Z}_2$ symmetry for the scalar therefore remove some of the tension on the Higgs-scalar coupling. The scalar is therefore no longer stable and we introduce a fermionic singlet to act as the DM.

3.2.1 The model

The most general renormalisable tree-level potential of the SM extended with a scalar singlet is given by

$$V = -\frac{1}{2}u_h^2 h^2 + \frac{1}{4}\lambda_h h^4 + \frac{1}{2}u_s^2 s^2 + \frac{1}{4}\lambda_s s^4 + \frac{1}{4}\lambda_{hs} s^2 h^2 + \mu_1^3 s + \frac{1}{3}\mu_3 s^3 + \frac{1}{4}\mu_m s h^2, \quad (3.14)$$

where h and s are the physical Higgs and singlet fields respectively. The final three terms are obtained by relinquishing the requirement of a $\mathbb{Z}_2$ symmetry for the s field. A shift of the singlet field, $s \to s + \delta$, just amounts to a redefinition of parameters so we will use this freedom to set $\mu_1 = 0$ throughout.

The singlet fermion enters through the Lagrangian

$$\mathcal{L}_{DM} = \bar{\psi}(i\partial\!\!\!/ - m)\psi - g_s s\bar{\psi}\psi, \tag{3.15}$$

where we a assumed parity conservation. Since s will in general attain a vev, $\langle s\rangle = w$, the dark matter mass is $m_\psi = m + g_s w$. We will take m_ψ to be a free parameter because m may be chosen freely. To prevent ψ from mixing with the SM fermions it must carry a global $U(1)$ fermion number symmetry. In the absence of this symmetry it could couple to the SM like a right-handed neutrino and would be unstable. We therefore have a renormalisable realisation of the fermionic Higgs portal model where the $\mathcal{O}_F$ operator can be generated by integrating out the s field. This model has been considered before in [172, 179–184].

For a general choice of parameters both h and s will attain vevs. This will introduce some mixing of the gauge eigenstates h and s. To describe physical processes we have to transform into the mass eigenbasis. The mass eigenstates are given by

$$\begin{aligned} h_1 &= \sin\alpha\ s + \cos\alpha\ h \\ h_2 &= \cos\alpha\ s - \sin\alpha\ h, \end{aligned}$$

where the mixing angle α is defined by

$$\tan\alpha = \frac{x}{1+\sqrt{1+x^2}} \tag{3.16}$$

with

$$x = \frac{2M_{sh}^2}{M_h^2 - M_s^2} \tag{3.17}$$

and

$$M_h^2 = \left.\frac{\partial^2 V}{\partial h^2}\right|_{(v,w)}, \quad M_s^2 = \left.\frac{\partial^2 V}{\partial s^2}\right|_{(v,w)}, \quad M_{sh}^2 = \left.\frac{\partial^2 V}{\partial h \partial s}\right|_{(v,w)}, \tag{3.18}$$

where $v = \langle h\rangle = 246$ GeV is the Higgs vev. The mass eigenvalues are given by

$$M_{h_{1,2}}^2 = \frac{1}{2}(M_h^2 + M_s^2) \pm \frac{M_{sh}^2}{x}\sqrt{1+x^2}. \tag{3.19}$$

The definition of α ensures that $\cos\alpha > \frac{1}{\sqrt{2}}$ so h_1 is identified as the Higgs-like state and h_2 as the singlet-like state.

3.2.2 Higgs physics constraints

This mixing will introduce a coupling both between h_1 and ψ, and between h_2 and the SM particles and so will modify the Higgs phenomenology of the SM as we will now discuss. Throughout the analysis we take the Higgs-like scalar mass to lie in the 95% confidence interval[2] [186],

$$M_{h_1} = 125.2 \pm 1.8 \text{ GeV}. \tag{3.20}$$

The search for a SM Higgs-like boson at the LHC and the subsequent measurement of its properties also provides constraints for any model with an extended Higgs sector. The mixing of the Higgs and singlet states introduces a universal $\cos\alpha$ suppression of all couplings of the Higgs-like particle, h_1, relative to the SM Higgs. The signal strength of a particular channel in Higgs production is measured as the production cross section times the branching ratio. The measured signal strengths of the 125 GeV Higgs boson will therefore constrain the allowed values of $\cos\alpha$.

Additionally, the possibility of non-SM decays of the Higgs will also introduce a universal suppression, because it will dilute the branching ratios to all SM final states. If kinematically allowed, this model provides new decay modes for the Higgs-like particle h_1: $h_1 \to 2h_2,\ \bar{\psi}\psi$. There is a degeneracy between a universal suppression factor and additional Higgs decay modes that cannot be lifted until any additional branching ratio is measured directly [187]. We therefore absorb the non-standard branching ratio into a redefined suppression factor. In the presence of both effects

[2]We note that in this section we use the constraints at the time when the original work was completed [39]. For comparison the current measurement from a combined combined ATLAS and CMS study [185] is $M_{h_1} = 125.09 \pm 0.32$ GeV. The updated constraints on the Higgs mass and couplings will not qualitatively affect our conclusions.

the signal strength, μ, will be modified according to

$$\mu = \cos^2\alpha \left(1 - BR^1_{BSM}\right) \mu_{SM} = a'^2 \mu_{SM}, \tag{3.21}$$

where BR^1_{BSM} is the branching ratio of h_1 to non-standard model final states. Global analyses of Higgs couplings [41, 188] found that such a suppression is required to have $a' > 0.9$ at 95% CL in order to account for the observed Higgs signal strengths. We will see later that this constraint can be easily satisfied while satisfying both DM and electroweak phase transition constraints.

The non-observation of an additional Higgs boson can also provide a constraint on our model. The exclusion plots produced by the ATLAS and CMS collaborations are however based on a particle with SM Higgs-like couplings. In our case, all couplings of the singlet-like state will be suppressed by a factor of $\sin\alpha$ relative to the Standard Model Higgs coupling. By analogy with Higgs-like state above, the signal strength, μ, will be modified to

$$\mu = \sin^2\alpha(1 - BR^2_{BSM})\mu_{SM} = b'^2 \mu_{SM}, \tag{3.22}$$

where BR^2_{BSM} includes decays to $\psi\bar{\psi}$ and $2h_1$. Using exclusion data [189] sets a conservative bound of $b'^2 \lesssim 0.1$ for $M_{h_2} \lesssim 400$ GeV but the bound becomes significantly weaker for larger scalar masses. This is again easily avoided in our model. A recent study [190] examined the potential for future discoveries in models with an extra singlet scalar. Extrapolating current bounds they forecast that constraints on the mixing angle, α, will tighten by a factor of $2 - 3$ after the 14 TeV run of the LHC so there is significant discovery potential in the coming months.

Finally, we ensure constraints coming for electroweak precision observables are avoided using [169, 191, 192]. We find, however, that this does not significantly add to the constraints on the model once other constraints are met.

3.2.3 Dark matter relic density

We will now consider the constraints coming from the requirement that the gauge singlet fermion, ψ, plays the role of the cold dark matter of our universe. The recent data from the *Planck* satellite [8] have provided the strongest constraints to date on cosmological parameters. The 95% CL on the physical DM relic density is

$$0.1134 < \Omega_{\rm cdm} h^2 < 0.1258. \tag{3.23}$$

The relic density of the ψ field is produced via the process of thermal freeze-out discussed in Sec. 1.1. It is therefore necessary to calculate the annihilation rate of the dark matter candidate. The annihilation of $\psi\bar{\psi}$ proceeds via h_i mediated $s-$channel diagrams $\psi\bar{\psi} \to f\bar{f},\ W^+W^-,\ ZZ,\ h_ih_j,\ h_ih_jh_k$, with $i,j,k = 1,2$. We also consider $t-$ and $u-$channel annihilation into h_ih_j final states. We consider only the dominate contribution of $b\bar{b}$ and $t\bar{t}$ to the two fermion final state and neglect other subdominate channels. The cross sections to 3 body final states were calculated but it was found they were highly suppressed by the three body phase space and so are neglected from the final analysis. The full expression of σv and the relevant couplings are contained in Appendix A.

Rather than using a velocity expansion to approximate the thermally averaged cross section we adopt the approach of [193] and preform the thermal averaging explicitly. This approach is more reliable than a velocity expansion in regions near resonances and thresholds which are often crucial. The thermally averaged cross section at temperature, T, is then given by

$$\langle \sigma v_{rel} \rangle = \frac{1}{8m_\psi^4 T K_2^2(\frac{m_\psi}{T})} \int_{4m_\psi^2}^{\infty} ds\ \sigma\ s^{3/2} \beta_\psi K_1\left(\frac{\sqrt{s}}{T}\right), \tag{3.24}$$

where $\beta_\psi = \sqrt{1 - 4m_\psi^4/s}$, $\sqrt{s}$ is the centre of mass energy, and $K_{1,2}$ are the modified Bessel functions.

The fulfilment of the relic density condition is highly constraining and permits only a narrow band in the (m_ψ, g_s) plane. Fig. 3.3 shows the result for two choices of singlet-like mass, M_{h_2}. Clear features can be seen in the figure. Notable are the s-channel resonances for both h_1 and h_2 and the thresholds corresponding the WW and $h_i h_i$ channels opening. Once all channels are open the (m_ψ, g_s) plane becomes even more constrained and the coupling g_s tends to 1 for $m_\psi = 1$ TeV.

We note that for $m_\psi > M_{h_{1,2}}$ the exchange of the light scalar $h_{1,2}$ fields creates an attractive potential for the ψ field. Sommerfeld enhancement [194] can therefore play a role [172] but is a small effect and it will not change the qualitative features of our result and so is neglected.

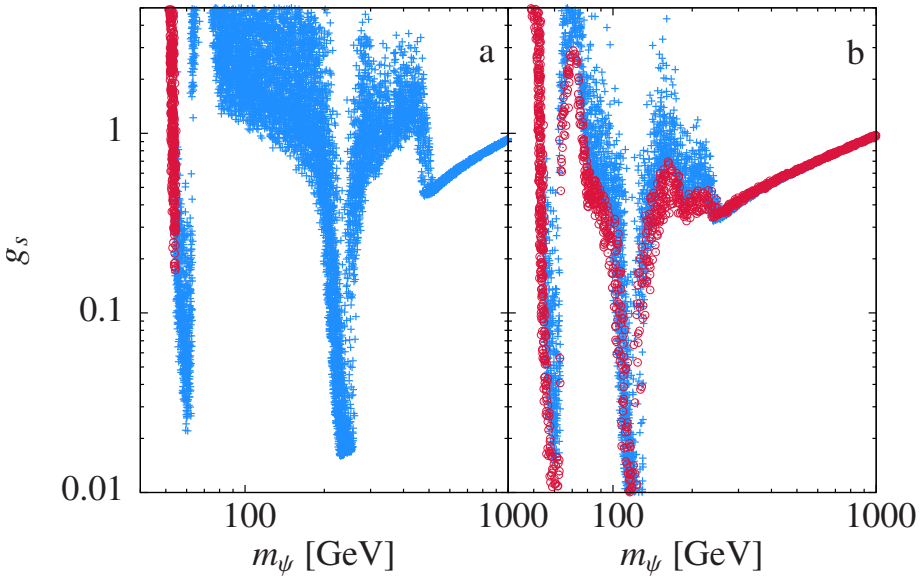

FIGURE 3.3: *Points in (g_s, m_ψ)-plane satisfying Planck relic density constraints for (a) $M_{h_2} = 500$ GeV ($\pm 5\%$), and (b) $M_{h_2} = 250$ GeV ($\pm 5\%$). The red points are ruled out by LHC Higgs physics.*

3.2.4 Direct detection of dark matter

There has been substantial effort to detect the presence of WIMP dark matter directly. Large nuclear recoil experiments are buried deep underground to shield from cosmic rays and search for WIMPs scattering elastically off heavy nuclei. The expected DM signal is model dependent and so must be calculated on a case by

case basis to constrain the model. The effective WIMP-nucleon couplings depend strongly on the details of the nuclear physics, and are given by [195, 196]

$$f_{p,n} = m_{p,n}\bar{\alpha}\left(\sum_{q=u,d,s} f_q^{p,n} + \frac{2}{9} f_g^{p,n}\right), \tag{3.25}$$

where the hadronic matrix elements, $f_q^{p,n}$, are given in [196], and $f_g^{p,n} = 1 - \sum f_q^{p,n}$. Here $\bar{\alpha}$ is related to the model-dependent coupling of the dark matter to quarks, α_q, by [180]

$$\bar{\alpha} = \frac{\alpha_q}{m_q} = \frac{g_s \cos\alpha \sin\alpha}{v}\left(\frac{1}{M_{h_1}^2} - \frac{1}{M_{h_2}^2}\right), \tag{3.26}$$

where the scattering proceeds via t-channel exchange of $h_{1,2}$. The cross section for WIMP-nucleus scattering is then

$$\sigma_N = \frac{4M_r^2}{\pi}\left(Z f_p + (A - Z) f_n\right)^2, \tag{3.27}$$

where $M_r = (1/m_\psi + 1/m_N)^{-1}$ is the reduced mass of the system. For ease of comparison with experiment this is translated into the spin-independent cross section per nucleon via [197]

$$\sigma_{SI} = \frac{1 + m_\psi^2/m_N^2}{1 + m_\psi^2/m_p^2}\frac{\sigma_N}{A^2}. \tag{3.28}$$

At the time of this work the best limits on σ_{SI} were provided by the Xenon100 experiment [198] so we use this data to constrain our model[3]. We see in Fig. 3.4 that when $m_\psi < \frac{1}{2}M_{h_2}$ we rely on resonant s-channel annihilation in order to satisfy the relic density constraints while evading direction detection. When $m_\psi > \frac{1}{2}M_{h_2}$ however we see that a large proportion of the parameter space is below the Xenon bound.

It is also worth noting that the h_2 resonance reaches $\sigma_{SI} \sim 10^{-51}$ cm^2, which would evade detection even by the next generation of direct detection experiments (e.g. [200]). These very low cross sections are a result of annihilation diagrams that are independent of $\sin\alpha$, g_s is constrained by relic density considerations but σ_{SI},

[3]We note that there has since been a factor ~ 2 improvement in these bounds by the LUX experiment [199]. Again, this improvement will have no qualitative effect on our results.

which is determined by $g_s \cos\alpha \sin\alpha$, can be very small because $\sin\alpha$ remains unconstrained. This is the case for t- and u-channel diagrams $\psi\bar{\psi} \to h_2 h_2$ and also for the s-channel diagram $\psi\bar{\psi} \to h_1 h_1$ (see Appendix A for the relevant coupling) which becomes important at the h_2 resonance.

It is important to mention that there is currently significant error in the values of the hadronic matrix elements. The points in Fig. 3.4 are quite sensitive to these errors but for simplicity we take central values and note that this may be subject to change.

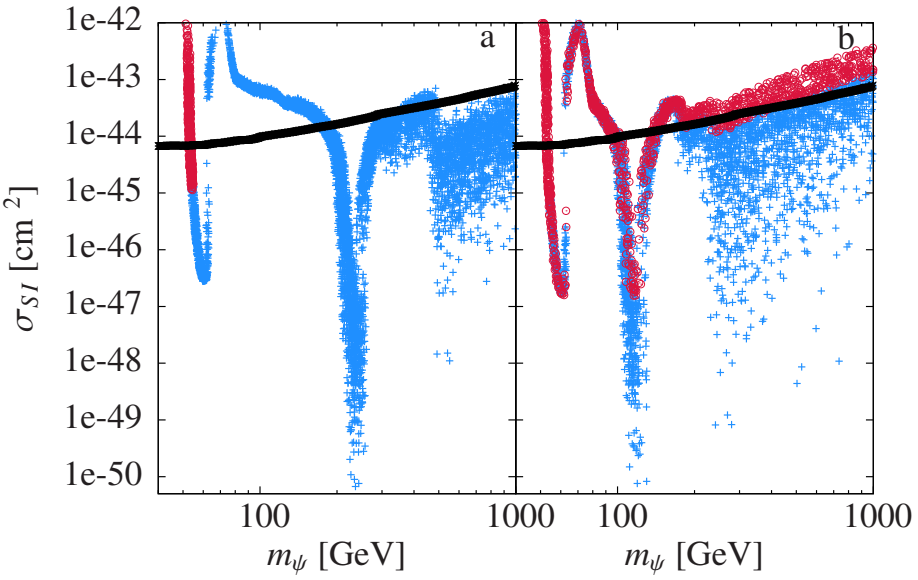

FIGURE 3.4: *The scattering cross section per nucleon satisfying Planck relic density constraints for (a) $M_{h_2} = 500$ GeV ($\pm 5\%$), and (b) $M_{h_2} = 250$ GeV ($\pm 5\%$). The red points are ruled out by LHC Higgs physics. The Xenon100 2012 bound is included for comparision.*

We do not explicitly compute constraints from indirect detections here because for this model they will be unconstraining. To understand why we can consider taking a velocity expansion of the full $\langle\sigma v_{\rm rel}\rangle$ shown in Appendix A. The procedure is to set $s = 4m_\psi^2 + m_\psi^2 v_{\rm rel}^2$ and expand $\langle\sigma v_{\rm rel}\rangle$ in powers of $v_{\rm rel}$. For the model shown here we find that $\langle\sigma v_{\rm rel}\rangle \sim v_{\rm rel}^2 + \mathcal{O}(v_{\rm rel}^4)$. When computing the annihilation cross section today to compute the flux from, say, the centre of the Galaxy we must use $v_{\rm rel}^{\rm today} \sim 10^{-3}$ which is significantly smaller than at the time of freeze-out $v_{\rm rel}^{\text{freeze-out}} \sim \sqrt{T_F/m_\psi} \sim 0.1 - 0.3$. We therefore expect very little flux from dark matter annihilating today and so cannot get useful constraints from indirect detection.

It is interesting to note however that if we allow for parity violating interactions,

$$\mathcal{L}_{DM} \to \mathcal{L}_{DM} + ig_p s\bar{\psi}\gamma_5\psi, \tag{3.29}$$

then the velocity suppression is removed [172, 201]. The velocity suppression instead appears in σ_{SI} so the direct detection results become unconstraining. This illustrates a nice complementarity between direct and indirect searches for dark matter.

3.2.5 Electroweak phase transition

The electroweak phase transition is the transition from $\langle h\rangle = 0$ to $\langle h\rangle = v$. In the case where there are two scalar fields the vev of the second field may also change. The transition therefore proceeds via $(\langle h\rangle, \langle s\rangle) = (0, w_0) \to (v, w)$, where w_0 is not necessarily zero (although it is always possible to make this choice by shifting s). As discussed in Sec. 3.1, in order for a phase transition to be considered strongly first order we must have $\bar{v}(T_c)/T_c > 1$, where T_c is the critical temperature for the phase transition and $\bar{v}(T)$ is a gauge-independent, temperature-dependent, scale that characterises the sphaleron energy [155, 202]. In the high-T effective theory considered here this scale coincides with v_c, the vev of the Higgs field at the critical temperature, although this is not true of the full 1-loop effective potential. Here we use a tree-level barrier to generate a large $\bar{v}(T_c)/T_c$ and so loop corrections are relatively small and it is sufficient to retain only the gauge invariant leading order terms in the leading order high-T expansion of the one-loop thermal potential

$$V_T = V + \left(\frac{1}{2}c_h h^2 + \frac{1}{2}c_s s^2 + m_3 s\right) T^2, \tag{3.30}$$

where

$$\begin{aligned} c_h &= \frac{1}{48}\left(9g^2 + 3g'^2 + 12y_t^2 + 24\lambda_h + 2\lambda_{hs}\right), \\ c_s &= \frac{1}{12}\left(2\lambda_{hs} + 3\lambda_s + g_s^2\right), \\ m_3 &= \frac{1}{12}\left(\mu_3 + \mu_m\right). \end{aligned} \tag{3.31}$$

Here, g and g' are the electroweak gauge couplings and y_t is the top quark Yukawa coupling (the contributions of the other quarks are sub-dominant and so have been neglected). In the $T \to \infty$ limit these thermal contributions drive $(\langle h \rangle, \langle s \rangle) \to (0, -m_3/c_s)$. The high-$T$ expansion can only be trusted up to $\bar{v}/T_c \sim 4$ so we do not consider values larger than this. It is also possible that if $\bar{v}/T_c$ becomes too large that the tunnelling probability becomes too small for the phase transition to take place during the age of the universe [203]. This typically occurs in the range $\bar{v}/T_c \sim 3 - 4$ but is model dependent, and removing these cases has no qualitative effect on our results so we omit this from the analysis.

We require our potential, V, to be well behaved. That is, we require V to be absolutely stable at tree-level by ensuring that it does not develop any directions which are unbounded from below. This requires

$$\lambda_h \lambda_s - \frac{1}{4}\lambda_{hs}^2 > 0 \qquad \text{for} \quad \lambda_{hs} < 0 \tag{3.32}$$

or,

$$\lambda_h \lambda_s > 0 \qquad \text{for} \quad \lambda_{hs} > 0. \tag{3.33}$$

We do not, however, require stability of the full quantum corrected potential but in light of the discussion of the previous chapter and recent interest in the stability of the electroweak vacuum to high scales [44, 76, 204–210] we note that models with additional scalars coupling to the Higgs are very effective at solving this problem [85, 182, 211–219]. We insist that the magnitude of all dimensionless couplings are reasonably small (< 1.5) so that the theory will remain perturbative, although a full analysis of the relevant renormalization group equations has not been carried out.

In order to search numerically for models with $\bar{v}/T_c > 1$ we must ensure that electroweak symmetry breaking is viable, and that the broken vacuum state we end up in is the global minimum of the zero temperature potential. One approach is to select a random set of parameters, ensure that the potential is bounded from below, find all the minima of the potential and examine how they change with changing T.

We can then check if (v, w) is the global minimum at $T = 0$, and locate the critical temperature T_c when we have two degenerate minima. To find the minima we need to find the intersection of the curves,

$$\frac{\partial V_T}{\partial h} = 0 \implies \begin{cases} h = 0 \\ h^2 = D_h^2(s) = \frac{1}{2\lambda_h}(2\mu_h^2 - \mu_m s - \lambda_{hs} s^2 - 2c_h T^2), \end{cases} \tag{3.34}$$

with the curve

$$\frac{\partial V_T}{\partial s} = 0 \implies h^2 = D_s^2(s) = -\frac{\mu_s^2 s + \lambda_s s^3 \mu_3 s^2 + (m_3 + c_s s)T^2}{\frac{1}{4}\mu_m + \frac{1}{2}\lambda_{hs} s}. \tag{3.35}$$

The points of intersection define critical points of which a subset are minima (determined in the usual way with the second derivative test). The problem with this approach is that for a random set of parameters we are not guaranteed to have a tree-level barrier and so may never find a situation with two distinct but degenerate minima.

Two illustrative examples are shown in Fig. 3.5 and Fig. 3.6 where we plot the minima evolving with temperature. The circles indicate minima and when there is more than one the black circle is the deepest. In Fig. 3.5 we can see that between $T = 100$ GeV and $T = 110$ GeV the deepest minimum switches from the broken minimum at $h \sim 150$ GeV to the symmetric minimum with $h = 0$ GeV. The critical temperature T_c at which these minima are degenerate is therefore in the range $100 - 110$ GeV so the order parameter is $\bar{v}/T_c \sim 1.5$ and we have a strongly first order phase transition. We can see in the case of Fig. 3.6 we never have a coexistence of broken and unbroken minima. Instead we have the broken minimum smoothly transitioning to the unbroken minimum as the temperature increases so we have a second order phase transition.

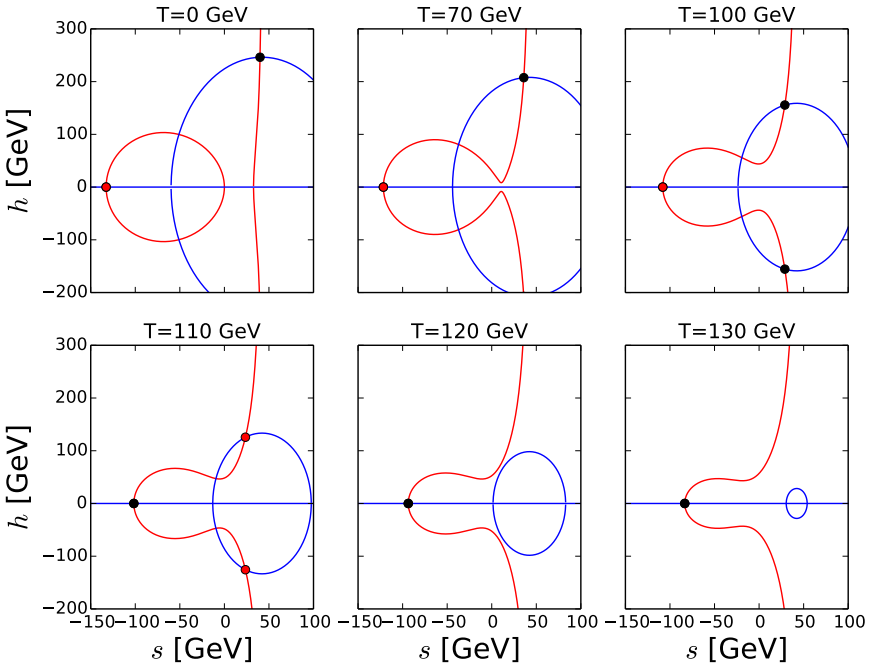

FIGURE 3.5: *Plot of D_h^2 and $h = 0$ (blue) with D_s^2 (red) in the $h - s$ plane. Intersection of the red and blue points are critical points of the thermal potential with dots indicating minima (black dots are deepest). We see the appearance of degenerate minima which are separated by a potential barrier.*

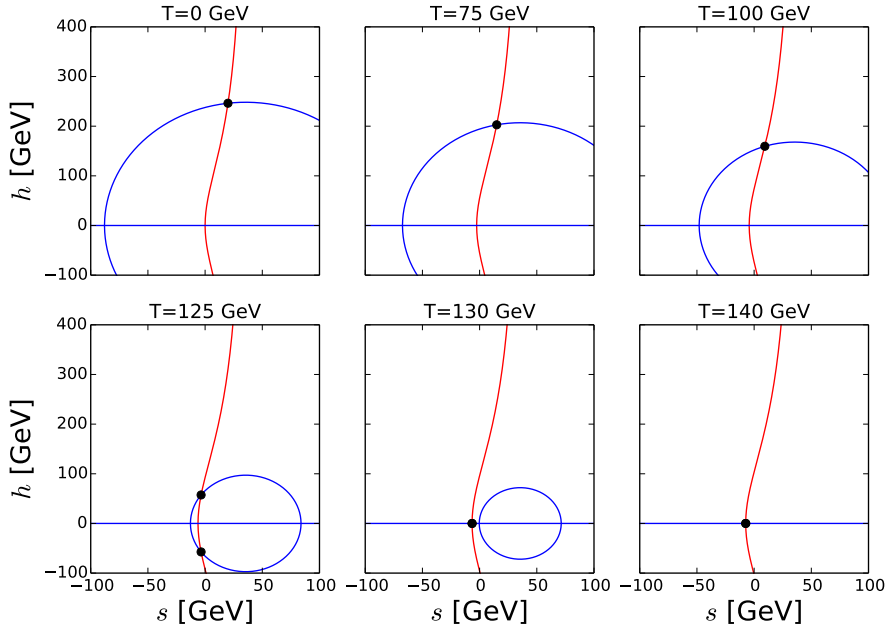

FIGURE 3.6: *Same as Fig. 3.5 but here we do not find coexisting broken and unbroken minima so we cannot have a first order phase transition.*

To remove the need for a numerical search for degenerate minima that may not exist we instead closely follow the recipe provided in [140]. In [140] the potential is re-parametrised using parameters that are central to the study of the critical points of the potential e.g. the second derivatives of the potential. In their parametrisation the conditions necessary for having coexisting degenerate minima become must simpler to write down analytically compared to using the Lagrangian parameters directly. We can then demand that these conditions are satisfied and therefore have a thermal potential at $T = T_c$ where T_c is now a free parameter. Once T_c is chosen we can determine the zero temperature parameters of the V_T in the parametrisation of Eq. (4.13) which we can then use in our dark matter calculation.

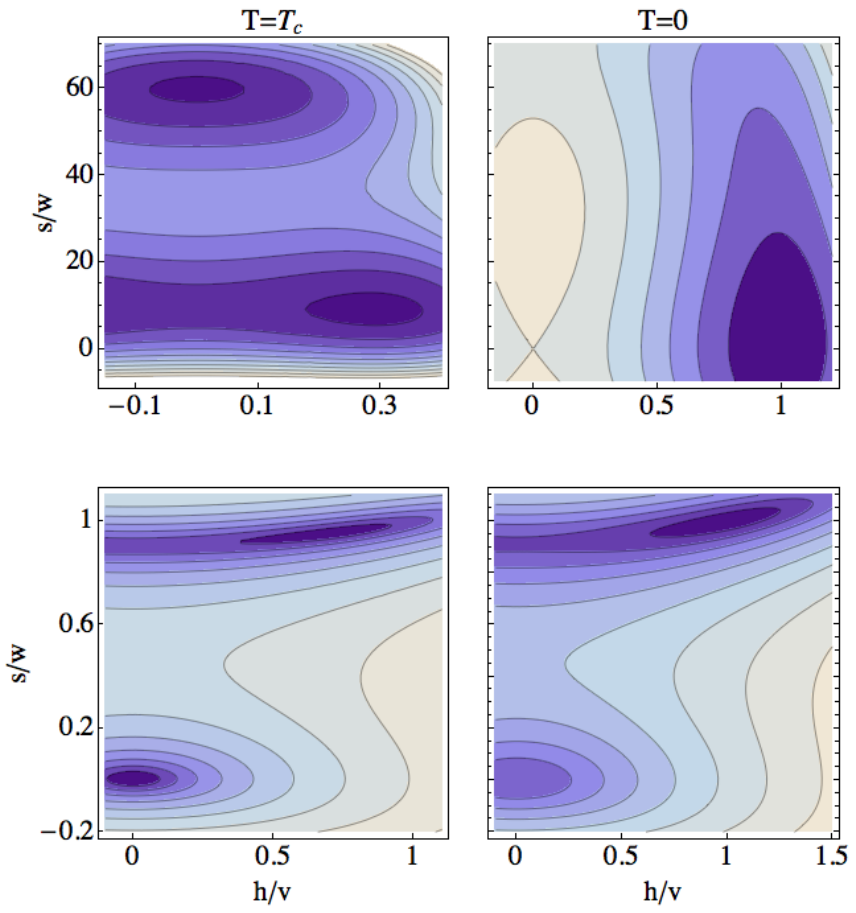

FIGURE 3.7: *Thermal effective potential at $T = 0$, T_c for $\Delta w < 0$ (top), and $\Delta w > 0$ (bottom). The potential at $T = T_c$ shows two degenerate minima and as T is lowered the electroweak breaking vacuum becomes the global minimum.*

We find that first order phase transitions mostly fall into two broad classes: a) $\Delta w = w - w_0 < 0$ and b) $\Delta w > 0$ (note that the sign is coordinate basis dependent and can always be swapped by relabelling $(s, \mu_m, \mu_1, \mu_3) \to (-s, -\mu_m, -\mu_1, -\mu_3)$ but the relative sign between the two modes of breaking will remain). Fig. 3.7 shows examples of the shape of the thermal potential at $T = 0, T_c$ for each case. If we were to use the $\mathbb{Z}_2$ model it was pointed out in [140] that for case b) it is not possible to have a tree-level barrier, and that the case (a) must proceed via $(0, w_0) \to (v, 0)$. If the vacuum had non-zero w the $\mathbb{Z}_2$ symmetry is broken by the vacuum and renders the scalar unstable preventing its use as a DM candidate.

After a large monte carlo scan[4] of the parameter space we found many models that satisfy all constraints. Fig. 3.8 shows the distribution of the derived values of $\bar{v}/T_c$. We see that we can easily achieve large values for $\bar{v}/T_c$. Fig. 3.9 shows the distribution of some of the key parameters after all cuts are made. We see that Higgs physics constraints, summarised in a' and b', are generically avoided in models that satisfy the DM and phase transition constraints.

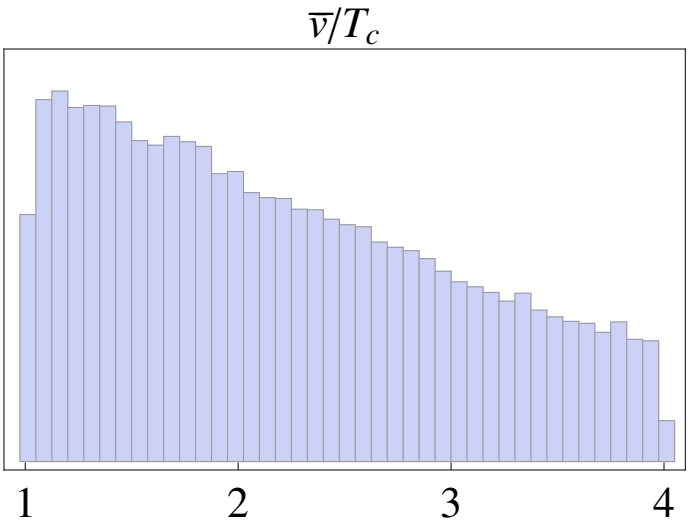

FIGURE 3.8: *Distribution of the order parameter, $\bar{v}/T_c$, for models satisying all constraints. We find many models with $\bar{v}/T_c \gg 1$ indicating a strong electroweak phase transition as required for electroweak baryogenesis.*

[4]We use flat priors for the convenient choice parameters described in [140]. These parameters are then transformed into those described in Eq. (4.13). As such, the density of points in plots (e.g. Fig. 3.3) does not necessarily correspond directly to regions of higher probability.

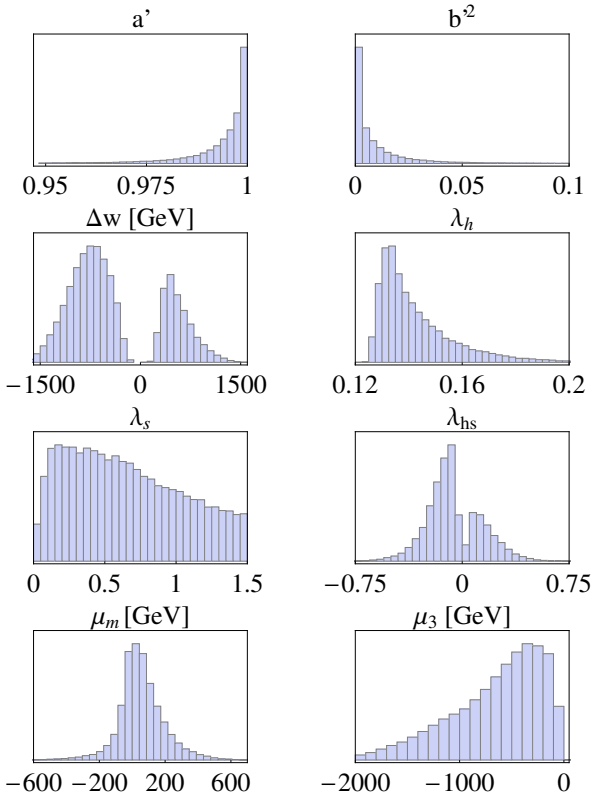

FIGURE 3.9: *Distribution of some key parameters that satisfy all constraints from dark matter, the electroweak phase transition, Higgs physics, and electroweak precision tests.*

3.3 Conclusion

We have considered a minimal extension of the SM and showed that it can simultaneously explain DM while providing a strongly first order electroweak phase transition as required for electroweak baryogenesis. In contrast with some recent attempts in this area we find that by considering terms linear and cubic in s and adding a singlet fermion both problems are easily solved. It is also possible to avoid current constraints from LHC Higgs physics because small mixing angles are preferred.

The next generation of dark matter direct detection experiments could push the upper bound on σ_{SI} to $\sim 10^{-47}$ cm^2 [200]. This would rule out a significant proportion of the parameter space but very small values of $\sin\alpha$ will allow these limits to be evaded for $m_\psi \sim \frac{1}{2}M_{h_2}$ or $m_\psi > M_{h_2}$. If future collider data can improve the Higgs physics constraints from the 10% level to the 1% level (e.g. with the HL-LHC [220])

this would still not be enough to rule out this model completely (see Fig. 3.10) but would explore large proportion of the parameter space, offering significant discovery potential.

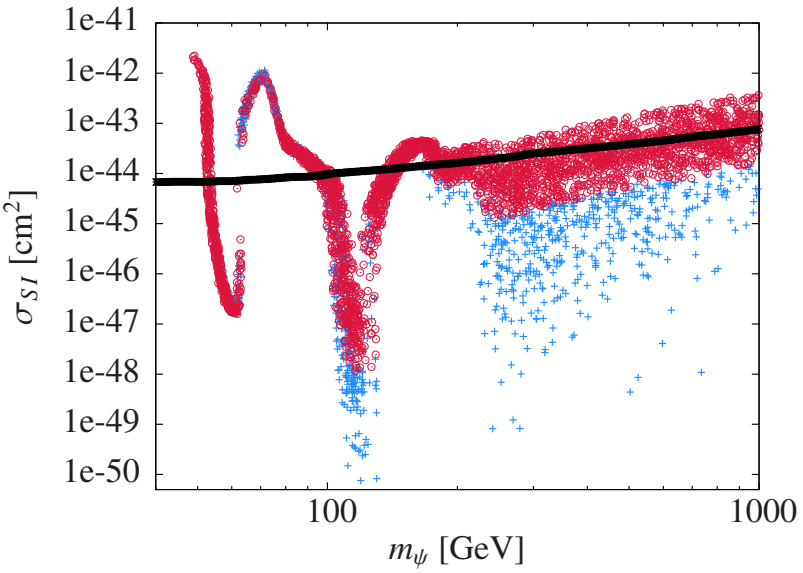

FIGURE 3.10: *Scattering cross section per nucleon for $M_{h_2} = 250$ GeV ($\pm 5\%$) with the constraints on a' and b'^2 improved from 10% level to 1% level. The Xenon100 2012 bound is included for comparision.*

Here we have limited our analysis to searching for first order phase transitions using only the leading order terms in the high-T expanded thermal potential. After the publication of this work a paper appeared [221] which included the full 1-loop contribution to the thermal effective potential and found that the parameter space of viable models was somewhat extended. The analysis does however suffer from the gauge dependence problem mentioned earlier. It would be interesting to see the result of a gauge independent 1-loop analysis using the approach of [156].

While the results presented here are encouraging we have not presented a full solution to the problem of electroweak baryogenesis. For a complete study we must include the origin of additional CP-violation and study the dynamics of the asymmetry accumulation near the bubble walls during the phase transition. Since we know that CP-violating interactions must occur in the bubble walls it must arise in the Higgs sector. An example of a suitable interaction (suggested in [154]) is a modification of

the top quark Yukawa interaction to

$$y_t \bar{Q}_L H \left(1 + \delta \frac{s}{\Lambda}\right) t_R, \tag{3.36}$$

where $\bar{Q}_L$ is the left-handed quark doublet, Λ is a mass scale for new physics that generates the interaction, and δ is a complex phase. It would be interesting to see if a complete solution to the baryogenesis problem will impact the parameter space much more than has been described here and perhaps make the model even more predictive.

Chapter 4

Unifying Inflation and Dark Matter with the Peccei-Quinn Field

4.1 Introduction

In Sec. 1.1 we said that there are two leading candidates for dark matter: WIMPs and axions. In Chapter 2 we presented an example of a WIMP dark matter model that can also give rise to a strongly first order electroweak phase transition. In this chapter we will discuss the axionic dark matter paradigm. As we will see, the cosmology of axionic dark matter is intimately linked with the details of primordial inflation. In fact, unless the scale of inflation is sufficiently low, the existence of axionic dark matter appears to be ruled out in most circumstances. Here we will present a new approach that aims to resolve this tension between high scale inflation and axionic dark matter by unifying both phenomenon with a single field. We will first discuss axions as a solution to the strong-CP problem and as a dark matter candidate. We will then introduce the idea of isocurvature perturbations that is the cause of the tension with high scale inflation. In the remainder of the chapter we will present our solution and discuss its phenomenology.

4.1.1 Axions and the strong-CP problem

The history of axions starts with the $U(1)_A$ problem of QCD . If we consider only light quark generations then the limit of massless quarks appears to be a good approximation to QCD since $m_u, m_d \ll \Lambda_{QCD} \sim 200$ MeV, where Λ_{QCD} is the QCD confinement scale. In this limit the theory has global $U(2)_V \times U(2)_A$ symmetry where the subscripts V and A stand for vector and axial vector respectively. In the real world, with light quarks that weakly break the symmetry, the $U(2)_V = SU(2)_I \times U(1)_B$ is manifested as the approximate isospin and baryon number symmetries. In the axial-vector case however the global symmetry is broken spontaneously by quark condensates (e.g. $\langle q\bar{q}\rangle \neq 0$), giving rise to the pions which are pseudo Nambu-Goldstone bosons of the $SU(2)_A$ subset of the approximate $U(2)_A$ symmetry. We should also expect an additional light meson as a result of the breaking of the remaining $U(1)_A$ symmetry with a mass $\sim m_\pi$ but such a meson is not observed. This apparent absence of an approximate $U(1)_A$ symmetry in QCD became known as the $U(1)_A$ problem [222].

It turns out that the $U(1)_A$ symmetry is anomalous and so breaks down in the quantum theory, resolving the problem. It was known for some time that the chiral current was apparently anomalous with

$$\partial_\mu J^\mu_5 \sim \text{Tr } G^{\mu\nu}\widetilde{G}_{\mu\nu}, \tag{4.1}$$

but this vanishes in perturbation theory. It was shown by 't Hooft [223] that the symmetry is violated by instantons, non-pertubative quantum mechanical objects that are a result of the vacuum structure of $SU(3)$. Similar to $SU(2)$ (discussed of Sec. 3.1.1) the non-trivial homotopy of $SU(3)$ means that there are an infinite number of distinct vacua that are related by large gauge transformations. The true vacuum of $SU(3)$ (known as the theta vacuum) is a superposition of all these distinct vacua,

$$|\theta\rangle = \sum_m e^{-im\theta}|m\rangle, \tag{4.2}$$

where m is the winding number of vacuum state $|m\rangle$. The effect of living in this theta vacuum can be incorporated into the theory in the classical vacuum by adding a term to the action given by

$$S_\theta = \frac{\theta}{32\pi^2}\int d^4x \ \mathrm{Tr}\ G^{\mu\nu}\widetilde{G}_{\mu\nu}\,. \tag{4.3}$$

The integrand is in fact a total divergence so we can see that it only has an effect as result of the existence of non-trivial boundary conditions for the gauge fields.

Before we discuss the implications of this term we might first ask why an analogous term is not found in the weak interactions. After all we saw in Sec. 3.1.1 that $SU(2)$ also had a non-trivial vacuum structure so we might expect that a weak interactions also have a superposition vacuum. In that case however we were free to use the anomalous $U(1)_{B+L}$ symmetry to rotate away the theta term without affecting the remainder of the Lagrangian i.e. we make a $U(1)_{B+L}$ transformation that generates an $F\widetilde{F}$ term that exactly cancels the theta term. In the case of QCD we might try to similarly rotate away the contribution of (4.3) using the $U(1)_A$ symmetry. This, however, does not work because the mass terms of the quark sector explicitly break the $U(1)_A$ symmetry and so will pick up an additional phase under chiral field transformations. When the quark mass matrix is diagonalised we will regain a contribution to (4.3). As result we can never fully rotate away the physical contribution of the theta term in QCD as we could for the weak interactions.

We are therefore forced to accept the presence of (4.3) in the SM. This term will however violate P and CP. For $\theta \neq 0$ this term will therefore contribute to the electric dipole moment for the neutron which is very tightly constrained ($d_n < 2.9 \times 10^{-26} e$ cm [224]) implying that θ must be tuned to be very small ($\lesssim 10^{-11}$ [225]). This unnatural tuning is known as the strong-CP problem.

The most popular solution to this problem was provided by Peccei and Quinn [226, 227]. The solution is to introduce another anomalous global chiral $U(1)$ symmetry (hereafter referred to as $U(1)_{PQ}$) that is spontaneously broken by a scalar field. The Goldstone boson of the broken symmetry scalar field is known as the axion, a

[228, 229]. $U(1)_{PQ}$ transformations of a then generates a contribution to the θ-term effectively replacing $\theta \to \theta_0 + a/f_a$, where θ_0 is the bare value in the theory without PQ symmetry[1] and f_a is the symmetry breaking scale. This therefore promotes θ to a dynamical field. The interaction with QCD instantons will then give rise to a scalar potential for a given by

$$V(a) \simeq m_a^2 f_a^2 (1 - \cos\theta)\,, \tag{4.4}$$

where m_a is the axion mass, f_a is the axion decay constant, and $\theta = a/f_a$. The θ dependence of the potential is required to be periodic in order to respect the shift symmetry of the axion (which is of course an angular variable). The scale of the potential is set by the instanton effects where $m_a^2 f_a^2 \sim \Lambda_{QCD}^4$ and $\Lambda_{QCD} \simeq 200$ MeV is the QCD scale. This potential causes the θ-term to dynamically relax to zero solving the strong CP problem (see Fig. 4.1).

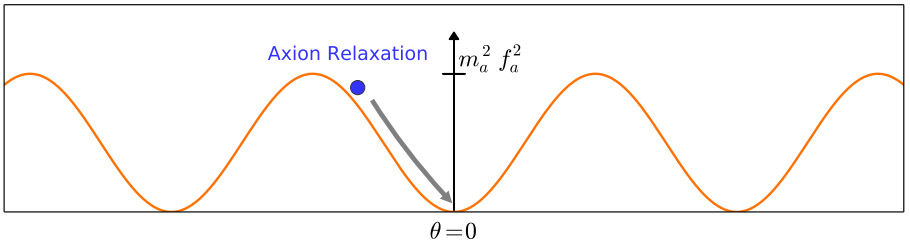

FIGURE 4.1: *A schematic representation of the dynamical relaxation of the QCD θ-term to zero as a result of the instanton induced axion potential.*

The original axion models had weak scale axions and were quickly ruled out when these axions could not be discovered. Since then there has been much work in so-called 'invisible' axion models where the scalar field that spontaneously breaks the PQ symmetry is a SM singlet and can easily be made to break the symmetry at a scale much higher that the weak scale. This renders the axion very weakly coupled and thus evades constraints. We will see however that these axions can still have very interesting phenomenology. The two most popular models for 'invisible' axions are so-called KSVZ [230, 231] and DFSZ [232, 233] models [2]. These models differ

[1] In what follows, unless otherwise specified, this θ_0 will be implicitly absorbed into θ.

[2] KSVZ axions are named after the authors Kim, Shifman, Vainshtein, and Zakharov. DFSZ axions are names after the authors Dine, Fischler, Srednicki, and Zhitnitsky.

in the content of fields which carry PQ charge and so have slight differences in how the axion will couple to SM fields. Here however we will mainly be concerned with the SM singlet PQ scalar that breaks the $U(1)_{PQ}$ which is common to both models.

4.1.2 Axionic dark matter

Soon after axions were first discussed it was realised that they may have cosmological consequences [234–241]. The breaking of the PQ symmetry in the early Universe can produce axion relics that are considered a promising alternative to thermal WIMP dark matter. Depending on the reheating temperature there are different ways that dominate the production of axions non-thermally. Firstly, if the reheating temperature is low such that the PQ symmetry is not restored by thermal corrections to the potential after inflation then the dark matter is produced by the misalignment mechanism. As the Universe cools during inflation the symmetry will break at a $T \sim f_a \gg \Lambda_{QCD}$ so the QCD instanton effects are not important and the axion potential is very nearly flat. We therefore generically expect an initial value $\theta_i \neq 0$. At $T \sim \Lambda_{QCD}$ the instanton effects become important, the axion mass becomes significant and θ begins to oscillate about $\theta = 0$. Since the axion is extremely weakly coupled there is almost no damping in this oscillation (apart from that caused by Hubble expansion) so this coherent state of axions can contribute significantly to the energy density today and behaves like cold dark matter. The relic density is then given by (e.g. [242])

$$\Omega_a^{\rm mis} h^2 = 0.1199 \left(\frac{\langle \theta_i^2 \rangle}{0.28}\right) \left(\frac{f_a}{10^{12}\ \text{GeV}}\right)^{7/6}, \tag{4.5}$$

where the angle brackets denote averaging over many possible values for the initial misalignment angle and so is a typical value and for simplicity we have dropped anharmonic contributions to the potential and possible dilution by entropy production after the QCD phase transition (see e.g. [243] for more details and discussions of the accuracy and limitations of this formula). It is important to note that we are not completely free to choose $\langle \theta_i^2 \rangle$. In the case where the bare theta term $\theta_0 \sim \mathcal{O}(1)$ and

the axion contribution $a/f_a \sim \mathcal{O}(1)$ then we expect in the absence of fine-tuning that the net θ to be uniformly distributed in the range $[-\pi, \pi]$, leading to $\langle\theta_i^2\rangle = \pi^2/3$. In this case, in order to avoid overclosing the Universe we must restrict $f_a < 10^{12}$ GeV. In order to allow for larger f_a there must be some cancellation in the bare and axion contributions such that $\langle\theta_i^2\rangle$ is smaller than we would otherwise expect. We can see from Eq. (4.5) that if $f_a \gg 10^{12}$ GeV we must reintroduce significant fine-tuning in θ_i. This has become known as the anthropic axion window. We cannot however arbitrarily tune θ_i because even if the initial value is zero the axion will receive quantum fluctuations $\sim H/2\pi$ during inflation that will give rise to a non-zero net θ_i. The allowable range for $\langle\theta_i^2\rangle$ is therefore $\sim [(H/2\pi f_a)^2, \pi^2/3]$.

If, on the other hand, the reheating temperature is large enough to restore to the symmetry then cosmic strings produced by the subsequent re-breaking of the symmetry cannot be inflated away. This will be the case if thermal contribution to the effective mass is enough to stabilise the potential at the origin, i.e.

$$m_{\text{eff}}^2 = \frac{\lambda T_{rh}^2}{2} > \lambda f_a^2, \tag{4.6}$$

or

$$T_{rh} > \sqrt{2} f_a, \tag{4.7}$$

where λ is the quartic self-coupling of the PQ scalar and the factor of $1/2$ is a 1-loop coefficient in the high temperature limit when we neglect possible couplings to other fields.

These cosmic strings quickly decay by radiating axions. After the QCD phase transition these axions will acquire a significant mass and behave like cold dark matter [244]. The energy density of dark matter axions produced in this phase can be calculated as [242, 245–247]

$$\Omega_a^{\text{str}} h^2 \simeq (1.16 - 11.6) 0.1199 \left(\frac{f_a}{10^{12}\ \text{GeV}}\right)^{1.18}, \tag{4.8}$$

where the prefactor reflects various theoretical uncertainties regarding string decay

and the QCD phase transition [243]. In this situation we can therefore also introduce a conservative upper bound on f_a in order not to over produce DM of

$$f_a < 1.25 \times 10^{11} \text{ GeV} . \tag{4.9}$$

Note that we will still have a contribution to the relic density from misalignment but it will be sub-dominant.

Axions can of course also be produced thermally by freeze-out. This however would require larger than typical axion masses (i.e. low f_a, so axions couple to matter more strongly) which, as we will see later, leads to tension with astrophysical constraints. This means that in practice only a negligible amount of dark matter can be produced this way so we do not consider it any further here.

4.1.3 Isocurvature from axions

As we have already mentioned, the axion will be approximately massless during inflation and will receive quantum fluctuations $\sim \mathcal{O}(H/2\pi)$ during each e-fold of inflation. If H is large compared to f_a then the fluctuations $\delta\theta$ will be large. Since, however, the axion is approximately massless during inflation these fluctuations will have negligible contribution to the total energy density. They are therefore isocurvature perturbations i.e. they do not contribute to the curvature perturbation but are instead perturbations in the axion number density. Following the QCD phase transition the axion acquires a mass and the axion density fluctuations contribute to energy density fluctuations. To conserve energy there are corresponding fluctuations in the photon density which are imprinted in the temperature fluctuations of the CMB. Since the axion couples very weakly to rest of the SM the isocurvature fluctuations will be uncorrelated with the adiabatic fluctuations. The presence of isocurvature fluctuations will modify the temperature power spectrum because the acoustic peaks are out of phase with the adiabatic mode by $\sim \pi/2$. Measurements of the CMB (by e.g. *Planck* [1]) can therefore put constraints on the relative fraction

of isocurvature modes,

$$\alpha = \frac{\langle (\delta T/T)^2_{iso} \rangle}{\langle (\delta T/T)^2_{tot} \rangle} \lesssim 0.036, \tag{4.10}$$

at $k = 0.002\ \mathrm{Mpc}^{-1}$. We will use this as our constraint at arbitrary r, but technically this is incomplete. As we will shortly see, isocurvature constraints usually force $r \approx 0$ for axions. Axion isocurvature as constrained in Ref. [1] therefore assumes $r = 0$, and consistent with this takes the isocurvature spectrum to be scale invariant. Constraints on α will also in general be correlated with those on r. The combined effect of r and α constraints on axions is so strong, however, that even an $\mathcal{O}(1)$ change to the constraint is relatively unimportant. Therefore, despite the complications just discussed, the percent-level bound of Eq. (4.10) will provide a good estimate of the constraints on the axion parameter space in our model including r.

The amplitude of isocurvature modes increase (decreases) with H (f_a) so Eq. (4.10) is a very useful observable to constrain the $H - f_a$ plane of axion models [248, 249]. We will see later this turns out to be a very strong constraint on axionic dark matter. In the remainder of this chapter we will introduce a new mechanism to alleviate the pressure imposed on axion models by this bound. The mechanism relies on inflating the Universe with the PQ field. The introduction of the PQ field could therefore be a very economical solution to three major problems of particle physics and cosmology: inflation, dark matter, and the strong-CP problem.

4.2 Axion dark matter and the tensor-to-scalar ratio

As we have already discussed there has been much progress in the experimental investigation of inflation in recent years. This culminated in BICEP2's now withdrawn claim of a measurement of primordial gravitational waves. In the wake of this claim there was some concern about its implications for axionic dark matter [250, 251]. In the last section we saw that axions can be a source of isocurvature modes. The BICEP2 claim of $r \sim 0.16$ would set the Hubble scale during inflation to be so large

as to firmly rule out axionic dark matter unless the PQ symmetry is restored after inflation. This can be difficult however in models with large f_a which are common in top-down approaches such as string theory [252][3].

Fortunately, as we mention already, the B-modes observed by BICEP2 were not completely primordial in origin so axionic dark matter survives. We will see later however that the problem persists for any value of r that is large enough to be observed. Such a detection could be made, for example, by SPIDER [105], and the consequences for inflationary cosmology and the axion would still be just as profound [248][4]. It would therefore be preferable to create a model of axionic dark matter that was not so sensitive to this problem.

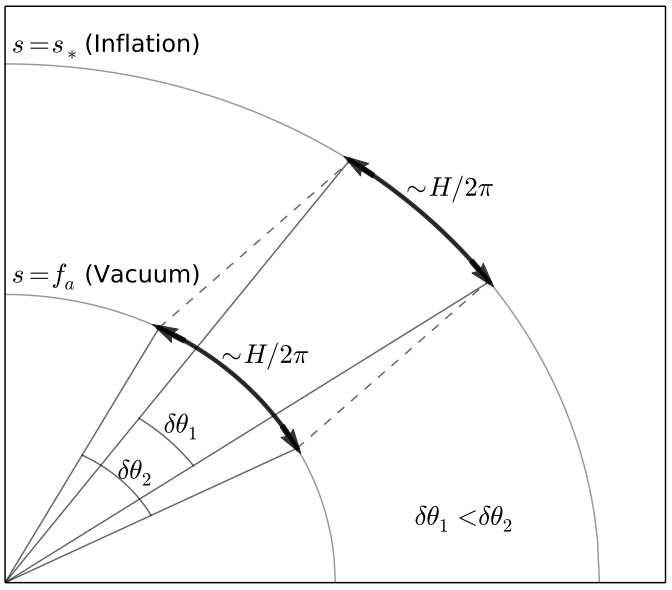

FIGURE 4.2: *Schematic of our mechanism. Isocurvature fluctuations in the axion field, $\delta\theta$, are reduced if the radial field, s, lies at higher values during inflation, s_*, compared to the low energy minimum, f_a.*

Here we propose such a model and show that if the PQ field itself plays the role of the inflaton then the problem of isocurvature modes can be dramatically reduced

[3]See [253, 254] for recent top-down models with small f_a.

[4]An ultimate, cosmic variance limited, measurement of r using 21cm lensing could in principle reach $r \sim 10^{-9}$ [255, 256]. As we will see, even this would provide a constraint on axion physics.

allowing for high f_a axion DM to be compatible with high scale inflation (see [257–260] for other recent attempts to suppress axion isocurvature modes).

Fig. 4.2 shows schematically that if the radial part of the PQ field, s, lies at values larger than f_a during inflation then the isocurvature fluctuations of the axion field will be reduced in amplitude. Isocurvature amplitude is proportional to the ratio $\delta\theta/\theta$, where θ is the axion (angular) direction of the PQ field. The DM abundance fixes θ. Inflation fixes the dimensionful field displacement at $H/2\pi$, however this subtends a smaller angle $\delta\theta$ if it is fixed at large rather than small radius (see Fig. 4.2).

4.2.1 Inflation with the radial PQ field

The PQ field, S, is a complex SM singlet charged under a global $U(1)_{PQ}$ symmetry broken at scale f_a. The axion, a, is the angular part of this field. The radial part, s, is minimised at f_a. Our mechanism for reducing isocurvature perturbations works by taking $s \gg f_a$ during inflation. One mechanism by which this can be achieved is to take s to be the inflaton.

The potential for the PQ field is given by

$$V = \frac{1}{4}\lambda\left(s^2 - f_a^2\right)^2, \tag{4.11}$$

where, following the case for the Higgs field in chapter 2, we have set $S = \frac{1}{\sqrt{2}}(0, s + f_a)^T$ in the vacuum. At large s this takes the form of a $\lambda\phi^4$ single-field inflation model. Such models are excluded at high confidence level by *Planck* constraints on r and the scalar spectral tilt, n_s [1]. To work around this we introduce a non-minimal coupling, ξ, between the s field and gravity in same way as we saw for Higgs inflation in Sec. 2.2.1 (see Refs. [261–267] for other treatments of this model and embeddings of it in supergravity/string theory)

$$S_J = \int d^4x\sqrt{-g}\left[-\left(\frac{M_{pl}^2 + \xi s^2}{2}\right)R + \frac{1}{2}(\partial s)^2 - V\right]. \tag{4.12}$$

This then gives rise to the Einstein frame potential,

$$V_E = \frac{V}{(1+\xi s^2/M_{pl}^2)^2} = \frac{\frac{1}{4}\lambda\left(s^2 - f_a^2\right)^2}{(1+\xi s^2/M_{pl}^2)^2}, \tag{4.13}$$

which can give rise to phenomenologically successful inflation. The slow roll parameters are then modified slightly to,

$$\epsilon = \frac{1}{2}M_{pl}^2\left(\frac{V_E'}{V_E\sigma'}\right)^2, \tag{4.14}$$

$$\eta = M_{pl}^2\left(\frac{V_E''}{V_E\sigma'^2} - \frac{V_E'\sigma''}{V_E\sigma'^3}\right). \tag{4.15}$$

For the analysis of inflation in this model it is sufficient to take the limit $f_a \to 0$ in equation (4.13). For $f_a < M_{pl}$ the effect of non-zero f_a is negligible and we may treat r and f_a as independent (in [262] the regime with $f_a \gg s$ during inflation is studied and then effect becomes substantial).

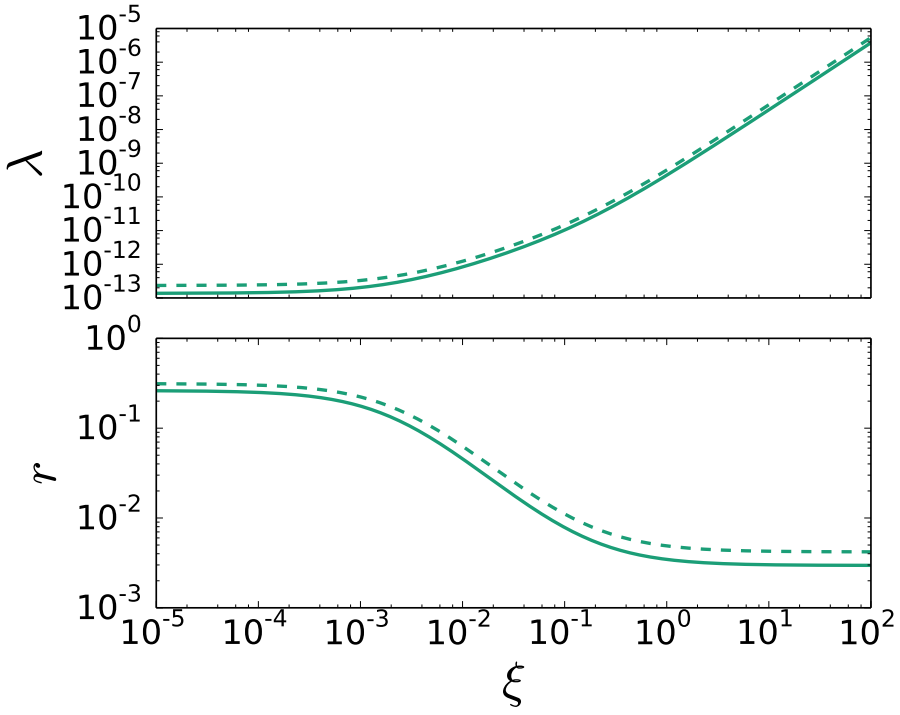

FIGURE 4.3: *The dependence of the self-coupling, λ, and the tensor-to-scalar ratio, r, on the non-minimal couping to gravity, ξ, for $N = 60$ (solid) and $N = 50$ (dashed). Here, for each value of ξ, λ is fixed using $A_s = 2.196 \times 10^{-9}$ and we take the limit $f_a \to 0$.*

Since r can be determined from ξ we have a two-parameter model of inflation. Holding the normalisation $A_s = 2.196 \times 10^{-9}$ fixed reduces this to a one-parameter family of models. This is demonstrated in Fig. 4.3 (upper panel) where we show the dependence of λ on ξ. We show $r(\xi)$ in one dimension in Fig. 4.3 (lower panel): as $\xi \to 0$, r asymptotes to its value in $\lambda\phi^4$ inflation. In the opposite regime of large ξ the tensor-to-scalar ratio goes to a minimum value $r_{\rm min} \simeq 3.3 \times 10^{-3}$ for $N = 60$, where N is the number of e-folds of observable inflation. In this large ξ limit this model is in fact an example of an α-attractor [268–271] with $\alpha = 1$, and has $n_s = 1 - 2/N$ and $r = 12/N^2$ in the large ξ limit.

This scenario is different from the Higgs inflation one of Sec. 2.2.1 because λ has not been determined by a mass measurement. We are therefore able to escape some of the technical difficulties of Higgs inflation. Recall that $M_h = 125$ GeV required $\xi \sim 10^4$ which caused problems with the unitarity of the theory at high scales. The theory will be free of these issues if the unitarity bound is much larger than the Hubble scale during inflation, i.e.,

$$\Lambda \simeq \frac{M_{\rm pl}}{\xi} \gg H \simeq \sqrt{\lambda}\frac{M_{\rm pl}}{\xi}, \tag{4.16}$$

or,

$$\sqrt{\lambda} \ll 1, \tag{4.17}$$

which is marginal at best in the case of $\lambda \sim 0.13$ for the Higgs case but we can see in Fig. 4.3 that this is readily achievable with the PQ field.

The resulting $n_s - r$ plane predictions are shown in Fig. 4.4, along with the 1 and 2σ contours from *Planck*. Our model is flexible enough to accommodate a large part of the interesting $n_s - r$ parameter space as we await future measurements.

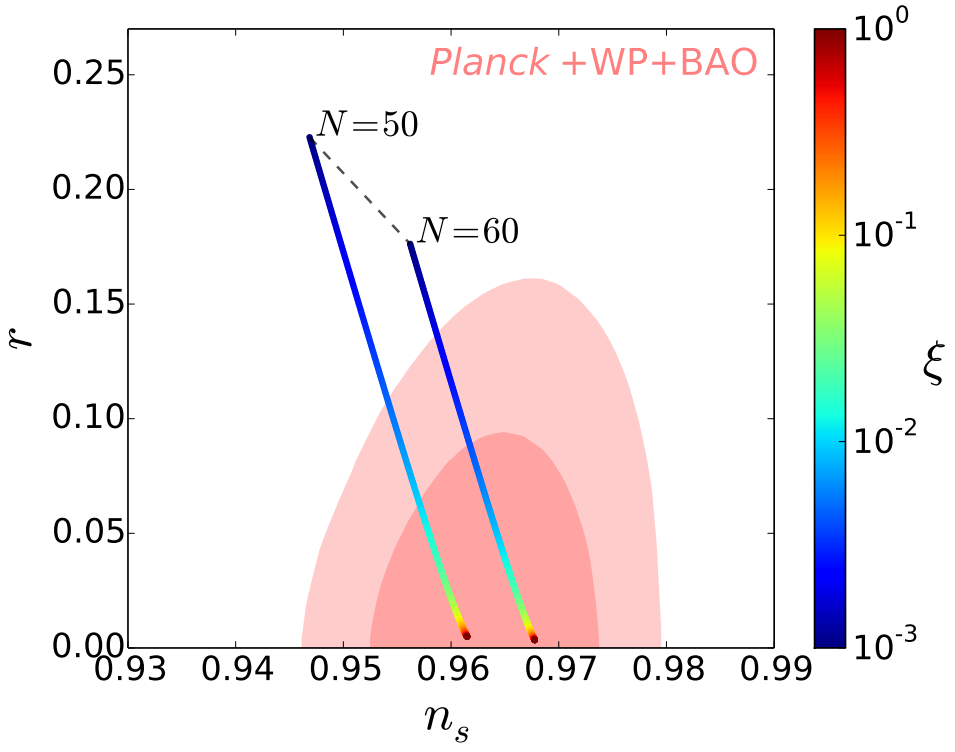

FIGURE 4.4: *The variation of the model prediction in the n_s-r plane for different values of ξ. We show the 1 and 2σ constraints from Planck with WMAP polarisation (WP) [272] and BAO from various surveys (see Ref. [273] for details). Our model is consistent with the data for $\xi \gtrsim \mathcal{O}(few) \times 10^{-3}$ depending on N, the number of e-folds of observable inflation.*

We note here that it is possible for quantum corrections to change the predictions of the theory. The case where the PQ scalar was also coupled to a fermion was considered in [261] where the effect of this correction on the inflationary parameters was analysed. In the interest of remaining as general as possible we do not consider any such couplings. There will also be quantum corrections from the running of λ and ξ on their own (see [267]). In our case we do not expect these corrections to have a large effect on our results because the bare coupling, λ, is very small.

4.2.2 Isocurvature constraints

The cosmological evolution of the axion field is determined by the epoch in which the PQ symmetry is broken. We have seen that the PQ symmetry can be restored after inflation if the reheating temperature is greater than the symmetry breaking

scale. It is also possible for the symmetry to be restored by the Gibbons-Hawking temperature ($T_{GH} = H/2\pi$) during inflation such that there is no axion present during inflation. In the standard scenario (when the radial field, s, plays no part in inflation) the symmetry is broken during inflation and remains broken after inflation if

$$f_a \gtrsim \mathrm{Max}[H/2\pi, T_{\mathrm{rh}}]. \tag{4.18}$$

When this inequality is satisfied all relics of the PQ phase transition are diluted away by inflation, and isocurvature perturbations in the axion field are present. In the opposite regime

$$f_a < \mathrm{Min}[H/2\pi, T_{\mathrm{rh}}]\,, \tag{4.19}$$

then the PQ symmetry is either unbroken during inflation so no isocurvature modes are produced or it is restored after inflation and all the isocurvature modes are wiped out. However, cosmic string relics of the phase transition that are produced when the symmetry re-breaks now play an important cosmological role.

In the model presented here where s plays the role of the inflaton the axion acquires isocurvature perturbations regardless of the value of f_a. This is because the s field no longer sits at the minimum of the potential so the symmetry is always broken during inflation and is unaffected by T_{GH}. The reheat temperature is then the only relevant scale in deciding whether these modes survive, and whether relics of the phase transition are cosmologically relevant.

We will now examine how the isocurvature constraints impact on the parameter space of the axion. The quantum fluctuations of the axion field during inflation produce a nearly scale invariant spectrum of perturbations with

$$\langle |\delta a|^2 \rangle = \left(\frac{H}{2\pi}\right)^2. \tag{4.20}$$

The amplitude of isocurvature perturbations for axions is then given by [242]

$$A_{\mathrm{iso},a} = \left\langle \left| \frac{\delta n_a}{n_a} \right|^2 \right\rangle = 4 \left\langle \left| \frac{\delta a}{a} \right|^2 \right\rangle = \frac{H^2}{\pi^2 f_a^2 \langle \theta_i^2 \rangle}, \tag{4.21}$$

where n_a is the number density of axions and the factor of 4 in the middle equality comes from $n_a \propto a^2$ when we approximate the axion potential as harmonic. We can then calculate the fractional contribution of isocurvature modes, α, and compare it to the experimental bound (4.10) using

$$\alpha = \frac{A_{\rm iso}}{A_{\rm iso} + A_s} = \frac{R_a^2\ A_{{\rm iso},a}}{R_a^2\ A_{{\rm iso},a} + A_s}, \tag{4.22}$$

where R_a is the fraction of cold dark matter made up of axions and we have assumed that there are no additional sources of isocurvature. Here A_s is the usual amplitude of adiabatic perturbations given by

$$A_s = \frac{1}{2\epsilon}\left(\frac{H}{2\pi M_{pl}}\right)^2. \tag{4.23}$$

In this work we assume $R_a = 1$ i.e. axions account for the dark matter, so we may write

$$\alpha = \frac{1}{1 + \frac{f_a^2\langle\theta_i^2\rangle}{8M_{pl}^2\epsilon}}, \tag{4.24}$$

We can now understand the tension between axionic dark matter and observable primordial tensor modes. Using $r = 16\epsilon$ and combining Eqs. (4.24) and (4.5) with the *Planck* constraints of Eq. (4.10) and $\Omega_{\rm cdm}h^2 = 0.1199 \pm 0.0027$ [273] we find the bound,

$$r \lesssim 10^{-10}\left(\frac{f_a}{10^{16}\ {\rm GeV}}\right)^{5/6}. \tag{4.25}$$

This result highlights that any conceivable detection of r will put severe constraints on axion dark matter with GUT scale f_a in the traditional setup.

If, however, the radial part, s, of the PQ field evolves considerably from inflation to the present, for example if it is the inflaton as we propose, the conclusion Eq. (4.25) can be radically changed. This is because the effective $f_{a,\rm eff} = s_*$ during inflation can be much larger than the vacuum value, f_a, appearing in the potential Eq. (4.11).

In this scenario Eq. (4.24) becomes

$$\alpha = \frac{1}{1 + \frac{s_*^2 \langle \theta_i^2 \rangle}{8 M_{pl}^2 \epsilon}}. \tag{4.26}$$

In this case the f_a dependence of isocurvature modes changes significantly. We see in Eq. (4.24) that it is usually preferable to have large f_a to avoid isocurvature bounds. In our model however f_a no longer directly enters the equation for α, and it is preferable to have a smaller f_a as a result of its indirect effect through $\langle \theta_i^2 \rangle$ when fixing the DM relic abundance in Eq. (4.5). The r dependence also changes because now the important r-dependent quantity is s_*^2/ϵ rather than just ϵ. The consequences of Eq. (4.26) in the parameter space (r, f_a) are discussed in Section 4.3.

Another realisation of our general scheme could be achieved in volume modulus inflation in the string theory large volume scenario [274]. Here the axion decay constant is inversely proportional to the volume of the compact dimensions, and so if the volume evolves from small values during inflation to large values (in string units) after inflation then this too will reduce the axion isocurvature amplitude. This is achieved in Ref. [274] by inflection point inflation along the decompactification direction at small volume, with reheating occuring in a large volume meta-stable de Sitter vacuum. An attractor solution prevents the field from overshooting the meta-stable end-point.

Since the decay constants of all axion-like particles in string theory depend inversely on the volume, the volume modulus model could dilute the isocurvature perturbations of many axions at once. In a field theory model like ours this could be achieved by inflation along a diagonal in field space with many s fields, i.e. a radial-field version of N-flation [275].

4.2.3 Direct detection and other constraints

The axion couples to photons through the term

$$\mathcal{L}_{a\gamma\gamma} = \frac{-g_{a\gamma\gamma}}{4}\frac{a}{f_a}F^{\mu\nu}\widetilde{F}_{\mu\nu} = g_{a\gamma\gamma}\frac{a}{f_a}\mathbf{E}\cdot\mathbf{B}. \tag{4.27}$$

The exact value of the dimensionless coupling $g_{a\gamma\gamma}$ is model dependent but generically of the same order (e.g. $g_{a\gamma\gamma} = 0.97$ for KSVZ axions and $g_{a\gamma\gamma} = -0.36$ for DFSZ axions [242]). The effective coupling is then inversely proportional to f_a. This coupling can be used to search for axions in the laboratory through axion-photon conversion. The Axion Dark Matter Experiment (ADMX) uses a large magnetic field to try to convert axions to photons in a tunable microwave cavity. This has provided additional constraints on the parameter space. Axion DM particles with masses in the the range $m_a = [1.9 - 3.3]$ μeV for KSVZ axions (or the slightly narrower range $m_a = [1.98 - 2.17]$ μeV for DFSZ axions) have been excluded [276]. We can convert this to a constraint on f_a using,

$$m_a = \frac{\sqrt{z}}{1+z}\frac{f_\pi m_\pi}{f_a} = 6.2\ \mu\text{eV}\left(\frac{10^{12}\ \text{GeV}}{f_a}\right), \tag{4.28}$$

where $z = m_u/m_d \simeq 0.56$. This yields an exclusion in the range $f_a = [1.88 - 3.26] \times 10^{12}$ GeV for KSVZ (or $f_a = [2.86 - 3.13] \times 10^{12}$ for DFSZ axions).

Axions can also have derivative couplings to SM fermions of the form

$$\mathcal{L}_{af\bar{f}} = \frac{g_{af\bar{f}}}{f_a}\bar{f}\gamma^\mu\gamma_5 f\partial_\mu a. \tag{4.29}$$

These couplings are much more model dependent because contrary to DFSZ axions, KSVZ axions do not couple to to quarks or leptons at tree-level and only have an effective coupling with hadrons (which gives the KSVZ axions the common name "hadronic axions").

We can put limits on these couplings using astrophysical observations [277]. For DFSZ axions the strongest limit comes from white dwarf stars which would cool

too quickly through axion emission if the axion-electron coupling is too large. The remaining limits are less model dependent because they rely on the axion-photon coupling. A large axion-photon coupling can significantly increase the Helium burning rate of globular cluster stars causing them to cool faster. It would also affect the neutrino flux from the Sun and from SN1987A. The Sun can lose energy through the emission of axions (which have also been directly searched for by the CAST experiment [278]) so for hydrodynamic stability we would require a higher fusion rate and we would therefore expect greater solar neutrino flux. For SN1987A we would expect less neutrinos emitted over a shorter time due to availability of more efficient energy release through axions. These complementary astrophysical measurements combine to give an upper bound on the axion mass of $m_a \lesssim 10^3$ μeV ($f_a \gtrsim 6.2 \times 10^9$ GeV) [277]. We also have a lower bound on the mass of the QCD axion follows from the phenomenon of black hole superradiance. The axions (or any massive boson) can form gravitational bound state of spinning holes. Infalling axions can extract energy from the spinning black hole which can be released when they decay to gravitons. For light axions this can cause the black hole to lose energy very efficiently. The observed spins of stellar mass blackholes can then constrain the presence of light axions excluding $f_a \gtrsim 10^{17}$ GeV [279].

4.3 Results and conclusions

As we have discussed, the value of the reheating temperature plays a crucial role in the phenomenology of this model. The precise value of $T_{\rm rh}$ is however model dependent because it is determined by the coupling of the PQ field to the SM (and possibly other) fields. In order to keep our discussion as general as possible we parametrise the uncertainty in $T_{\rm rh}$ using an efficiency parameter, $\epsilon_{\rm eff} < 1$, with

$$T_{\rm rh} = \sqrt{\epsilon_{\rm eff} H M_{pl}}, \tag{4.30}$$

where for ease in translating to CMB observables we take H at 60 e-folds before the end of inflation. The phenomenology of different scenarios can then be investigated by varying $\epsilon_{\rm eff}$.

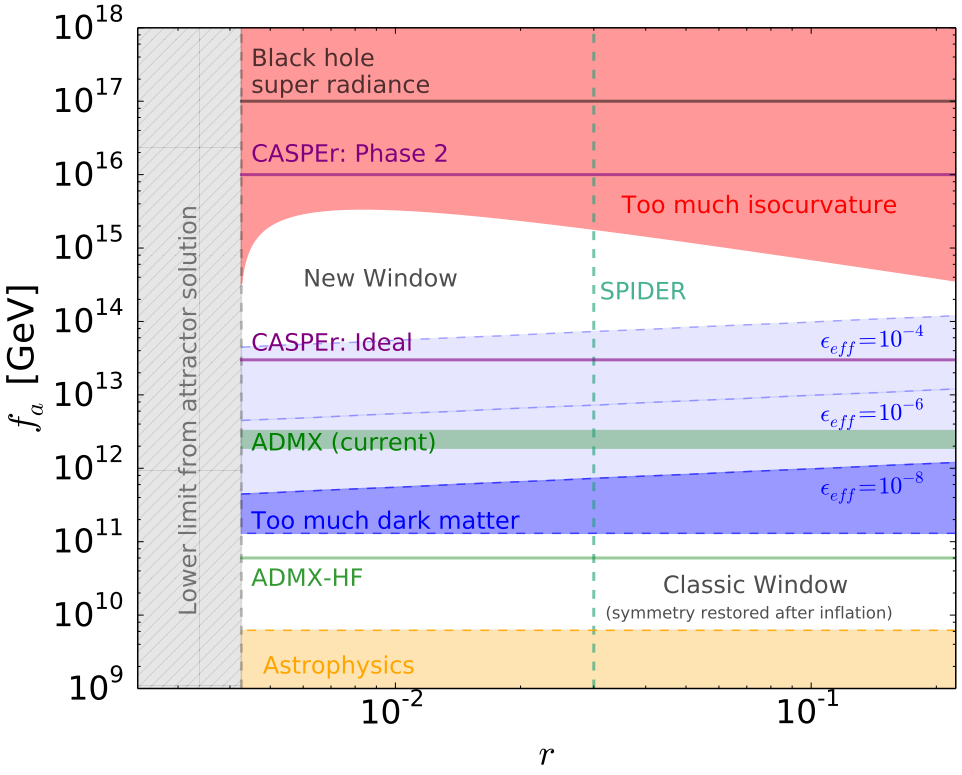

FIGURE 4.5: *Axion DM constraints for non-minimal PQ inflation model showing the new window unavailable to other axion models. The colored regions are ruled out by: isocurvature constraints (red); astrophysical constraints on the axion coupling to SM particles (orange); overproduction of DM from cosmic strings (for three different values of T_{rh} parameterised by ϵ_{eff}) (blue); direct searches for DM axions by ADMX (green). The purple lines show the projected lower bounds of the CASPEr experiment. Together,* SPIDER *and CASPEr/ADMX-HF can probe a large part of the parameter space of our model.*

The resulting updated constraints are summarised in Fig. 4.5 where we show the constraints on f_a as a function of the tensor-to-scalar ratio in our model of inflation driven by the radial PQ field. The upper portion of the plot is ruled out by excess isocurvature modes for any observable value of r even when our mechanism is employed. Our mechanism opens up a new window for intermediate-scale axions with 10^{12} GeV $\lesssim f_a \lesssim 10^{15}$ GeV to be consistent with observable primordial B-modes, as could be observed, for example, by near future experiments like SPIDER. As a side note, since it is now possible to have axionic dark matter for relatively low f_a

even when the symmetry is not restored after inflation, the need for fine-tuning of $\langle\theta_i\rangle$ is considerably reduced for a large range of r.

The exact size of the new window depends on the value of r, which has a minimum value, $r_{\rm min} \approx 3.3 \times 10^{-3}$ in our model. This is below what is accessible to SPIDER, but it is not impossible to imagine this as detectable at some stage in the future. In standard inflation $r \lesssim 10^{-10}$ is required for high f_a axions to be viable in the so-called anthropic window [249]. If r were detected, for example by 21cm lensing, in the range $10^{-9} \lesssim r \lesssim 10^{-3}$ then a mechanism other than that presented here would be necessary to save the high f_a QCD axion.

Remaining agnostic about the model of reheating and allowing $\epsilon_{\rm eff}$ to vary by orders of magnitude has a strong effect on the size of the new window, with the lower bound of the window $f_{a,\rm low} \propto \epsilon_{\rm eff}^{0.5}$. Even when reheating is quite efficient (up to $\epsilon_{\rm eff} \sim 10^{-2}$) our model still offers new, previously unavailable regions of the parameter space with simultaneously large values of r and f_a. The size of the new window is maximised when reheating is inefficient and the blue region disappears; this occurs for $\epsilon_{\rm eff} \lesssim 10^{-10}$.

We have also highlighted the presence of the classic window for axion DM, when the PQ symmetry is restored after inflation. Here the lower bound on f_a is imposed by astrophysical constraints [277], while the upper bound is imposed by the DM abundance from string decay. When the reheating is very inefficient ($\epsilon_{\rm eff} \lesssim 10^{-10}$) the size of the classic window can be reduced significantly because the symmetry cannot be restored.

The ADMX exclusion lies in the new window so we can look forward to more explorations of this window (and the classic window) with the proposed ADMX-HF experiment [280] that will extend the sensitivity to masses as large as ~ 100 μeV ($f_a \sim 6 \times 10^{10}$ GeV). The CASPEr experiment [281] has proposed a search for axions with large f_a using the precession of CP-odd nuclear moments of the target caused by interacting with DM axions. Phase 2 of the experiment can rule out axions with $f_a > 1.3 \times 10^{16}$ GeV. With improvements in magnetometer technology the

experiment can be used to search for axions with $f_a > 4 \times 10^{13}$ GeV. Without some mechanism to dilute isocurvature, such as ours, the entire range for CASPEr would be excluded on cosmological grounds if r is observed by SPIDER.

We have shown that it is possible for large f_a axion DM to coexist with high scale inflation, with observably large tensor modes and accompanying isocurature. If a non-negligible measurement of r is reported in future by e.g. Keck-Array [106] or SPIDER this would be selective in the available parameter space of our model. Furthermore if large f_a axions are found by CASPEr or ADMX then a mechanism such as that presented here will be needed to reconcile the two measurements. Additional probes of the model could come if isocurvature perturbations are observed at the percent level by future CMB measurements [282]. Axion DM direct detection and CMB polarisation experiments are complementary in many ways and together can access physics at extremely high energies and discriminate between models of inflation.

Chapter 5

Conclusion

In this thesis we have presented some new results for astroparticle phenomenology. In chapter 1 we argued that a minimal, bottom-up approach to model building is an attractive alternative to the more typical top-down approach. While the motivations for top-down model building are clear, sometimes we are guilty of losing track of the original motivation to explain the Universe we observe and become attached to the seductive ideas. In this thesis we have therefore tried another approach by focusing on the phenomenology of simple models that can fill in some of the missing pieces of the current best theories of particle physics and cosmology, the Standard Model and ΛCDM.

In chapter 2 we examined the role of the Higgs in inflation. We argued that it was natural to consider whether the first (seemingly) fundamental scalar that we have discovered could play the role of the scalar inflaton. We reviewed some previous attempts at this problem, most notably Higgs inflation with a non-minimal coupling, and concluded that while the model is initially very attractive is has some theoretical issues with unitarity that must be addressed satisfactorily before the model is accepted. We also presented some new results on the false vacuum Higgs inflation scenario. Motivated by the peculiar possibility of a false vacuum appearing in the quantum effective potential of the Higgs we took a closer look at this possibility. We came to the unfortunate conclusion that, contrary to previous claims in the

literature, it is not possible to inflate the Universe in a way that is simultaneously compatible with both particle physics experiments and cosmological observations. We therefore concluded that some new ideas are needed in order to make Higgs inflation a compelling idea again.

With this, we were naturally driven to consider the consequences of a theory with an inflaton that is separate from the Higgs. It was immediately clear that the appearance of an instability in the Higgs potential (for the central values of M_h, M_t, and α_s) might result in the Higgs destabilising during inflation. Without inflation the Higgs is safe in the electroweak vacuum because the tunnelling rate to the true vacuum is extremely small compared to the age of the Universe. In an inflationary Universe however we expect the Higgs to receive quantum fluctuations which could kick the Higgs into the true vacuum during inflation. We found that if the scale of inflation is high then this becomes a problem. While the details of post-inflationary evolution of the bubbles of true vacuum makes the analysis a little bit more subtle we argued that the intuitive conclusion remains intact: this is not compatible with our Universe. It would, however, be very interesting to study the evolution of these bubbles in a more quantitative way using a numerical GR code (e.g. [125]). We analysed two potential remedies to this problem (apart from the obvious absence of an instability) that use a direct coupling between the Higgs and the inflaton or a finite temperature during inflation to stabilise the Higgs field. If we discover evidence for high scale inflation in the coming years by, for example, measuring the tensor-to-scalar ratio, then this will provide concrete evidence for new physics. This new physics could be the introduction of new bosonic particles to stabilise the Higgs potential or, alternatively, could teach us about the coupling of the inflaton to other particles.

In chapter 3 we addressed the problem of the baryon asymmetry of the Universe. In the context of electroweak baryogenesis it is necessary to modify the electroweak symmetry breaking sector in order to produce a first order phase transition. We saw that by introducing a new singlet scalar that couples to the Higgs this could be readily achieved. In addition, this singlet scalar can act as a mediator between

the SM and dark matter. We saw that if we introduce a singlet fermion that can couples to the singlet scalar then this can successfully explain the dark matter relic density through thermal freeze-out. While the dark matter currently evades all constraints the most promising avenue for discovery is using direct detection experiments. We can simultaneously constrain this model by studying Higgs physics because the mixing of a singlet scalar with the Higgs will modify its coupling to other particles relative to that expected in the SM. It would be interesting for future work to include a full analysis of the baryon asymmetry generation by studying the quantum transport of the asymmetry near the bubble walls. This may lead to new and complimentary constraints on the parameter space of this model.

In chapter 4 we presented a new unified picture of inflation and dark matter with the Peccei-Quinn field. By introducing a non-minimal coupling between the PQ singlet and gravity we can reproduce an inflationary cosmology compatible with *Planck* and allow the angular part of the field (the axion) to both solve the strong-CP problem and play the role of cold dark matter. The isocurvature modes of the axion field are also suppressed by having a large effective decay constant, f_a, during inflation so that axion becomes compatible with high scale inflation (even if the PQ symmetry remains broken after inflation). This model therefore opens up a new window for axion cosmology that can be tested in the coming years. Direct detection of axions and measurements of primordial tensor or isocurvature modes in the CMB provide complementary search strategies that could significantly constrain this model. An interesting future direction for this work would be to study the reheating dynamics in detail. Up to now we have remained agnostic about the details but for a particular axion model this could be computed in order to determine the size of the new axion window. In addition we could consider a coupling between the Higgs and the PQ scalar and study its effect on stabilising the electroweak vacuum.

In this thesis we have therefore shown that minimal models can be very successful in solving the various problems with our current models. Perhaps by beginning with the simplest possible solutions and examining their phenomenology we may illuminate the path forward towards a more complete understanding of the Universe.

Appendix A

Fermionic Dark Matter Cross Sections and Formulae

The cross section for $\psi\bar{\psi} \to h_i h_j$ (with $i,j \in \{1,2\}$) is given by $s-$, $t-$, and $u-$channel terms, and the interference term [181],

$$\sigma v_{rel}^{ij,s} = \frac{\beta_{ij}}{16\pi s}(s-4m_\psi^2)\left|\sum_{r=1,2}\frac{g_r\Lambda_r^{ij}}{s-m_{h_r}^2+im_{h_r}\Gamma_{h_r}}\right|^2, \tag{A.1}$$

$$\begin{aligned}\sigma v_{rel}^{ij,t/u} =& \frac{\beta_{ij}}{8\pi s}g_i^2 g_j^2\Bigg[\frac{(4m_\psi^2-m_{h_i})(4m_\psi^2-m_{h_j})}{B^2-A^2} \\ &- \ln\left|\frac{A+B}{A-B}\right|\left(\frac{s+8m_\psi^2-m_{h_i}^2-m_{h_i}^2}{2B}+\frac{16m_\psi^4-4sm_\psi^2-m_{h_i}^2m_{h_j}^2}{AB}-2\right)\Bigg],\end{aligned} \tag{A.2}$$

$$\sigma v_{rel}^{ij,int} = \frac{\beta_{ij}}{4\pi s}g_i g_j m_\psi\left(\sum_{r=1,2}\frac{g_r\Lambda_r^{ij}(s-m_{h_r}^2)}{(s-m_{h_r}^2)^2+m_{h_r}^2\Gamma_{h_r}^2}\right)\left(\ln\left|\frac{A+B}{A-B}\right|\left(\frac{A}{B}+\frac{1}{2}\frac{\beta_\psi}{\beta_{ij}}-2\right)\right), \tag{A.3}$$

where

$$\beta_{ij} = \sqrt{1-\frac{(m_{h_i}+m_{h_j})^2}{s}}\sqrt{1-\frac{(m_{h_i}-m_{h_j})^2}{s}}, \tag{A.4}$$

$$A = \frac{1}{2}(m_{h_i}^2 + m_{h_j}^2 - s), \quad D = \frac{s}{2}\beta_\psi \beta_{ij}, \tag{A.5}$$

and there is an additional symmetry factor of $\frac{1}{2}$ when $i = j$.

The cross-section for SM finals states is given by [180]

$$\begin{aligned}\sigma v_{rel} =& \frac{(g_s \sin\alpha \cos\alpha)^2}{16\pi}\beta_\psi^2 \left| \sum_{r=1,2} \frac{g_r \Lambda_r^{ij}}{s - m_{h_r}^2 + i m_{h_r}\Gamma_{h_r}} \right|^2 \times \\ & \left(\sum_{V=W,Z} \epsilon \left(\frac{2m_V^2}{v}\right)^2 \left(2 + \frac{(s-2m_V^2)^2}{4m_V^4}\right)\beta_V + \sum_{q=b,t} N_c y_q s \beta_q^{3/2} \right),\end{aligned} \tag{A.6}$$

where $N_c = 3$ is the number of colors, y_q are the quark Yukawa couplings, $\beta_i = \sqrt{1 - 4m_i^2/s}$, and $\epsilon = 1/2$ for $V = Z$ and otherwise unity. In the above the Standard Model contribution to Γ_{h_i} was calculated using the HDECAY code [283].

The couplings for the cross sections are given by

$$g_r = \begin{cases} g_s \sin\alpha, & \text{if } i = 1 \\ g_s \cos\alpha, & \text{if } i = 2 \end{cases} \tag{A.7}$$

$$\begin{aligned}\Lambda_1^{12} =& c^3\left(\frac{\mu_m}{4} + \frac{\lambda_{hs} w}{2}\right) - c^2 s\,(3\lambda_h v + \lambda_{hs} v) \\ & + s^2 c\,\left(\mu_3 - \frac{\mu_m}{2} - \lambda_{hs} w + 3\lambda_s w\right) - s^3\,\frac{1}{2}\lambda_{hs} v,\end{aligned} \tag{A.8}$$

$$\begin{aligned}\Lambda_2^{12} =& s^3\left(\frac{\mu_m}{4} + \frac{\lambda_{hs} w}{2}\right) + s^2 c\,(3\lambda_h v + \lambda_{hs} v) \\ & + c^2 s\,\left(\mu_3 - \frac{\mu_m}{2} - \lambda_{hs} w + 3\lambda_s w\right) + c^3\,\frac{1}{2}\lambda_{hs} v,\end{aligned} \tag{A.9}$$

$$\Lambda_1^{11} = c^3 \lambda_h v + c^2 s\left(\frac{\mu_m}{4} + \frac{\lambda_{hs} w}{2}\right) + s^2 c \frac{\lambda_{hs} v}{2} + s^3\left(\frac{\mu_3}{3} + \lambda_s w\right), \tag{A.10}$$

$$\Lambda_2^{22} = -\,s^3\,\lambda_h v + s^2 c\left(\frac{\mu_m}{4} + \frac{\lambda_{hs} w}{2}\right) - c^2 s\,\frac{\lambda_{hs} v}{2} + c^3\,\left(\frac{\mu_3}{3} + \lambda_s w\right), \tag{A.11}$$

where $c = \cos\alpha$ and $s = \sin\alpha$.

Bibliography

[1] Planck, P. Ade *et al.*, Astron.Astrophys. **571**, A22 (2014), 1303.5082.

[2] ATLAS Collaboration, G. Aad *et al.*, Phys.Lett. **B716**, 1 (2012), 1207.7214.

[3] CMS Collaboration, S. Chatrchyan *et al.*, Phys.Lett. **B716**, 30 (2012), 1207.7235.

[4] G. Bertone, D. Hooper, and J. Silk, Phys.Rept. **405**, 279 (2005), hep-ph/0404175.

[5] F. Zwicky, Helv.Phys.Acta **6**, 110 (1933).

[6] T. S. van Albada, J. N. Bahcall, K. Begeman, and R. Sancisi, Ap. J. **295**, 305 (1985).

[7] A. G. Riess *et al.*, The Astrophysical Journal **607**, 665 (2004).

[8] Planck Collaboration, P. Ade *et al.*, (2013), 1303.5076.

[9] T. P. Walker, G. Steigman, D. N. Schramm, K. A. Olive, and H.-S. Kang, Astrophys.J. **376**, 51 (1991).

[10] J. F. Navarro, C. S. Frenk, and S. D. White, Astrophys.J. **462**, 563 (1996), astro-ph/9508025.

[11] J. F. Navarro, C. S. Frenk, and S. D. White, Astrophys.J. **490**, 493 (1997), astro-ph/9611107.

[12] G. Jungman, M. Kamionkowski, and K. Griest, Phys.Rept. **267**, 195 (1996), hep-ph/9506380.

[13] J. McDonald, Phys.Rev. **D50**, 3637 (1994), hep-ph/0702143.

[14] D. Hooper, Particle Dark Matter, in *TASI 2008*, pp. 709–764, 2010, 0901.4090.

[15] L. J. Hall, K. Jedamzik, J. March-Russell, and S. M. West, JHEP **1003**, 080 (2010), 0911.1120.

[16] A. G. Cohen, A. De Rujula, and S. Glashow, Astrophys.J. **495**, 539 (1998), astro-ph/9707087.

[17] Particle Data Group, K. A. Olive *et al.*, Chin. Phys. **C38**, 090001 (2014).

[18] R. H. Cyburt, B. D. Fields, and K. A. Olive, JCAP **0811**, 012 (2008), 0808.2818.

[19] A. Sakharov, Pisma Zh.Eksp.Teor.Fiz. **5**, 32 (1967).

[20] V. Kuzmin, V. Rubakov, and M. Shaposhnikov, Phys.Lett. **B155**, 36 (1985).

[21] M. Fukugita and T. Yanagida, Phys.Lett. **B174**, 45 (1986).

[22] M. Yoshimura, Phys.Rev.Lett. **41**, 281 (1978).

[23] I. Affleck and M. Dine, Nucl.Phys. **B249**, 361 (1985).

[24] Planck, P. Ade *et al.*, (2015), 1502.01589.

[25] J. Preskill, Phys. Rev. Lett. **43**, 1365 (1979).

[26] D. Baumann, Inflation, in *TASI 09*, pp. 523–686, 2011, 0907.5424.

[27] A. H. Guth, Phys.Rev. **D23**, 347 (1981).

[28] A. D. Linde, Phys.Lett. **B129**, 177 (1983).

[29] BICEP2 Collaboration, P. Ade *et al.*, Phys.Rev.Lett. **112**, 241101 (2014), 1403.3985.

[30] S. Coleman and E. Weinberg, Physical Review D **7**, 1888 (1973).

[31] M. Bando, T. Kugo, N. Maekawa, and H. Nakano, Phys.Lett. **B301**, 83 (1993), hep-ph/9210228.

[32] S. R. Coleman and J. Mandula, Phys.Rev. **159**, 1251 (1967).

[33] K. de Vries *et al.*, (2015), 1504.03260.

[34] LHC New Physics Working Group, D. Alves *et al.*, J.Phys. **G39**, 105005 (2012), 1105.2838.

[35] J. Abdallah *et al.*, (2015), 1506.03116.

[36] P. W. Graham, D. E. Kaplan, and S. Rajendran, (2015), 1504.07551.

[37] M. Fairbairn, P. Grothaus, and R. Hogan, JCAP **1406**, 039 (2014), 1403.7483.

[38] M. Fairbairn and R. Hogan, Phys. Rev. Lett. **112**, 201801 (2014), 1403.6786.

[39] M. Fairbairn and R. Hogan, JHEP **1309**, 022 (2013), 1305.3452.

[40] M. Fairbairn, R. Hogan, and D. J. Marsh, Phys.Rev. **D91**, 023509 (2015), 1410.1752.

[41] J. Ellis and T. You, JHEP **1306**, 103 (2013), 1303.3879.

[42] J. Ellis, V. Sanz, and T. You, JHEP **1407**, 036 (2014), 1404.3667.

[43] J. Ellis, V. Sanz, and T. You, JHEP **1503**, 157 (2015), 1410.7703.

[44] G. Degrassi *et al.*, JHEP **1208**, 098 (2012), 1205.6497.

[45] D. Buttazzo *et al.*, JHEP **1312**, 089 (2013), 1307.3536.

[46] D. S. Salopek, J. R. Bond, and J. M. Bardeen, Phys. Rev. D **40**, 1753 (1989).

[47] F. L. Bezrukov and M. Shaposhnikov, Phys.Lett. **B659**, 703 (2008), 0710.3755.

[48] A. Barvinsky, A. Y. Kamenshchik, and A. Starobinsky, JCAP **0811**, 021 (2008), 0809.2104.

[49] J. Garcia-Bellido, D. G. Figueroa, and J. Rubio, Phys.Rev. **D79**, 063531 (2009), 0812.4624.

[50] F. L. Bezrukov, A. Magnin, and M. Shaposhnikov, Phys.Lett. **B675**, 88 (2009), 0812.4950.

[51] F. Bezrukov, D. Gorbunov, and M. Shaposhnikov, JCAP **0906**, 029 (2009), 0812.3622.

[52] A. De Simone, M. P. Hertzberg, and F. Wilczek, Phys.Lett. **B678**, 1 (2009), 0812.4946.

[53] A. Barvinsky, A. Y. Kamenshchik, C. Kiefer, A. Starobinsky, and C. Steinwachs, JCAP **0912**, 003 (2009), 0904.1698.

[54] F. Bezrukov and M. Shaposhnikov, JHEP **0907**, 089 (2009), 0904.1537.

[55] F. Bezrukov, A. Magnin, M. Shaposhnikov, and S. Sibiryakov, JHEP **1101**, 016 (2011), 1008.5157.

[56] F. Bezrukov, Class.Quant.Grav. **30**, 214001 (2013), 1307.0708.

[57] C. P. Burgess, S. P. Patil, and M. Trott, JHEP **06**, 010 (2014), 1402.1476.

[58] F. Bezrukov and M. Shaposhnikov, Phys. Lett. **B734**, 249 (2014), 1403.6078.

[59] Y. Hamada, H. Kawai, K.-y. Oda, and S. C. Park, Phys. Rev. Lett. **112**, 241301 (2014), 1403.5043.

[60] C. Burgess, H. M. Lee, and M. Trott, JHEP **0909**, 103 (2009), 0902.4465.

[61] J. Barbon and J. Espinosa, Phys.Rev. **D79**, 081302 (2009), 0903.0355.

[62] R. N. Lerner and J. McDonald, JCAP **1004**, 015 (2010), 0912.5463.

[63] C. Burgess, H. M. Lee, and M. Trott, JHEP **1007**, 007 (2010), 1002.2730.

[64] M. P. Hertzberg, JHEP **1011**, 023 (2010), 1002.2995.

[65] M. Atkins and X. Calmet, Phys.Lett. **B697**, 37 (2011), 1011.4179.

[66] S. Ferrara, R. Kallosh, A. Linde, A. Marrani, and A. Van Proeyen, Phys.Rev. **D83**, 025008 (2011), 1008.2942.

[67] R. N. Lerner and J. McDonald, Phys.Rev. **D82**, 103525 (2010), 1005.2978.

[68] G. F. Giudice and H. M. Lee, Phys.Lett. **B694**, 294 (2011), 1010.1417.

[69] C. Germani and A. Kehagias, Phys.Rev.Lett. **105**, 011302 (2010), 1003.2635.

[70] K. Kamada, T. Kobayashi, M. Yamaguchi, and J. Yokoyama, Phys.Rev. **D83**, 083515 (2011), 1012.4238.

[71] C. Germani, Y. Watanabe, and N. Wintergerst, JCAP **1412**, 009 (2014), 1403.5766.

[72] G. Isidori, G. Ridolfi, and A. Strumia, Nucl.Phys. **B609**, 387 (2001), hep-ph/0104016.

[73] G. Isidori, V. S. Rychkov, A. Strumia, and N. Tetradis, Phys.Rev. **D77**, 025034 (2008), 0712.0242.

[74] N. Arkani-Hamed, S. Dubovsky, L. Senatore, and G. Villadoro, JHEP **0803**, 075 (2008), 0801.2399.

[75] J. Ellis, J. Espinosa, G. Giudice, A. Hoecker, and A. Riotto, Phys.Lett. **B679**, 369 (2009), 0906.0954.

[76] J. Elias-Miro *et al.*, Phys.Lett. **B709**, 222 (2012), 1112.3022.

[77] V. Branchina and E. Messina, Phys.Rev.Lett. **111**, 241801 (2013), 1307.5193.

[78] A. D. Linde, Inflation, quantum cosmology and the anthropic principle, in *In *Barrow, J.D. (ed.) et al.: Science and ultimate reality* 426-458*, 2002, hep-th/0211048.

[79] Y. Hamada, H. Kawai, and K.-y. Oda, PTEP **2014**, 023B02 (2014), 1308.6651.

[80] I. Masina and A. Notari, Phys.Rev. **D85**, 123506 (2012), 1112.2659.

[81] I. Masina and A. Notari, JCAP **1211**, 031 (2012), 1204.4155.

[82] I. Masina, Phys. Rev. **D89**, 123505 (2014), 1403.5244.

[83] A. H. Guth, Phys.Rev. **D23**, 347 (1981).

[84] A. D. Linde, Phys.Rev. **D49**, 748 (1994), astro-ph/9307002.

[85] J. Elias-Miro, J. R. Espinosa, G. F. Giudice, H. M. Lee, and A. Strumia, JHEP **1206**, 031 (2012), 1203.0237.

[86] ATLAS Collaboration, CDF Collaboration, CMS Collaboration, D0 Collaboration, (2014), 1403.4427.

[87] S. Bethke, Eur.Phys.J. **C64**, 689 (2009), 0908.1135.

[88] F. Feroz, M. Hobson, and M. Bridges, Mon.Not.Roy.Astron.Soc. **398**, 1601 (2009), 0809.3437.

[89] A. De Simone and A. Riotto, JCAP **1302**, 014 (2013), 1208.1344.

[90] K. Enqvist, D. G. Figueroa, and R. N. Lerner, JCAP **1301**, 040 (2013), 1211.5028.

[91] K. Enqvist, T. Meriniemi, and S. Nurmi, JCAP **1310**, 057 (2013), 1306.4511.

[92] K. Enqvist, R. N. Lerner, and T. Takahashi, JCAP **1401**, 006 (2014), 1310.1374.

[93] J. Espinosa, G. Giudice, and A. Riotto, JCAP **0805**, 002 (2008), 0710.2484.

[94] O. Lebedev and A. Westphal, Phys.Lett. **B719**, 415 (2013), 1210.6987.

[95] A. Kobakhidze and A. Spencer-Smith, Phys.Lett. **B722**, 130 (2013), 1301.2846.

[96] G. W. Gibbons and S. W. Hawking, Phys. Rev. D **15**, 2752 (1977).

[97] BICEP2 Collaboration, P. Ade *et al.*, (2014), 1403.3985.

[98] K. Enqvist, T. Meriniemi, and S. Nurmi, JCAP **1407**, 025 (2014), 1404.3699.

[99] A. Hook, J. Kearney, B. Shakya, and K. M. Zurek, JHEP **1501**, 061 (2015), 1404.5953.

[100] A. Spencer-Smith, (2014), 1405.1975.

[101] M. J. Mortonson and U. Seljak, JCAP **1410**, 035 (2014), 1405.5857.

[102] R. Flauger, J. C. Hill, and D. N. Spergel, JCAP **1408**, 039 (2014), 1405.7351.

[103] Planck Collaboration, R. Adam *et al.*, (2014), 1409.5738.

[104] BICEP2 Collaboration, Planck Collaboration, P. Ade *et al.*, Phys.Rev.Lett. (2015), 1502.00612.

[105] A. S. Rahlin *et al.*, Proc. SPIE Int. Soc. Opt. Eng. **9153**, 915313 (2014), 1407.2906.

[106] C. Sheehy *et al.*, (2011), 1104.5516.

[107] A. Starobinsky, in *Field Theory, Quantum Gravity and Strings*, , Lecture Notes in Physics Vol. 246, pp. 107–126, Springer Berlin Heidelberg, 1986.

[108] A. D. Linde, Nucl.Phys. **B372**, 421 (1992), hep-th/9110037.

[109] J. Kearney, H. Yoo, and K. M. Zurek, Phys. Rev. **D91**, 123537 (2015), 1503.05193.

[110] M. Herranen, T. Markkanen, S. Nurmi, and A. Rajantie, Phys.Rev.Lett. **113**, 211102 (2014), 1407.3141.

[111] M. Herranen, T. Markkanen, S. Nurmi, and A. Rajantie, (2015), 1506.04065.

[112] A. Berera, Phys.Rev.Lett. **75**, 3218 (1995), astro-ph/9509049.

[113] A. Berera, M. Gleiser, and R. O. Ramos, Phys.Rev. **D58**, 123508 (1998), hep-ph/9803394.

[114] A. Berera, M. Gleiser, and R. O. Ramos, Phys.Rev.Lett. **83**, 264 (1999), hep-ph/9809583.

[115] A. Berera, I. G. Moss, and R. O. Ramos, Rept.Prog.Phys. **72**, 026901 (2009), 0808.1855.

[116] M. Bastero-Gil and A. Berera, Int.J.Mod.Phys. **A24**, 2207 (2009), 0902.0521.

[117] J. Yokoyama and A. D. Linde, Phys.Rev. **D60**, 083509 (1999), hep-ph/9809409.

[118] M. Bastero-Gil, A. Berera, and R. O. Ramos, JCAP **1109**, 033 (2011), 1008.1929.

[119] H. Mishra, S. Mohanty, and A. Nautiyal, Phys.Lett. **B710**, 245 (2012), 1106.3039.

[120] D. Lopez Nacir, R. A. Porto, L. Senatore, and M. Zaldarriaga, JHEP **1201**, 075 (2012), 1109.4192.

[121] M. Bastero-Gil, A. Berera, R. O. Ramos, and J. G. Rosa, JCAP **1301**, 016 (2013), 1207.0445.

[122] R. Cerezo and J. G. Rosa, JHEP **1301**, 024 (2013), 1210.7975.

[123] S. Bartrum *et al.*, Phys.Lett. **B732**, 116 (2014), 1307.5868.

[124] A. M. Green, (2014), 1403.1198.

[125] K. Clough *et al.*, (2015), 1503.03436.

[126] G. 't Hooft, Phys. Rev. Lett. **37**, 8 (1976).

[127] S. L. Adler, Phys.Rev. **177**, 2426 (1969).

[128] J. Bell and R. Jackiw, Nuovo Cim. **A60**, 47 (1969).

[129] V. Rubakov and M. Shaposhnikov, Usp.Fiz.Nauk **166**, 493 (1996), hep-ph/9603208.

[130] P. B. Arnold and L. D. McLerran, Phys.Rev. **D36**, 581 (1987).

[131] S. Y. Khlebnikov and M. Shaposhnikov, Nucl.Phys. **B308**, 885 (1988).

[132] J. Baacke and S. Junker, Phys.Rev. **D49**, 2055 (1994), hep-ph/9308310.

[133] M. Gavela, P. Hernandez, J. Orloff, and O. Pene, Mod.Phys.Lett. **A9**, 795 (1994), hep-ph/9312215.

[134] M. Gavela, P. Hernandez, J. Orloff, O. Pene, and C. Quimbay, Nucl.Phys. **B430**, 382 (1994), hep-ph/9406289.

[135] P. Huet and E. Sather, Phys.Rev. **D51**, 379 (1995), hep-ph/9404302.

[136] K. Kajantie, M. Laine, K. Rummukainen, and M. Shaposhnikov, Nuclear Physics B **493**, 413 (1997).

[137] K. Rummukainen, M. Tsypin, K. Kajantie, M. Laine, and M. Shaposhnikov, Nuclear Physics B **532**, 283 (1998).

[138] F. Csikor, Z. Fodor, and J. Heitger, Physical Review Letters **82**, 21 (1999).

[139] C. Grojean, G. Servant, and J. D. Wells, Phys.Rev. **D71**, 036001 (2005), hep-ph/0407019.

[140] J. R. Espinosa, T. Konstandin, and F. Riva, Nucl.Phys. **B854**, 592 (2012), 1107.5441.

[141] D. J. Chung, A. J. Long, and L.-T. Wang, Phys.Rev. **D87**, 023509 (2013), 1209.1819.

[142] P. Huet and A. E. Nelson, Phys.Rev. **D53**, 4578 (1996), hep-ph/9506477.

[143] D. Curtin, P. Jaiswal, and P. Meade, JHEP **1208**, 005 (2012), 1203.2932.

[144] M. Pietroni, Nucl.Phys. **B402**, 27 (1993), hep-ph/9207227.

[145] A. Menon, D. Morrissey, and C. Wagner, Phys.Rev. **D70**, 035005 (2004), hep-ph/0404184.

[146] S. Profumo, M. J. Ramsey-Musolf, and G. Shaughnessy, JHEP **0708**, 010 (2007), 0705.2425.

[147] J. M. Cline, G. Laporte, H. Yamashita, and S. Kraml, JHEP **0907**, 040 (2009), 0905.2559.

[148] J. M. Cline and K. Kainulainen, JCAP **1301**, 012 (2013), 1210.4196.

[149] H. H. Patel and M. J. Ramsey-Musolf, Phys.Rev. **D88**, 035013 (2013), 1212.5652.

[150] J. Espinosa and M. Quiros, Phys.Lett. **B305**, 98 (1993), hep-ph/9301285.

[151] J. Choi and R. Volkas, Phys.Lett. **B317**, 385 (1993), hep-ph/9308234.

[152] S. Ham, Y. Jeong, and S. Oh, J.Phys. **G31**, 857 (2005), hep-ph/0411352.

[153] A. Ahriche, Phys.Rev. **D75**, 083522 (2007), hep-ph/0701192.

[154] J. R. Espinosa, B. Gripaios, T. Konstandin, and F. Riva, JCAP **1201**, 012 (2012), 1110.2876.

[155] H. H. Patel and M. J. Ramsey-Musolf, JHEP **1107**, 029 (2011), 1101.4665.

[156] C. L. Wainwright, S. Profumo, and M. J. Ramsey-Musolf, Phys.Rev. **D86**, 083537 (2012), 1204.5464.

[157] A. Pomarol and F. Riva, JHEP **1401**, 151 (2014), 1308.2803.

[158] J. Ellis, V. Sanz, and T. You, JHEP **1407**, 036 (2014), 1404.3667.

[159] A. Drozd, J. Ellis, J. Quevillon, and T. You, JHEP **06**, 028 (2015), 1504.02409.

[160] B. Patt and F. Wilczek, (2006), hep-ph/0605188.

[161] C. Burgess, M. Pospelov, and T. ter Veldhuis, Nucl.Phys. **B619**, 709 (2001), hep-ph/0011335.

[162] V. Barger, P. Langacker, M. McCaskey, M. J. Ramsey-Musolf, and G. Shaughnessy, Phys.Rev. **D77**, 035005 (2008), 0706.4311.

[163] O. Bertolami and R. Rosenfeld, Int.J.Mod.Phys. **A23**, 4817 (2008), 0708.1784.

[164] J. March-Russell, S. M. West, D. Cumberbatch, and D. Hooper, JHEP **0807**, 058 (2008), 0801.3440.

[165] S. Andreas, T. Hambye, and M. H. Tytgat, JCAP **0810**, 034 (2008), 0808.0255.

[166] R. N. Lerner and J. McDonald, Phys.Rev. **D80**, 123507 (2009), 0909.0520.

[167] S. Andreas, C. Arina, T. Hambye, F.-S. Ling, and M. H. Tytgat, Phys.Rev. **D82**, 043522 (2010), 1003.2595.

[168] O. Lebedev, H. M. Lee, and Y. Mambrini, Phys.Lett. **B707**, 570 (2012), 1111.4482.

[169] S. Baek, P. Ko, and W.-I. Park, JHEP **1202**, 047 (2012), 1112.1847.

[170] X. Chu, T. Hambye, and M. H. Tytgat, JCAP **1205**, 034 (2012), 1112.0493.

[171] A. Djouadi, O. Lebedev, Y. Mambrini, and J. Quevillon, Phys.Lett. **B709**, 65 (2012), 1112.3299.

[172] L. Lopez-Honorez, T. Schwetz, and J. Zupan, Phys.Lett. **B716**, 179 (2012), 1203.2064.

[173] A. Djouadi, A. Falkowski, Y. Mambrini, and J. Quevillon, Eur.Phys.J. **C73**, 2455 (2013), 1205.3169.

[174] F. S. Queiroz and K. Sinha, Phys.Lett. **B735**, 69 (2014), 1404.1400.

[175] V. Barger, P. Langacker, M. McCaskey, M. Ramsey-Musolf, and G. Shaughnessy, Phys.Rev. **D79**, 015018 (2009), 0811.0393.

[176] T. A. Chowdhury, M. Nemevsek, G. Senjanovic, and Y. Zhang, JCAP **1202**, 029 (2012), 1110.5334.

[177] A. Ahriche and S. Nasri, Phys.Rev. **D85**, 093007 (2012), 1201.4614.

[178] J. M. Cline and K. Kainulainen, Phys.Rev. **D87**, 071701 (2013), 1302.2614.

[179] Y. G. Kim and K. Y. Lee, Phys.Rev. **D75**, 115012 (2007), hep-ph/0611069.

[180] Y. G. Kim, K. Y. Lee, and S. Shin, JHEP **0805**, 100 (2008), 0803.2932.

[181] H.-Y. Qin, W.-Y. Wang, and Z.-H. Xiong, Chin.Phys.Lett. **28**, 111202 (2011).

[182] S. Baek, P. Ko, W.-I. Park, and E. Senaha, JHEP **1211**, 116 (2012), 1209.4163.

[183] M. Farina, D. Pappadopulo, and A. Strumia, JHEP **1308**, 022 (2013), 1303.7244.

[184] K. Petraki and A. Kusenko, Phys.Rev. **D77**, 065014 (2008), 0711.4646.

[185] ATLAS, CMS, G. Aad *et al.*, Phys.Rev.Lett. **114**, 191803 (2015), 1503.07589.

[186] CERN Report No. ATLAS-CONF-2012-163, 2012 (unpublished).

[187] J. R. Espinosa, M. Muhlleitner, C. Grojean, and M. Trott, JHEP **1209**, 126 (2012), 1205.6790.

[188] A. Falkowski, F. Riva, and A. Urbano, JHEP **1311**, 111 (2013), 1303.1812.

[189] CMS, S. Chatrchyan *et al.*, Eur.Phys.J. **C73**, 2469 (2013), 1304.0213.

[190] D. Buttazzo, F. Sala, and A. Tesi, (2015), 1505.05488.

[191] M. Baak *et al.*, Eur.Phys.J. **C72**, 2205 (2012), 1209.2716.

[192] O. Eberhardt *et al.*, Phys.Rev.Lett. **109**, 241802 (2012), 1209.1101.

[193] P. Gondolo and G. Gelmini, Nucl.Phys. **B360**, 145 (1991).

[194] A. Sommerfeld, Annalen der Physik **403**, 257 (1931).

[195] T. Nihei and M. Sasagawa, Phys.Rev. **D70**, 055011 (2004), hep-ph/0404100.

[196] J. R. Ellis, A. Ferstl, and K. A. Olive, Phys.Lett. **B481**, 304 (2000), hep-ph/0001005.

[197] A. Bottino *et al.*, Phys.Lett. **B402**, 113 (1997), hep-ph/9612451.

[198] XENON100 Collaboration, E. Aprile *et al.*, Phys.Rev.Lett. **109**, 181301 (2012), 1207.5988.

[199] LUX, D. Akerib *et al.*, Phys.Rev.Lett. **112**, 091303 (2014), 1310.8214.

[200] XENON1T, E. Aprile, Springer Proc. Phys. **148**, 93 (2013), 1206.6288.

[201] S. Esch, M. Klasen, and C. E. Yaguna, Phys.Rev. **D88**, 075017 (2013), 1308.0951.

[202] L. Carson, X. Li, L. McLerran, and R.-T. Wang, Phys. Rev. D **42**, 2127 (1990).

[203] J. Espinosa, T. Konstandin, J. No, and M. Quiros, Phys.Rev. **D78**, 123528 (2008), 0809.3215.

[204] M. Holthausen, K. S. Lim, and M. Lindner, JHEP **1202**, 037 (2012), 1112.2415.

[205] Z.-z. Xing, H. Zhang, and S. Zhou, Phys.Rev. **D86**, 013013 (2012), 1112.3112.

[206] W. Rodejohann and H. Zhang, JHEP **1206**, 022 (2012), 1203.3825.

[207] F. Bezrukov, M. Y. Kalmykov, B. A. Kniehl, and M. Shaposhnikov, JHEP **1210**, 140 (2012), 1205.2893.

[208] S. Alekhin, A. Djouadi, and S. Moch, Phys.Lett. **B716**, 214 (2012), 1207.0980.

[209] I. Masina, Phys.Rev. **D87**, 053001 (2013), 1209.0393.

[210] W. Chao, M. Gonderinger, and M. J. Ramsey-Musolf, Phys.Rev. **D86**, 113017 (2012), 1210.0491.

[211] M. Gonderinger, Y. Li, H. Patel, and M. J. Ramsey-Musolf, JHEP **1001**, 053 (2010), 0910.3167.

[212] S. Profumo, L. Ubaldi, and C. Wainwright, Phys.Rev. **D82**, 123514 (2010), 1009.5377.

[213] C.-S. Chen and Y. Tang, JHEP **1204**, 019 (2012), 1202.5717.

[214] M. Gonderinger, H. Lim, and M. J. Ramsey-Musolf, Phys.Rev. **D86**, 043511 (2012), 1202.1316.

[215] C. Cheung, M. Papucci, and K. M. Zurek, JHEP **1207**, 105 (2012), 1203.5106.

[216] O. Lebedev, Eur.Phys.J. **C72**, 2058 (2012), 1203.0156.

[217] M. Frigerio, A. Pomarol, F. Riva, and A. Urbano, JHEP **1207**, 015 (2012), 1204.2808.

[218] A. Abada and S. Nasri, Phys.Rev. **D88**, 016006 (2013), 1304.3917.

[219] A. Barroso, P. Ferreira, I. Ivanov, and R. Santos, JHEP **1306**, 045 (2013), 1303.5098.

[220] F. Gianotti *et al.*, Eur.Phys.J. **C39**, 293 (2005), hep-ph/0204087.

[221] T. Li and Y.-F. Zhou, JHEP **1407**, 006 (2014), 1402.3087.

[222] S. Weinberg, Phys. Rev. D **11**, 3583 (1975).

[223] G. 't Hooft, Phys.Rept. **142**, 357 (1986).

[224] C. A. Baker *et al.*, Phys. Rev. Lett. **97**, 131801 (2006).

[225] J. E. Kim and G. Carosi, Rev.Mod.Phys. **82**, 557 (2010), 0807.3125.

[226] R. D. Peccei and H. R. Quinn, Phys. Rev. Lett. **38**, 1440 (1977).

[227] R. D. Peccei and H. R. Quinn, Phys. Rev. D **16**, 1791 (1977).

[228] S. Weinberg, Phys.Rev.Lett. **40**, 223 (1978).

[229] F. Wilczek, Phys.Rev.Lett. **40**, 279 (1978).

[230] J. E. Kim, Phys. Rev. Lett. **43**, 103 (1979).

[231] M. A. Shifman, A. Vainshtein, and V. I. Zakharov, Nucl.Phys. **B166**, 493 (1980).

[232] A. Zhitnitsky, Sov.J.Nucl.Phys. **31**, 260 (1980).

[233] M. Dine, W. Fischler, and M. Srednicki, Phys.Lett. **B104**, 199 (1981).

[234] J. Preskill, M. B. Wise, and F. Wilczek, Phys.Lett. **B120**, 127 (1983).

[235] L. Abbott and P. Sikivie, Phys.Lett. **B120**, 133 (1983).

[236] M. Dine and W. Fischler, Phys.Lett. **B120**, 137 (1983).

[237] M. S. Turner, Phys.Rev. **D28**, 1243 (1983).

[238] M. S. Turner, F. Wilczek, and A. Zee, Phys.Lett. **B125**, 35 (1983).

[239] M. S. Turner, Phys.Rev. **D33**, 889 (1986).

[240] J. E. Kim, Phys.Rept. **150**, 1 (1987).

[241] Z. Berezhiani, A. Sakharov, and M. Y. Khlopov, Sov.J.Nucl.Phys. **55**, 1063 (1992).

[242] M. Beltran, J. Garcia-Bellido, and J. Lesgourgues, Phys.Rev. **D75**, 103507 (2007), hep-ph/0606107.

[243] Wantz, O. and Shellard, E.P.S., Phys.Rev. **D82**, 123508 (2010), 0910.1066.

[244] R. L. Davis, Phys.Lett. **B180**, 225 (1986).

[245] R. Battye and E. Shellard, Nucl.Phys.Proc.Suppl. **72**, 88 (1999), astro-ph/9808221.

[246] M. Yamaguchi, M. Kawasaki, and J. Yokoyama, Phys.Rev.Lett. **82**, 4578 (1999), hep-ph/9811311.

[247] C. Hagmann, S. Chang, and P. Sikivie, Phys.Rev. **D63**, 125018 (2001), hep-ph/0012361.

[248] P. Fox, A. Pierce, and S. D. Thomas, (2004), hep-th/0409059.

[249] M. P. Hertzberg, M. Tegmark, and F. Wilczek, Phys.Rev. **D78**, 083507 (2008), 0807.1726.

[250] D. J. E. Marsh, D. Grin, R. Hlozek, and P. G. Ferreira, Phys.Rev.Lett. **113**, 011801 (2014), 1403.4216.

[251] P. Gondolo and L. Visinelli, Phys.Rev.Lett. **113**, 011802 (2014), 1403.4594.

[252] P. Svrcek and E. Witten, JHEP **0606**, 051 (2006), hep-th/0605206.

[253] L. J. Hall, Y. Nomura, and S. Shirai, JHEP **1406**, 137 (2014), 1403.8138.

[254] K. Choi, K. S. Jeong, and M.-S. Seo, JHEP **1407**, 092 (2014), 1404.3880.

[255] K. Sigurdson and A. Cooray, Phys.Rev.Lett. **95**, 211303 (2005), astro-ph/0502549.

[256] L. Book, M. Kamionkowski, and F. Schmidt, Phys.Rev.Lett. **108**, 211301 (2012), 1112.0567.

[257] T. Higaki, K. S. Jeong, and F. Takahashi, Phys.Lett. **B734**, 21 (2014), 1403.4186.

[258] E. J. Chun, Phys. Lett. **B735**, 164 (2014), 1404.4284.

[259] M. Kawasaki, N. Kitajima, and F. Takahashi, Phys. Lett. **B737**, 178 (2014), 1406.0660.

[260] T. Moroi, K. Mukaida, K. Nakayama, and M. Takimoto, JHEP **11**, 151 (2014), 1407.7465.

[261] N. Okada, M. U. Rehman, and Q. Shafi, Phys.Rev. **D82**, 043502 (2010), 1005.5161.

[262] A. Linde, M. Noorbala, and A. Westphal, JCAP **1103**, 013 (2011), 1101.2652.

[263] R. Kallosh and A. Linde, JCAP **1306**, 027 (2013), 1306.3211.

[264] R. Kallosh and A. , JCAP **1310**, 033 (2013), 1307.7938.

[265] A. Linde, Inflationary Cosmology after Planck 2013, in *Les Houches, 2013*, 2014, 1402.0526.

[266] J. Joergensen, F. Sannino, and O. Svendsen, Phys.Rev. **D90**, 043509 (2014), 1403.3289.

[267] T. Inagaki, R. Nakanishi, and S. D. Odintsov, Astrophys. Space Sci. **354**, 2108 (2014), 1408.1270.

[268] R. Kallosh and A. Linde, JCAP **1307**, 002 (2013), 1306.5220.

[269] R. Kallosh and A. Linde, JCAP **1312**, 006 (2013), 1309.2015.

[270] R. Kallosh, A. Linde, and D. Roest, JHEP **1311**, 198 (2013), 1311.0472.

[271] M. Galante, R. Kallosh, A. Linde, and D. Roest, Phys.Rev.Lett. **114**, 141302 (2015), 1412.3797.

[272] WMAP, C. Bennett *et al.*, Astrophys.J.Suppl. **208**, 20 (2013), 1212.5225.

[273] Planck Collaboration, P. Ade *et al.*, Astron.Astrophys. (2014), 1303.5076.

[274] J. P. Conlon, R. Kallosh, A. D. Linde, and F. Quevedo, JCAP **0809**, 011 (2008), 0806.0809.

[275] S. Dimopoulos, S. Kachru, J. McGreevy, and J. G. Wacker, JCAP **0808**, 003 (2008), hep-th/0507205.

[276] ADMX Collaboration, S. J. Asztalos *et al.*, Phys.Rev. **D69**, 011101 (2004), astro-ph/0310042.

[277] G. G. Raffelt, Lect.Notes Phys. **741**, 51 (2008), hep-ph/0611350.

[278] CAST, K. Zioutas *et al.*, Phys.Rev.Lett. **94**, 121301 (2005), hep-ex/0411033.

[279] A. Arvanitaki, S. Dimopoulos, S. Dubovsky, N. Kaloper, and J. March-Russell, Phys.Rev. **D81**, 123530 (2010), 0905.4720.

[280] K. van Bibber and G. Carosi, (2013), 1304.7803.

[281] Budker, D. and Graham, P.W. and Ledbetter, M. and Rajendran, S. and Sushkov, A.O., Phys.Rev. **X4**, 021030 (2014), 1306.6089.

[282] J. Hamann, S. Hannestad, G. G. Raffelt, and Y. Y. Y. Wong, JCAP **06**, 22 (2009), 0904.0647.

[283] A. Djouadi, J. Kalinowski, and M. Spira, Comput.Phys.Commun. **108**, 56 (1998), hep-ph/9704448.